FE-2550-4
Distribution Category UC-90d

PHYSICAL AND CHEMICAL BEHAVIOR OF LIQUEFIED COAL IN SOLIDS SEPARATION

Annual Report for the
Year Ending September 30, 1977

Dale E. Briggs
David V. Addington
Clinton E. Berry, Jr.
Shang-Shing Chou
Douglas Greminger
Kurt A. Heringhausen
John D. Jones
Jeffrey A. McKeen
James C. Romine
Jerome R. Skelly
J. Andrew Stirling
Peter A. S. Smith
W. Brian Bedwell
John R. Cameron
Mustafa I. El-Shaikh
Levon Hachigian
Benedict Ho
David B. McAlpine
Lionel D. Moore
Utpal Sen Gupta
Karen C. Steinke

Department of Chemical Engineering
Department of Chemistry

University of Michigan

Under Contract No. EX-76-S-01-2550

Administered Through

Division of Research Development and Administration
DRDA Project 014933

Ann Arbor, Michigan 48109

October 1977

TABLE OF CONTENTS

LIST OF TABLES

LIST OF TABLES (concluded)

LIST OF FIGURES

LIST OF FIGURES (concluded)

PHYSICAL AND CHEMICAL BEHAVIOR OF LIQUEFIED COAL IN SOLIDS SEPARATION

Annual Report for the Year
Ending September 30, 1977

Dale E. Briggs
David V. Addington
W. Brian Bedwell
Clinton E. Berry, Jr.
John R. Cameron
Shang-Shing Chou
Mustafa I. El-Sheikh
Peter A. S. Smith
Douglas Greminger
Levon Hachigian
Kurt A. Heringhausen
Benedict Ho
John D. Jones
David B. McAlpine
Jeffrey A. McKeen
Lionel D. Moore
James C. Romine
Utpal Sen Gupta
Jerome R. Skelly
Karen C. Steinke
J. Andrew Stirling

ABSTRACT

Four bis-(hydroxyphenyl)alkanes and four α,ω-dipyridyl or diquinolyl-alkanes were synthesized, purified, and examined by proton NMR. The compounds are believed to possess characteristics of asphaltenes.

Solvent extracted asphaltenes from an H-coal liquefaction of an Illinois No. 6 Coal were fractioned in a 10.16-cm x 122-cm long GPC column. Fractions were characterized by molecular weight, elemental and proton NMR analyses. Oxygen and metals levels were determined by neutron activation. Exploratory experiments to separate asphaltenes into acidic and basic fractions were conducted.

Filtration data were taken at 232°C (450°F) at different concentrations of oils, resins, asphaltenes, and preasphaltenes with 13.8 wt. % THF insoluble solids. At comparable asphaltene and preasphaltene concentrations, the specific cake resistance is less with oils and resins than with tetralin. The colloid micelles which form in tetralin above 16-18% asphaltenes at 177°C (350°F) are substantially peptized by resins.

Electrophoresis experiments with asphaltene and preasphaltene fractions gave deposition on both electrodes, being largest on the positive electrode with pyridine, THF, and m-cresol and on the negative electrode with benzene and tetralin as solvents. The amount of deposition is directly related to the extent of asphaltene or preasphaltene solubilization being greatest in pyridine at elevated temperatures.

Adsorption characteristics of GPC fractionated asphaltenes were examined. The analysis included the effects of concentration, temperature, solvent and solid adsorbent. Micelle formation was apparent with the higher molecular weight asphaltene fractions. The critical micelle concentration is temperature dependent. Adsorption experiments on two and three ring aromatic compounds were conducted to assess the adsorption tendency of various functional groups.

Streaming potential measurements were made for the flow of asphaltene solutions through fixed beds of solids to assess the effects of concentration, temperature, solvent, and solid adsorbent. There is consistency in the electrophoresis, adsorption and streaming potential data.

OBJECTIVE AND SCOPE OF WORK

The objective of this program is to study the physical and chemical behavior of liquefied coal. The interactions between various fractions of liquefied coal, solvents, mineral matter, and catalysts will be experimentally measured to provide solubility, colloid behavior, adsorption, viscosity, and surface tension data for the design and operation of coal liquefaction processes. Model compounds will be synthesized and examined in combinations to simulate coal liquids.

The scope of work to accomplish the program objects include the following five tasks and sub-tasks:

Task 1. Separation, Characterization, and Chemistry of Liquefied Coal.

- A. Chemical investigations
  1. Synthesis and analysis of heterocyclic compounds
  2. Chemical analysis of fractionated asphaltene samples
  3. Reactivity of asphaltene fractions
- B. Preparative scale separation and characterization of liquefied coal samples for experimental work under Tasks 1-5

Task 2. Solids-Separations-Filtration Experiments.

- A. Filtration of preasphaltene-free solids in tetralin to obtain specific cake resistances and compressibilities
- B. Filtration of oils, resins, asphaltenes, and preasphaltenes dissolved either singularly or in combination in tetralin to determine the effect on precoat materials
- C. Filtration of solids residues dispersed in tetralin and/or selected fractions of liquefied coal from which the residues originated to obtain the specific cake resistance at different concentrations of dissolved fractions
- D. Filtration of dispersed residues pretreated with extenders

Task 3. Colloid Chemistry of Liquefied Coal Slurries.

- A. Determination of the solubility of fractionated asphaltenes and preasphaltenes and mixtures of the two in oils, resins, and selected solvents
- B. Measurement of the electrical charge associated with asphaltenes, preasphaltenes, and resin fractions from electrophoresis experiments
- C. Assessment of mineral particle agglomeration in the presence of asphaltenes and preasphaltenes by observation under a 1000X research microscope

D. Deduction of intermolecular bonding between fractionated samples from molecular weight determinations by vapor pressure osmometry when samples are dissolved in different solvents

E. Characterization of vacuum dried asphaltene residues by electron microscopy and X-ray analysis

Task 4. Adsorption Characteristics of Asphaltenes.

A. Measurement of adsorption isotherms for narrow molecular weight fractions of asphaltenes, preasphaltenes, and resins dissolved in solvents or oils when in contact with mineral solids and catalysts

B. Measurement of the streaming potential when asphaltenes, preasphaltenes, and resins dissolved in solvents flow through beds of mineral solids

Task 5. Viscosity and Surface Tension Characteristics of Coal Liquids.

A. Measurement of the viscosity of asphaltenes with narrow ranges of molecular weight

B. Development of prediction rules for viscosities of mixtures of asphaltenes, preasphaltenes, resins, and oils

C. Measurement of the viscosities of liquefied coal slurries

D. Measurement of viscosities of prepared liquefied coal samples at high temperatures and at pressures high enough to prevent boiling

E. Measurement of the surface tension of prepared liquefied coal samples

SUMMARY OF PROGRESS

This contract for the study of the physical and chemical behavior of liquefied coal in solids separation was awarded on September 30, 1976 for a period of 34 months. The contract work is a continuation of the study initiated under an Advanced Energy Research Grant of NSF RANN. The final report of that effort was completed during the first quarter.[1]

The contract work covers five major tasks:

1. Separation, characterization and chemistry of liquefied coal,
2. Solids separation-filtration experiments,
3. Colloid chemistry of liquefied coal slurries,
4. Adsorption characteristics of asphaltenes,
5. Viscosity and surface tension characteristics of coal liquids.

Work was accomplished on all five tasks.

Task 1. An objective of Task 1 is to synthesize a series of compounds having either two or more heterocyclic rings joined by a saturated carbon chain or two or more phenolic groups joined in the same way. p,p'-tetramethylene bisphenol and four bis-(hydroxyphenyl)alkanes were synthesized and purefied into crystalline solids. The compounds include 1,5-bis-(2-hydroxy-5-methylphenyl)pentane, 1,4-bis(2-hydroxy-5-methylphenyl)hexane, 1,4-bis-(2-hydroxy-5-methylphenyl) butane and 1,2-bis-(p-hydroxyphenyl)ethane. α,α'-hexamethylenebisquinoline, 1,2-bis-(2-quinolyl)ethane, 1,5-bis-(2-pyridyl)pentane and 1,6-bis-(2-pyridyl)hexane have been synthesized. NMR spectra and melting points were obtained for each compound after purification.

A 10.16-cm ID x 122-cm long gel permeation chromatography (GPC) column containing an 8% divinylbenzene-styrene copolymer was used to fractionate an asphaltene from the H-Coal process liquefaction of an Illinois No. 6 Coal into seven fractions for the adsorption experiments. A total of seven identical runs were made and corresponding fractions mixed. Samples of the asphaltene fractions and a preasphaltene fraction were characterized by molecular weight, elemental and proton NMR analyses. The molecular weight distribution in four asphaltene fractions was determined by fractionation in a 2.5-cm ID x 100-cm long GPC column followed by molecular weight measurements by vapor pressure osmometry.

A procedure was developed to measure the oxygen content of liquefied coal samples by neutron activation. Neutron activation was also used to measure the concentrations of Na, K, Ca, Mg, Mn, Al, Ti, and V in coal liquefaction residues, extract and GPC separation fractions.

Exploratory work was initiated to separate asphaltenes and/or preasphaltenes into acidic and basic components.

A 30 gallon extraction vessel was constructed and put into operation for solvent extraction of liquefied coal.

Task 2. During the first quarter, Mr. Stirling completed his Ph.D. research and dissertation on the filtration of liquefied coal. Data were taken at 232°C (450°F) on extracts from H-Coal vacuum bottoms at different concentrations of oils, resins, asphaltenes, and preasphaltenes with 13.8 wt. % THF insoluble solids. At comparable asphaltene and preasphaltene concentrations, the specific cake resistance is less with oils and resins than with tetralin. The colloid micelles which form in tetralin above 16-18% asphaltenes at 177°C (350°F) are substantially peptized by resins.

Major modifications to the filtration equipment were effected. The slurry preparation vessel heating system was put on a separate circuit to reduce heating time from three hours to one hour. The filtrate density and flow rate measuring systems were modified to simplify operations. Recalibration of the differential pressure instruments was completed and the precoating procedure checked-out.

Task 3. An experimental procedure to measure the size-configuration of asphaltene colloids by small angle X-ray scattering was developed. This technique should be useful in determining changes in solution behavior at conditions found in coal liquefaction. An experimental cell was designed and constructed to be used in existing X-ray equipment.

Three experimental electrophoresis cells were designed, constructed and operated to measure the charge associated with different fractions of liquefied coal. Runs were made with asphaltene and preasphaltene samples in five different solvents and the deposition on the electrodes determined as a function of concentration, voltage and time.

A Balsbaugh Model LRC-1 Liquid Reference Cell, a Keithley Model 610C Electrometer and a Radiometer MM2 RLC Meter have been put together to measure electrical conductivity and dielectric of asphaltene solutions. Some electrical conductivity data have been taken.

Task 4. Nine solids were characterized as to pore size distribution, surface area, and true density for the adsorption experiments.

Eighteen two and three ring aromatic compounds with various functional groups were obtained and their retention volumes measured on 2.5 wt. % water deactivated Alcoa F-20 alumina by the LEAC procedure. Compounds with basic

nitrogen atoms and phenolic groups had the greatest affinity for adsorption. A synthesized bifunctional compound containing two basic nitrogen atoms had a retention volume seven times larger than 5,6-benzoquinoline which contains one basic nitrogen atom. Adsorption experiments with acidic and basic asphaltene fractions showed substantial tailing indicating the presence of many heteroatom compounds in each mixture. The adsorption of selected compounds in benzene, chloroform, and THF onto 4% water deactivated Grace 923 silica gel was measured by the LEAC procedure.

The narrow molecular weight fractions from the 10.16-cm ID x 122-cm long GPC fractionation were used to study the effect of asphaltene molecular weight, temperature, solvent, and solid adsorbent on asphaltene adsorption. Five asphaltene fractions and one preasphaltene fraction were used to assess the effect of molecular weight on adsorption. The effect of temperature range on asphaltene adsorption was investigated from 30° to 180°C using tetralin as a solvent. The effect of solvent properties was studied by using pyridine, tetrahydrofuran, tetralin, nitrobenzene and toluene as solvents. Finally seven solids, solids present in coal liquefaction processes and two laboratory standards, were used as adsorbents to show any effect of surface area, pore size, and surface properties.

Streaming potential measurements were made for the flow of asphaltenes in solution through fixed beds of solids.

Task 5. A literature review was initiated to find and evaluate methods for measuring viscosity at high temperatures and at pressures high enough to avoid boiling. The review included both solutions and slurries.

A Brookfield Viscometer was modified to permit viscosity measurements with a UV adaptor extender to keep the viscometer clean and cool when viscosity is measured at or above 250°C. Calibration was started, but more calibration work is needed.

The viscosity of asphaltenes from GPC fraction 77-4 in tetralin before and after vacuum drying at 150°C was measured to assess if the method of solution preparation is critical to the results.

Table 1 contains a summary of effort on the various tasks and subtasks.

Table 1. Work Accomplished During First Year, October 1, 1976 to September 31, 1978.

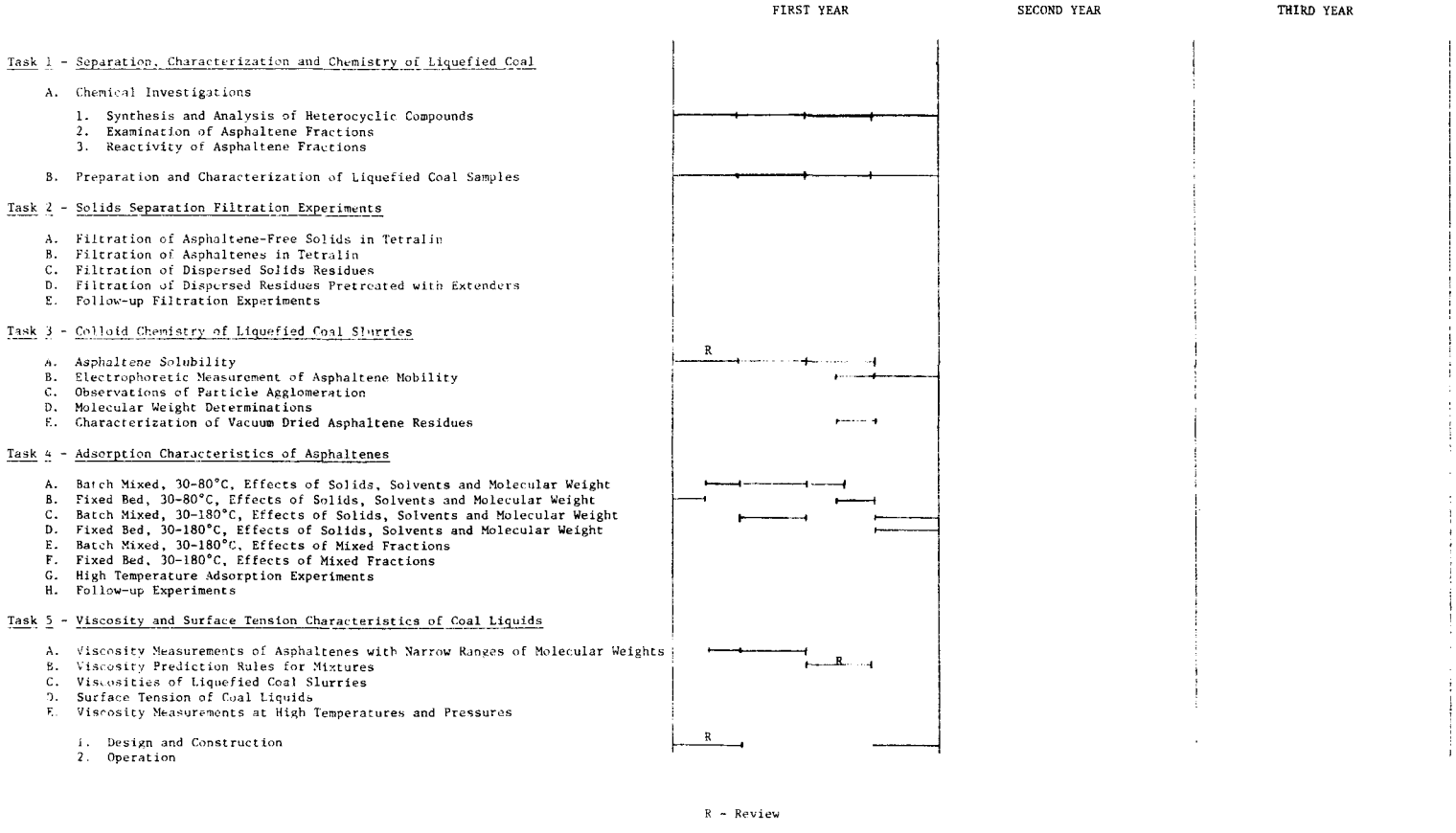

R - Review

I. SEPARATION, CHARACTERIZATION, AND CHEMISTRY OF LIQUEFIED COAL

A. Chemical Investigations

(P. Chou, J. Romine, M. El-Sheikh)

1. Synthesis and Examination of Heterocyclic Compounds as Models of Asphaltene Components

In this part of the program, two classes of substance are under investigation: compounds with two or more heterocyclic nuclei attached to a chain of saturated carbon atoms, and compounds with two or more phenolic groups similarly attached. The interaction between these two classes will then be examined.

a. Phenols

p,p'-Tetramethylenebisphenol was synthesized from anisole and succinic anhydride by a multi-step route. The Friedel-Crafts reaction produced β-(p-methoxybenzoyl) propionic acid in good yield. Several attempts were made to convert this product to an acid chloride, followed by a second Friedel-Crafts condensation, but only tarry products resulted. The acid was therefore reduced by catalytic hydrogenation over palladium on charcoal to γ-p-anisyl-p-methoxybutyrophenone (40% yield). This product was a light yellow solid, m.p. 91-92°C after recrystallization from ether and methanol. Its NMR spectrum was consistent with the assigned structure, as was its infrared spectrum (carbonyl stretch at 1680-1700 cm^{-1}).

Hydrogenation of the foregoing ketone over palladium on charcoal gave p,p'-tetramethylenebisanisole as pure white crystals (64% yield). This product was demethylated to the corresponding bisphenol by refluxing with HBr in acetic acid. A seemingly pure product was obtained, m.p. 156-157°C, in about 50% yield, but its NMR spectrum (δ 1.7, 2.7, 6.7-7.3 ppm) showed in addition an unexpected singlet at the position expected for the O-methyl group of the starting material. It was presumed that demethylation was not complete, but numerous attempts at purification by recrystallization and chromatography failed to improve the spectrum. Eventually, it was found that the NMR solvent used, d_6-dimethyl sulfoxide, was contaminated with something unknown that was responsible for the extraneous singlet, and the bisphenol had been obtained pure after all.

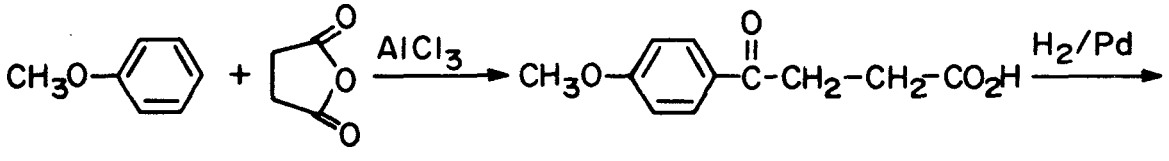

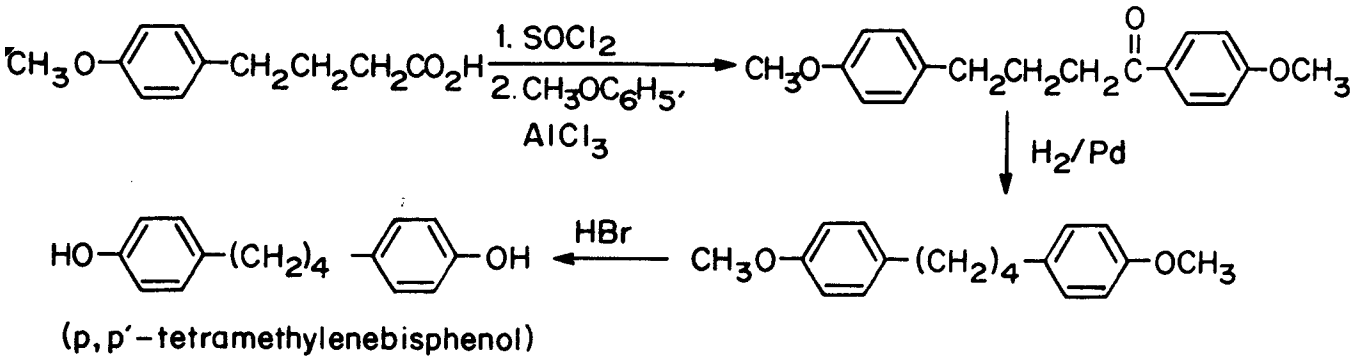

Another area of synthesis is bis-(o-hydroxyphenyl)-alkanes having the phenolic substituents at the terminal positions of chains of methylene groups two to six carbons in length. Our synthesis begins with the preparation of phenyl esters (II) of dicarboxylic acids from the acid chlorides (I) and phenol, followed by Fries rearrangement to the corresponding bis-(o-hydroxyphenyl)-alkanediones (III). Attempts to hydrogenate the carbonyl groups in the diones to methylene groups were unsatisfactory, apparently owing to interaction of the adjacent hydroxy group with the carbonyl. The problem was overcome by blocking the hydroxy group by acetylation, but the phenols eventually obtained by removal of the acetyl groups were difficult to crystallize. Better results were obtained by Clemmensen reduction of the non-acetylated diones.

The acetylated bis-phenols were reduced by catalytic hydrogenation (paladium catalyst) and were hydrolyzed during work-up. It became evident from the spectra of the crude products that there was contamination with the isomeric para-hydroxy compounds. When it was found to be difficult to remove the contaminant satisfactorily, it was decided to prevent formation of the para isomers by having that position blocked with a methyl group. By this means, some of the desired bis-(o-hydroxyphenyl)-alkanes were obtained. The results are tabulated in Table 2.

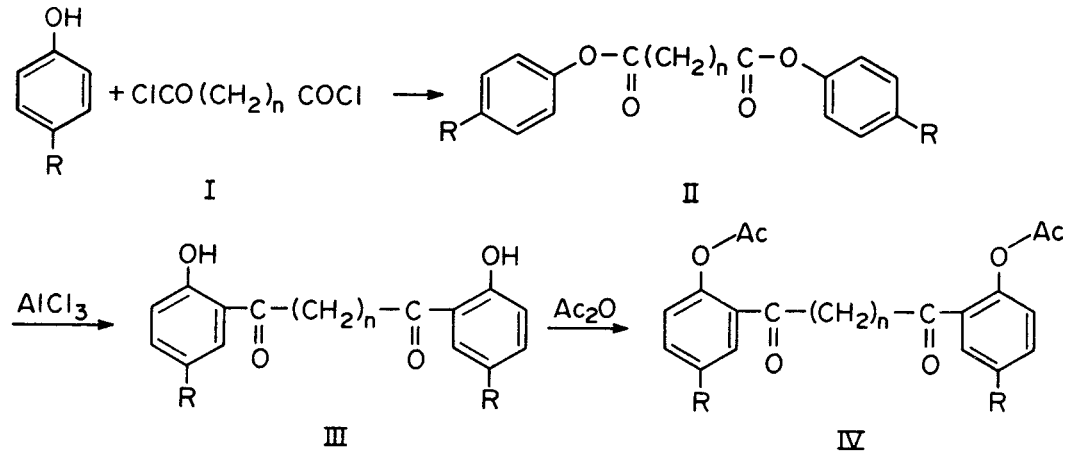

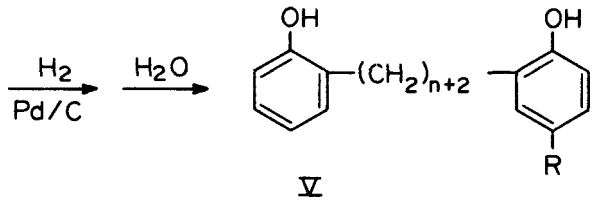

V

R = H or CH_3 n = 0 to 4

Because the reduction using the acetyl blocking group was still not completely satisfactory, we are experimenting with the use of methyl as a blocking group.

Table 2. Bis-phenol Derivatives.

Compound	n	R	m.p., °C	Yield	Remarks
Acid Chlorides:					
Ia	1				b.p. 78-80°/85mm
Ib	2				b.p.105-110°/45mm
Ic	3			100%	not distilled
Id	4			96%	not distilled
Esters:					
IIa	3	H	53		
IIb	4	H	105-106	72%	
IIc	0	CH_3	150-151	62%	
IId	2	CH_3	118-120	74%	
IIe	3	CH_3	83-86	92%	
IIf	4	CH_3	92-95	50%	hydrolysis occurred during recrystallization
Diketones:					
IIIa	0	CH_3	200	3%	
IIIb	3	CH_3	135-137	51%	
IIIc	4	CH_3	158-160	66%	
Diacetoxy Diketones:					
IVa	3	CH_3	99-102	98%	
IVb	4	CH_3	133-135	97%	
Bis-(hydroxyphenyl)alkanes:					
Va	3	CH_3	101-103	89%	
Vb	4	CH_3	123-124	100%	

1,5-bis-(2-hydroxy-5-methylphenyl)pentane was originally prepared as an oil by catalytic hydrogenation of the diacetate of the corresponding 1,5-diketone. Clemmensen reduction of the dihydroxy diketone gave a crystalline product, m.p. 101-103°, NMR δ 6.5-6.0 multiplet, 4.07 (OH); 2.9, 2.2-2.6, 2.1 singlet; 1.4 multiplet.

Similarly, 1,6-bis-(2-hydroxy-5-methylphenyl)hexane which had been obtained as an oil from the acetate, was obtained crystalline by Clemmensen reduction. It had m.p. 123-124°; NMR δ 7.8 (OH), 6.7-6.9 multiplet, 2.5, 2.1 singlet, 1.4 multiplet. This compound was later also obtained crystalline from the oil from the acetate by use of column chromatography.

A third member of this series, 1,4-bis-(2-hydroxy-5-methylphenyl) butane, has been prepared by the same route: Fries rearrangement of p-cresyl succinate, followed by Clemmensen reduction. The product had an unexpectedly high m.p. (>200°, with shrinking at 145°), and its identity is consequently in doubt.

The compound 1,2-bis-(p-hydroxyphenyl)ethane has been synthesized by the route shown in the equations:

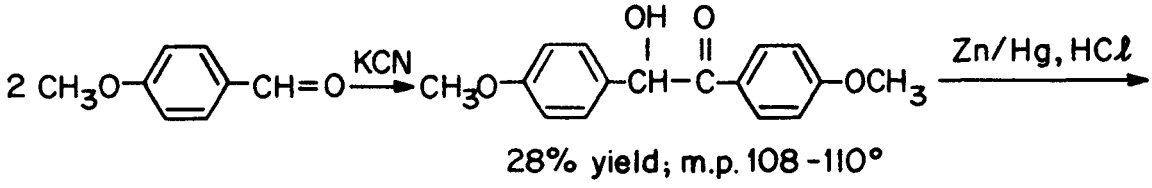

28% yield; m.p. 108-110°

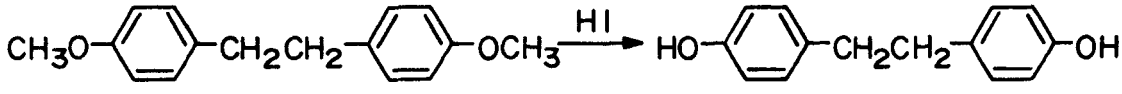

92% yield; m.p. 124-125°

~100% yield; m.p. 198-199°
(reported m.p. 199°)

Its NMR spectrum was similar to the ortho-hydroxy analogs: δ 7.8 (OH), 6.65-6.95, 2.2-2.65, 1.4.

The next higher homolog has been synthesized in the form of an oil by the following route:

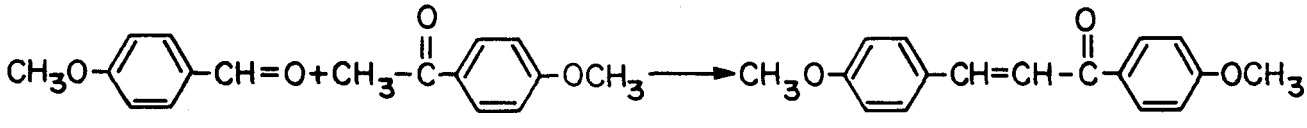

95% yield; m.p. 100-102°

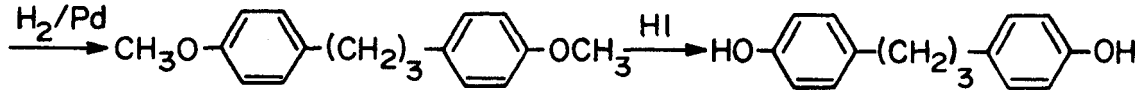

89% yield

Oil

The crude oil had an NMR spectrum similar to the lower homolog, and showed no carbonyl stretching in the infrared. Purification is underway.

The meta-hydroxy analogs of the foregoing two bis-phenols have been synthesized by analogous routes.

b. Basic Heterocycles

α,α'-Hexamethylenebisquinoline was prepared from 2-methylquinoline by converting it to its lithio derivative with butyllithium, and then treating it with tetramethylene bromide. The oily product was crystallized from ethanol and chloroform, but it was obtained only as impure, brown crystals. Digestion of these with petroleum ether gave a cleaner product, which had m.p. 90-91.5°C after a further crystallization from ethanol, in a total yield of 18%. Attempts to purify the crude product by crystallization of an oxalate salt failed.

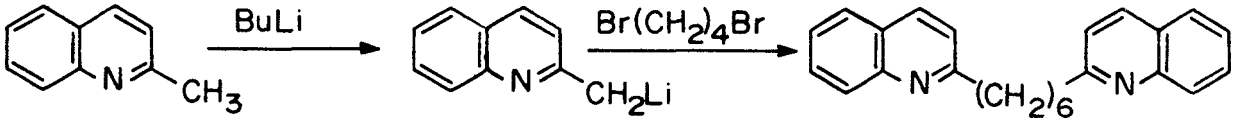

The NMR spectrum of the product showed the expected aromatic multiplet at δ 7.2-8.2, a ragged triplet (α-CH_2's) at δ 2.9-3.2 and a broad multiplet at δ 1.3-2.2 (β and γ CH_2's). The α-methylenes thus could account for some of the low-field aliphatic region of the spectrum of asphaltenes. A chain of fewer than six methylenes between the two heterocyclic nuclei should result in a slight shift further downfield, which would correspond even more closely to what is seen in asphaltenes. 2-Methylquinoline was treated first with butyllithium, and then with 2-bromomethylquinoline, to give 1,2-bis-(2-quinolyl)ethane: m.p. 162-163° NMR δ 7.1-8.1 multiplet, 3.55 singlet. The spectrum is of special interest for the fact that it can account for the low-field end of the "aliphatic" portion of asphaltene NMR spectra.

1,5-Bis-(2-pyridyl)pentane has been prepared from α-picoline by treatment first with butyllithium, then with 1,3-tribromopropane.

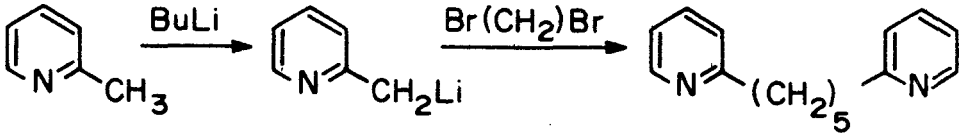

It is an oil; b.p. 141-146°/0.7 mm, NMR δ 8.4-8.6 (m), 7.3-7.6 (m), 6.8-7.2 (m), 2.6-2.9 (triplet), 1.1-2.1 (m).

In an analogous manner, 1,6-bis-(2-pyridyl)hexane was prepared. It is also an oil; b.p. 167-170°/0.8 mm, NMR δ 8.2-8.4 (m), 7.0-7.8 (m), 2.4-3.0 (triplet), 1.0-2.0 (m).

1,2-bis-(4-pyridyl)ethane was prepared, along with 1,2-bis-(4-pyridyl) ethylene, by heating γ-picoline with sulfur: m.p. 99-104°; NMR δ 8.4-8.6 (m), 7.0-7.5 (m), 2.95 (singlet).

A similar experiment using α-picoline gave 1,2-bis-(2-pyridyl) ethane: m.p. 46-48°; NMR δ 7.8.5 (m), 3.3 singlet.

An attempt was made to synthesize 1,3-bis-(2-pyridyl)propane from a α-picoline and 2-vinylpyridine in the presence of sodium. An oil of the expected volatility was obtained: m.p. 123-126°/0.5 mm, NMR δ 7.0-8.5 (m), 2.6-3.18 (triplet), 1.9-2.5 (quartet?). We are not certain that the NMR spectrum in the high-field region is fully consistent with the expected structure, and are attempting further purification. A crystalline perchlorate has been obtained: m.p. 208-210°.

The analogous reaction with γ-picoline gave an oil, b.p. 136-142°/0.8 mm.

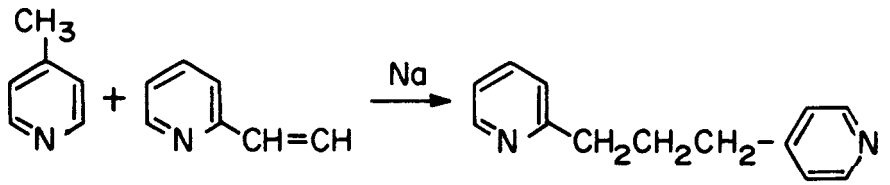

An alternative route to dipyridylalkanes is shown in the following equation.

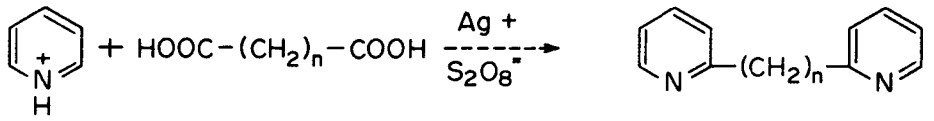

This method involves forming the free radical by decarboxylation:

F. Minisci[2] has shown that free radicals will attach a protonated pyridine ring at the gamma and alpha positions.

We were successful in alkylating quinaldine and lutidine by free radicals of monocarboxylic acids:

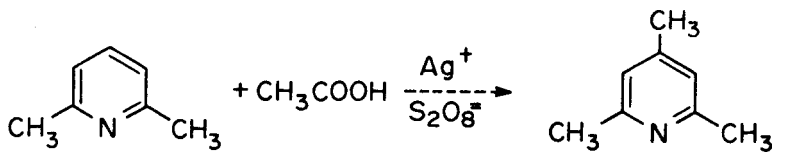

Although these reactions took place according to Minisci's report, the yields were low (10-20%).

Many attempts were made to use this process to form the bis-heterocyclic compounds. Only two reactions were successful, and then only after considerable modification of Minisci's procedure. The following reaction was carried out in a yield of about 7%.

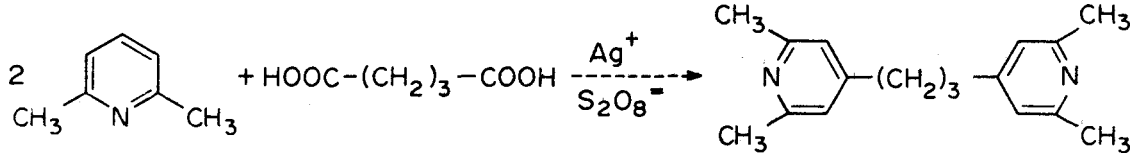

In the hope of improving the yield of this type of reaction, several syntheses were carried out in which one end of the dicarboxylic acid was protected as the amide. The following compounds were successfully produced by this method:

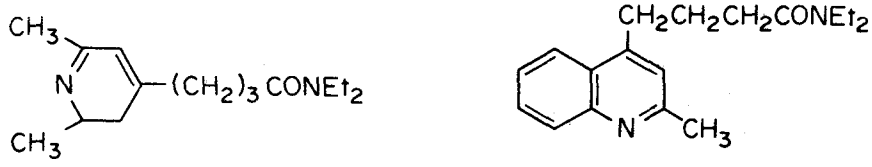

We had originally expected to have been able to begin ^{14}N NMR investigations of asphaltene fractions and components by this time. Unfortunately, the manufacturer of the required NMR accessories has not been able to deliver, and has estimated a six-month or greater lead time.

c. Spectrographic Studies: Mixtures of Phenol and Pyridine

This work was begun in order to obtain reference data for assessing the contribution of O-H-N hydrogen bonding to the NMR spectra of asphaltenes.

From the data in Table 3, one can see that the shift of the phenolic proton depends on the ratio of phenol to pyridine to a marked extent. As the ratio decreases, the proton signal appears further downfield. This is reasonable, considering the deshielding effect of hydrogen bonding. Some values show deviation from the trend, most probably owing to uncertainties in the concentrations. To obtain a more precise relationship between the ratio of proton donor to acceptor and the PMR shift, it will be necessary to examine solutions of more accurately controlled concentrations. Solvent can also play an obvious role, as seen in the spectrum A20, which was determined in carbon tetrachloride instead of chloroform solution.

A preliminary examination has been made of the interaction between the two model compounds that are in hand, 1,4-bis-(p-hydroxyphenyl) butane and 1,6-hexamethylene-2, 2'-quinoline. Complex patterns in the

NMR spectrum were obtained. Although this study is not through, it appears that the change in shift of the phenolic proton may not be great.

Table 3. PMR Shifts in Phenol-Pyridine Mixtures ($CDCL_3$ Solution).

Spectrum No.	Pyridine: Phenol Ratio	Shift of Phenolic Proton, ppm.	Change from Phenol Alone, ppm
A5	0.1M phenol alone	5.78	--
A6	4.8:1	10.2	4.4
A10	1.38:1	9.75	3.97
A16	0.88:1	10.0	4.2
A7	0.32:1	7.58	1.80
A20*	0.28:1	7.53	1.75
A18	0.21:1	7.60	1.82

*in CCl_4 instead of $CDCl_3$

B. Preparation and Characterization of Liquefied Coal Samples
(D. V. Addington, W. B. Bedwell, D. Greminger, J. A. McKeen, L. D. Moore, U. Sen Gupta, and J. A. Stirling)

Under this phase of the work, liquefied coal was solvent extracted into oils and resins, asphaltene and preasphaltene fractions; asphaltenes were fractionated by gel permeation chromatography and subsequently analyzed and asphaltenes were separated into acidic and basic fractions. The acidic and basic fractions are of particular interest since the functional groups in these fractions play a significant role in hydrogen bonding and in the tendency for colloid micellization.

1. Solvent Extraction
(D. V. Addington, J. A. McKeen, and J. A. Stirling)

Large quantities of both coal-derived mineral solids and organic compounds generated during coal liquefaction processes (including oils and resins, asphaltenes, and preasphaltenes) were required for the experimental work. Two main sources of coal-derived mineral solids and organic compounds were used. These were:

a. Vacuum Still Bottoms from the H-Coal Process of Hydrocarbon Research, Incorporated (HRI), Trenton, New Jersey. This material was produced during H-Coal run No. 130-62 while feeding Illinois No. 6 Coal (River King Mine) to the H-Coal Process operating in the Syncrude Mode. Analyses of the feed coal and the vacuum still bottoms are given in Reference 1.

b. Centrifuge solids and centrifuged product oil from the SYNTHOIL Process of the Bureau of Mines, United States Department

of Interior. These materials were produced from West Virginia Coal from the Pittsburgh Seam of the Ireland Mine. An analysis of the feed coal is given in Reference 1.

The H-Coal vacuum still bottoms and the SYNTHOIL centrifuge solids were processed by a series of refluxing, batch, solvent extractions to separate various soluble organic fractions from them. The SYNTHOIL product oil was not processed by extraction but was used directly in some filtration experiments.

A diagram which illustrates the solvent extraction procedure is presented in Figure 1. A known mass (usually 1100 g) of SYNTHOIL centrifuge solids or H-Coal vacuum still bottoms was placed in a three-necked, 12 liter round-bottom boiling flask. A volume in milliliters of pentane (at room temperature) equal to four times the mass of the solids in grams that was already charged to the flask was then added to the flask. A thermometer, stirrer, and cold-water condenser were installed on the three openings in the flask, and the flask and condenser were purged with nitrogen gas to remove oxygen from the system; the motor-driven stirrer was turned on, and heat was applied to the flask by a hemispherical heating mantle. The pentane in the flask was then heated under the reflux at about 37°C.

The stirrer and heater were operated for ten hours in the case of a pentane extraction. This allowed the pentane and the stirrer, which had two pieces of light-weight chain and a teflon-encased piece of chromel wire attached to it, an opportunity to penetrate and break up the pieces of centrifuge solids or vacuum still bottoms. If these pieces were sufficiently reduced in size, the pentane would be able to extract substantially all the molecules which were pentane soluble.

At the end of ten hours, the flask heater was turned off, and the slurry in the flask was allowed to cool below its boiling temperature. The condenser, thermometer, and stirrer were removed from the flask, and the warm extract slurry was poured into a #4A Buchner funnel (151 mm ID x 221 mm high) with a 15.0-cm diameter piece of Whatman No. 42 filter paper in the bottom. The pentane-soluble portion (oils and resins) of the centrifuged solids or vacuum still bottoms passed through the filter paper while the pentane-insoluble portion (a solid) was retained in the Buchner funnel with mineral solids and undissolved coal or char. The pentane-insoluble portion was washed with about 500 ml of pure pentane to remove retained pentane-solubles and then placed in a vacuum oven at room temperature to remove the pentane.

The pentane-soluble extract was placed in a 5 liter round-bottom boiling flask which served as the reboiler for a small distillation column packed with glass beads. The distillation unit was used to recover extraction solvent, in this case pentane, for reuse in the extraction unit and, at the same time, to concentrate the coal-derived extract for use in the filtration system. The distillation unit also had a cold-water condenser and was purged with nitrogen before boil-up was started. Two small samples of known volume of the extract were taken before the pentane was removed, so that a mass balance could be computed on the extraction process.

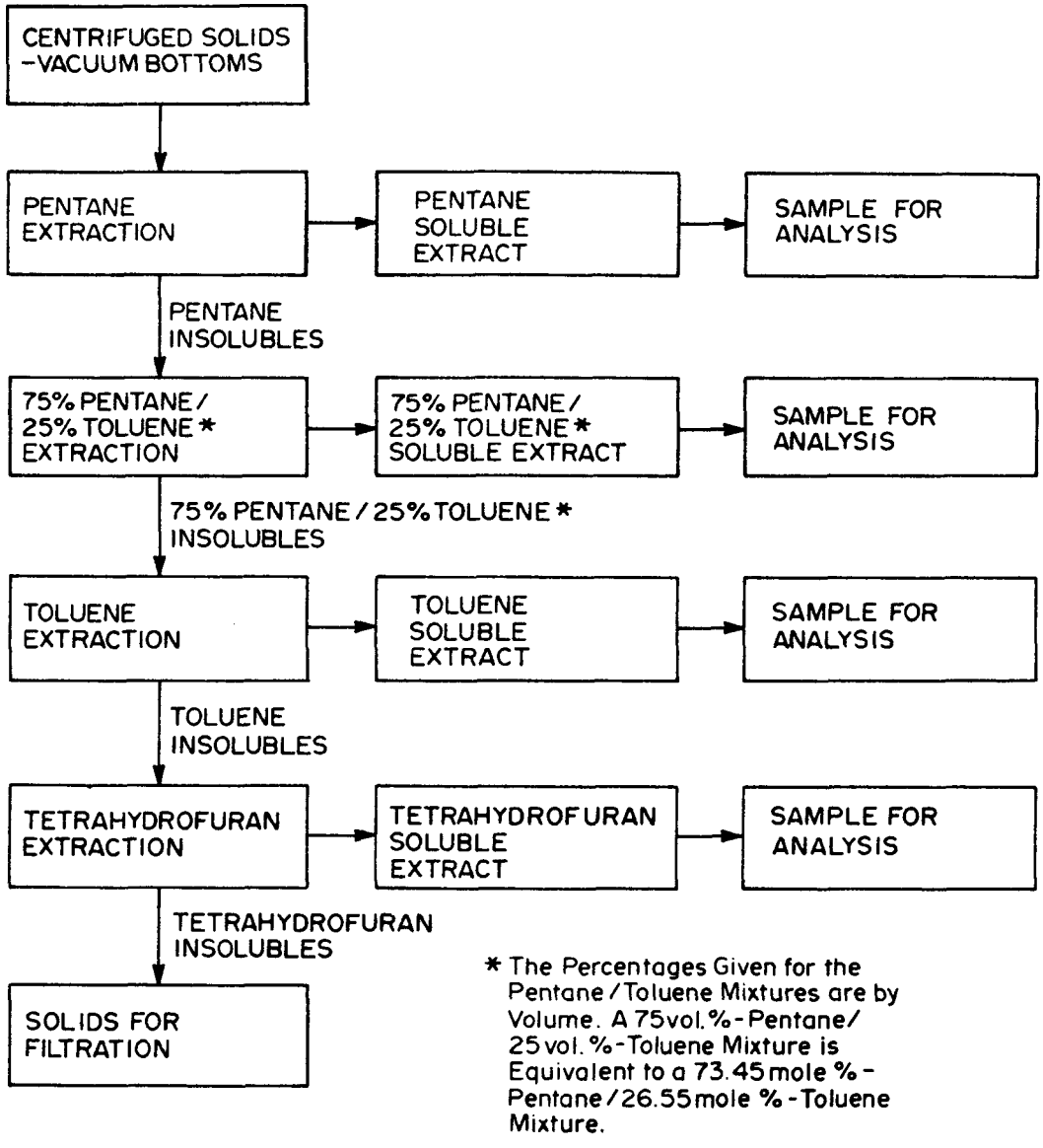

Figure 1. Diagram of Batch Solvent Extraction Procedure.

After the pentane-insoluble solids from the pentane extraction had been dried long enough in the vacuum oven to remove all of the residual pentane, they were weighed to obtain a mass balance and were placed in the 12 liter extraction flask again. A mixture of 25% by volume toluene and 75% by volume pentane was added to the flask. The volume of this mixture was that added in the first extraction. The stirrer, thermometer, and condenser were again installed, and the contents of the vessel were stirred and heated so that the solvent mixture boiled (~39°C). This second extraction was conducted for only five hours, instead of the original ten, since the solids had already been dispersed once, and the solvent mixture of toluene and pentane was much stronger than the original pentane alone.

At the end of five hours, the extract mixture was allowed to cool slightly and then was separated into the soluble and insoluble portions by filtering the mixture through Whatman No. 42 filter paper in the Buchner funnel again. Samples of the 25%-toluene/75%-pentane-soluble extract were taken and the rest was placed in the distillation system to recover solvent and concentrate the extract. The 25%-toluene/75%-pentane-insoluble solids were dried in the vacuum oven to remove retained pentane and toluene.

The 25%-toluene/75%-pentane-insoluble solids were taken from the vacuum oven after the retained solvent had been removed, were weighed, and then were placed in the 12 liter extraction flask again. A volume of technical grade toluene equal to the volume of pentane used in the first extraction was added to the flask. The hot, stirred extraction was carried out at the boiling point of the toluene-slurry mixture (~107°C) for five hours. The toluene-soluble and toluene-insoluble portions were then separated from each other using the Buchner funnel. The toluene-soluble extract was sampled and then concentrated in the distillation apparatus. The toluene-insoluble solids were dried in the vacuum oven to remove retained toluene.

For the final extraction, the toluene-insoluble solids were removed from the vacuum oven after toluene removal, weighed, and then placed in the 12 liter extraction flask again. A volume of tetrahydrofuran (THF) equal to the volume of pentane used in the first extraction was added to the flask. The hot, stirred extraction was carried out near the boiling point of THF (~66°C) for five hours. The THF-soluble extract was separated from the THF-insoluble solids using the Buchner funnel. The THF-soluble extract was sampled and then concentrated by distillation. The THF-insoluble solids were placed in the vacuum oven to remove retained THF.

The net result of the above series of extractions was that the H-Coal vacuum still bottoms or the SYNTHOIL centrifuge solids were divided up into five portions, based on their solubilities in the various solvents. This is shown in Figure 1. The pentane-soluble extract contained the oils and resins. The pentane-insoluble, 25%-toluene/75%-pentane-soluble extract contained a lower molecular weight fraction of the asphaltenes along with some oils and resins not removed by the batch pentane extraction. The 25%-toluene/75%-pentane-insoluble, toluene-

soluble extract contained the higher molecular weight fraction of the asphaltenes. The toluene-insoluble, THF-soluble extract contained the preasphaltenes and some residual asphaltenes from the toluene extraction. The THF-insoluble solids contain the mineral solids, undissolved coal, and char from the coal liquefaction process.

When necessary extracts of similar nature were added together to provide sufficient material of comparable composition for a series of experiments.

A 30 gallon covered stainless steel tank has been modified to serve as an extraction vessel. This will increase the amount of material which can be extracted at one time by a factor of eight. The unit, shown in Figure 2, will be operated to carry out the extraction procedure as before.

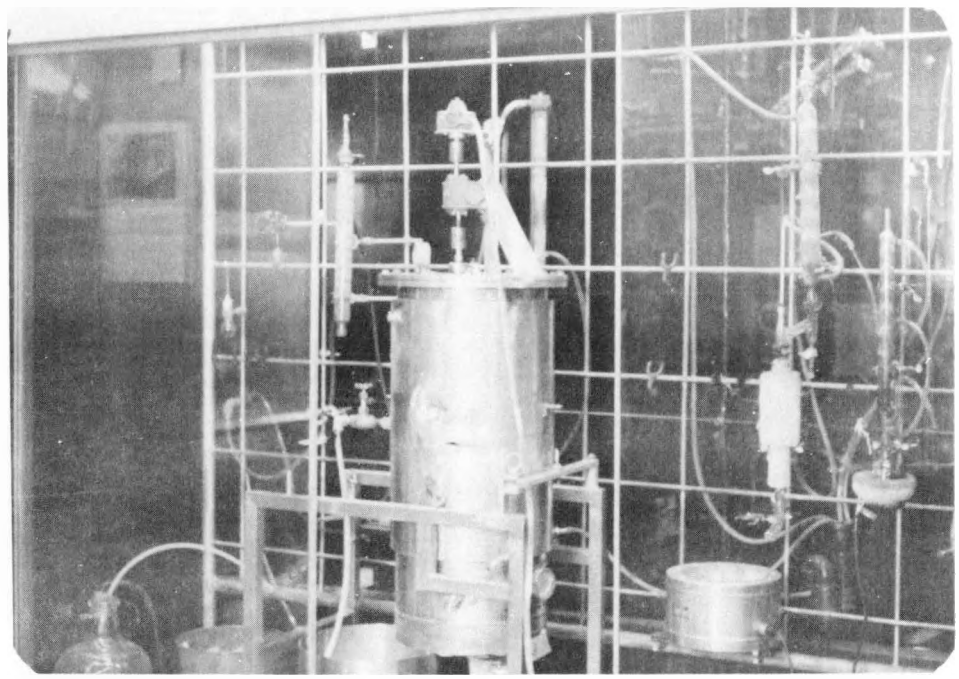

Figure 2. 30 Gallon Stainless Steel Extraction Vessel.

2. Large Scale GPC Fractionations and Analysis
(D. V. Addington and U. Sen Gupta)

Asphaltenes were fractionated in the 10.16-cm ID x 122-cm long (4 in. ID x 4 ft long) column shown in Figure 3. The column packing was an 8% divinylbenzene-styrene copolymer supplied by Dow Chemical Company. The fractions were used in the adsorption experiments.

The following procedure was used in the GPC fractionation of asphaltenes for the adsorption work. Feed material was prepared by combining

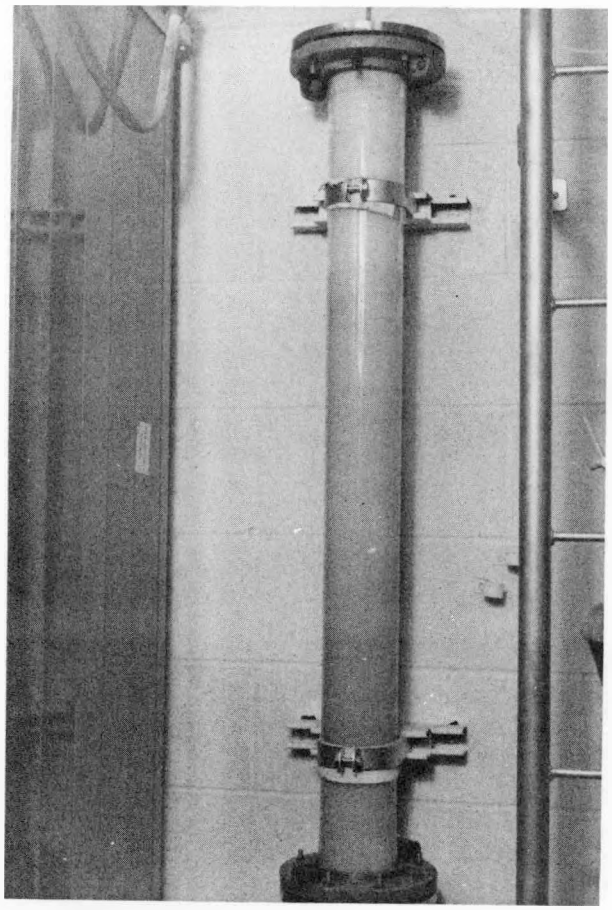

Figure 3. Photograph of the 10.16-cm ID x 122-cm long (4-in ID x 4-ft long) Gel Permeation Chromatography Column.

the toluene soluble, 75%-pentane/25%-toluene-insoluble extracts from four separate batch solvent extraction series (H-Coal vacuum still bottoms, Extraction Series 43, 44, 47, and 48). These extracts were thoroughly mixed and then dried under vacuum for four days at room temperature. A total of 236.5 g of these asphaltenes were then dissolved in 150 ml of tetrahydrofuran (THF) to make approximately 360 ml of feed solution.

Seven identical GPC runs were made. In each case the feed solution volume was 50 ml. The 50 ml samples were injected into the column through an Altex slider injection valve and an 8-mm ID x 1.16-m long glass tube sample loop. This resulted in an intermediate column loading of approximately 330 mg sample/100 ml column volume. The eluent was run through a continuous refractive index (RI) detector with a flow rate of approximately 520 ml/hr and a pressure drop of 20-25 psi across the column and detector. Seven sample fractions were taken in each run. The sample volumes after breakthrough were 300, 360, 550, 550, 360, 360 ml, and the remaining volume to the end of the run. The volumes were of unequal size due to the quantity of each fraction required in the adsorption experiments.

Figure 4 shows a plot of the concentration of each collected fraction as a function of the elution volume for the large scale GPC fractionation. Also indicated is the response curve of the continuous RI detector. The sample volumes and weight of solids recovered in each fraction are shown in Table 4 along with the molecular weight of each fraction. All molecular weights were determined by vapor pressure osmometry in pyridine at 75°C. The molecular weights of the first two fractions are probably somewhat higher than actually exist because of hydrogen bonding of the fractions with pyridine. Good asphaltene and preasphaltene solvents such as pyridine and THF hydrogen bond to the hydroxyl groups of the acidic molecules.

Each corresponding fraction from the seven repetitive runs was mixed, dried, and finally vacuum dried at room temperature. These samples were then stored under nitrogen in a freezer. Small samples from each of the seven composite fractions were further fractionated by running them through the smaller 25-mm ID x 100-cm long GPC column. After breakthrough, 15 ml samples were taken, the solvent evaporated to determine mass and the molecular weight determined by vapor pressure osmometry. This was done to establish a molecular weight distribution for each composite fraction. Figures 5-8 show the results of the small column GPC fractionations as a function of the elution volume for Fractions GPC-72-2, 72-3, 72-4, and 72-5, respectfully. By plotting the molecular weights versus the accumulated mass fraction (at the midpoint of each sample), a molecular weight distribution can be drawn for these fractions. Figure 9 shows this type of distribution for the extract feed for Fraction GPC-72 and a distribution for the Fractions GPC-72-2, 72-3, 72-4, and 72-5.

The feed material, toluene-soluble, 75%-pentane/25%-toluene-insoluble asphaltenes, has a molecular weight range from 280 to about 1350 with a large amount of material on the low end. Fraction GPC-72-5 shows a narrow molecular weight range of 305 to 385 with a linear distribution when plotted in this manner. Fraction GPC-72-4 shows a wider range, 330

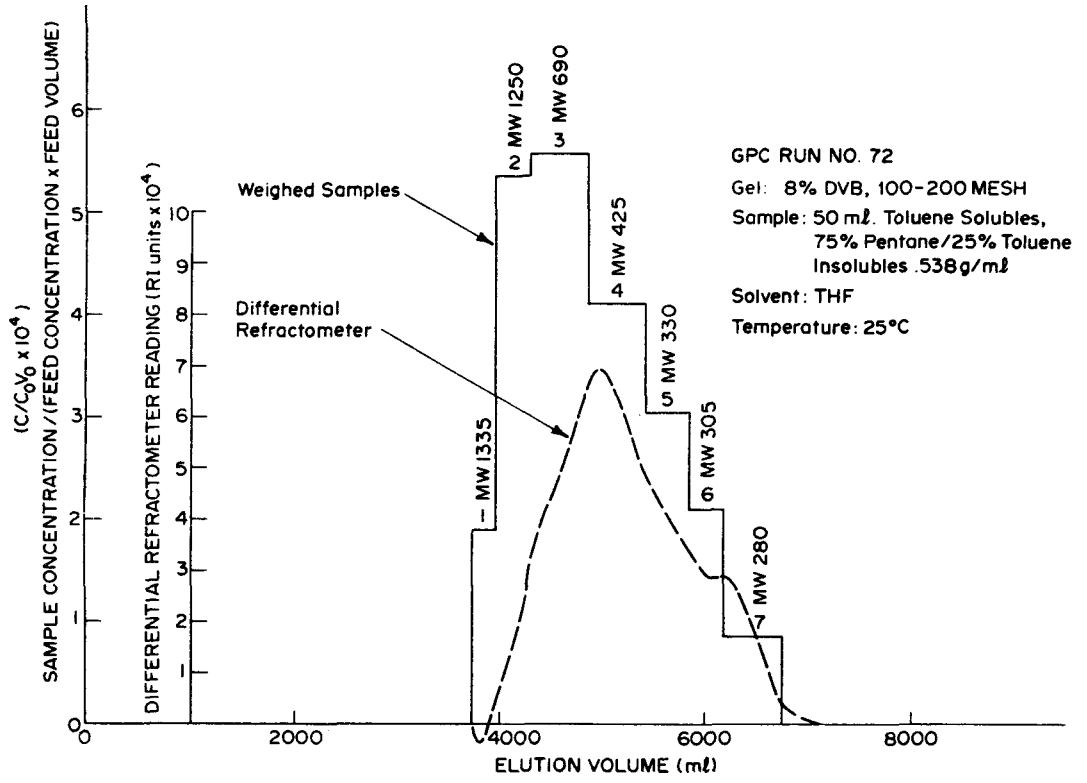

Figure 4. GPC Fractionation of Toluene Soluble, 75%-Pentane/25%-Toluene-Insoluble Extract from Hydrocarbon Research, Inc., H-Coal Vacuum Bottoms, Illinois No. 6, River King Mine Coal.

Table 4. GPC Composite Results for Seven Runs in the 10.16-cm ID x 122-cm Long Column, Fractionation (GPC-72).

Feed Sample: Toluene Solubles, 75%-Pentane/25%-Toluene-Insolubles from Hydrocarbon Research, Inc., H-Coal Vacuum Bottoms from an Illinois No. 6 Coal, River King Mine

Fraction Number	Average Sample Volume	Total Sample Weight Seven Runs	Weight %	Molecular Weight
	(ml)	(g)		
72-1	286	10.3	5.5	1335
72-2	353	35.2	18.7	1250
72-3	547	55.6	29.5	690
72-4	563	43.5	23.1	425
72-5	359	20.5	10.9	330
72-6	348	13.7	7.3	305
72-7	600	9.5	5.0	280
		188.3	100.0	

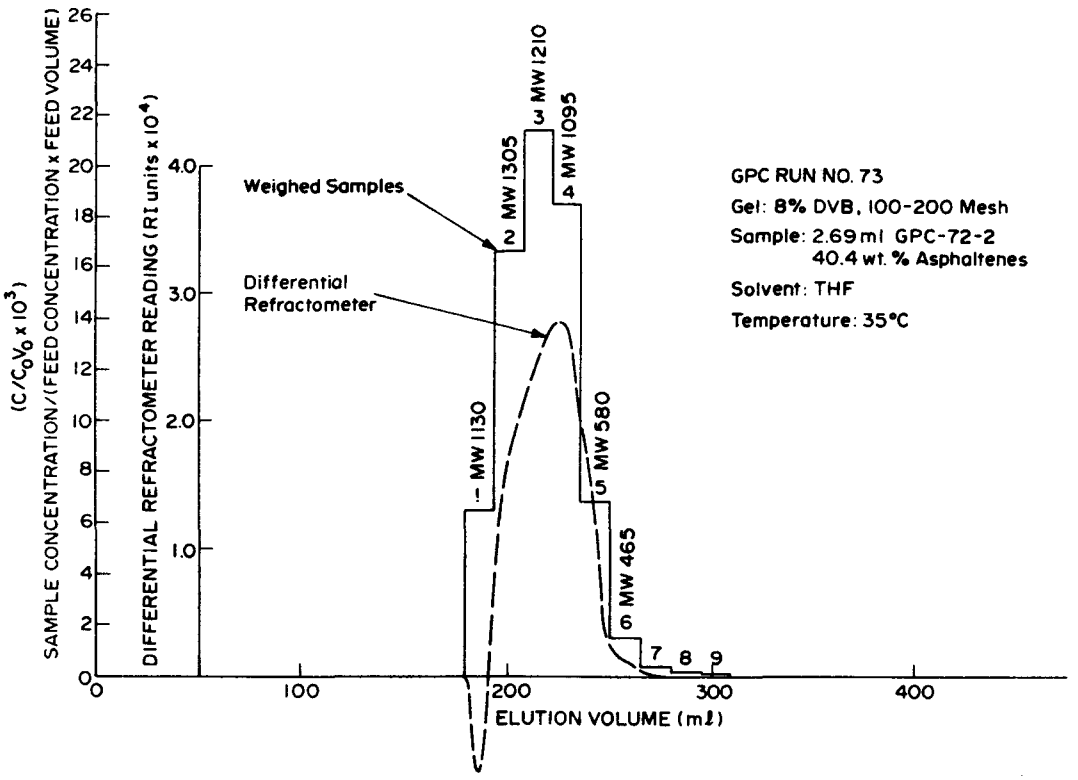

Figure 5. GPC Fractionation of Fraction GPC-72-2 in 25-mm ID x 100-cm Long Column.

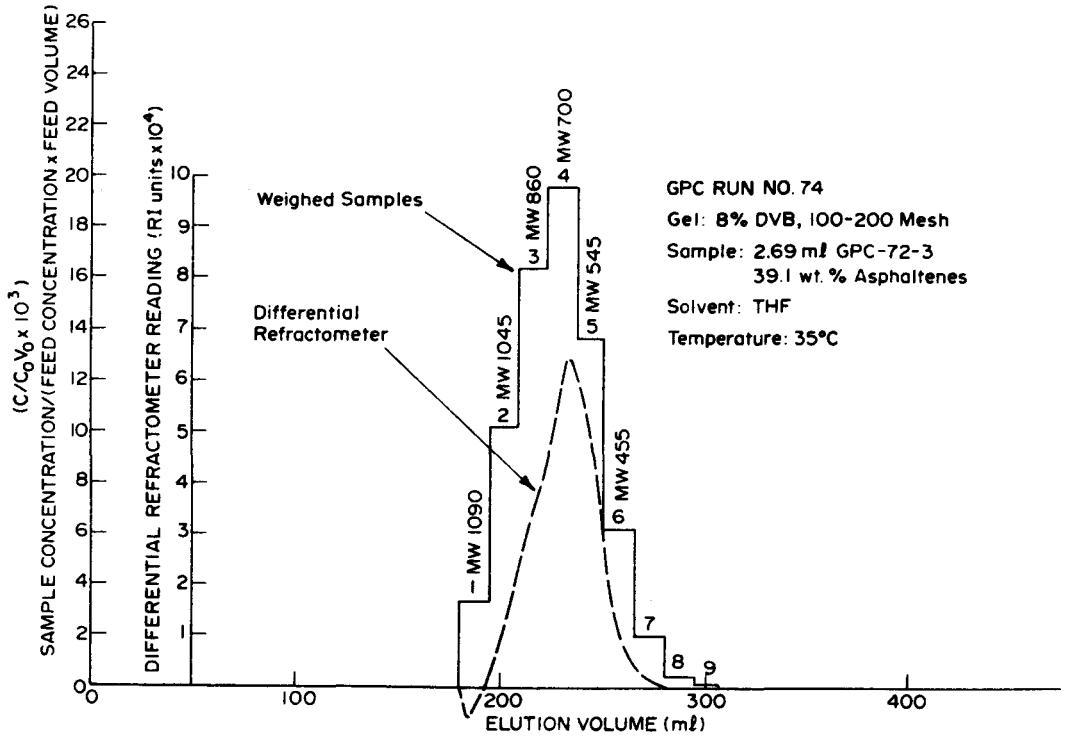

Figure 6. GPC Fractionation of Fraction GPC-72-3 in 25-mm ID x 100-cm Long Column.

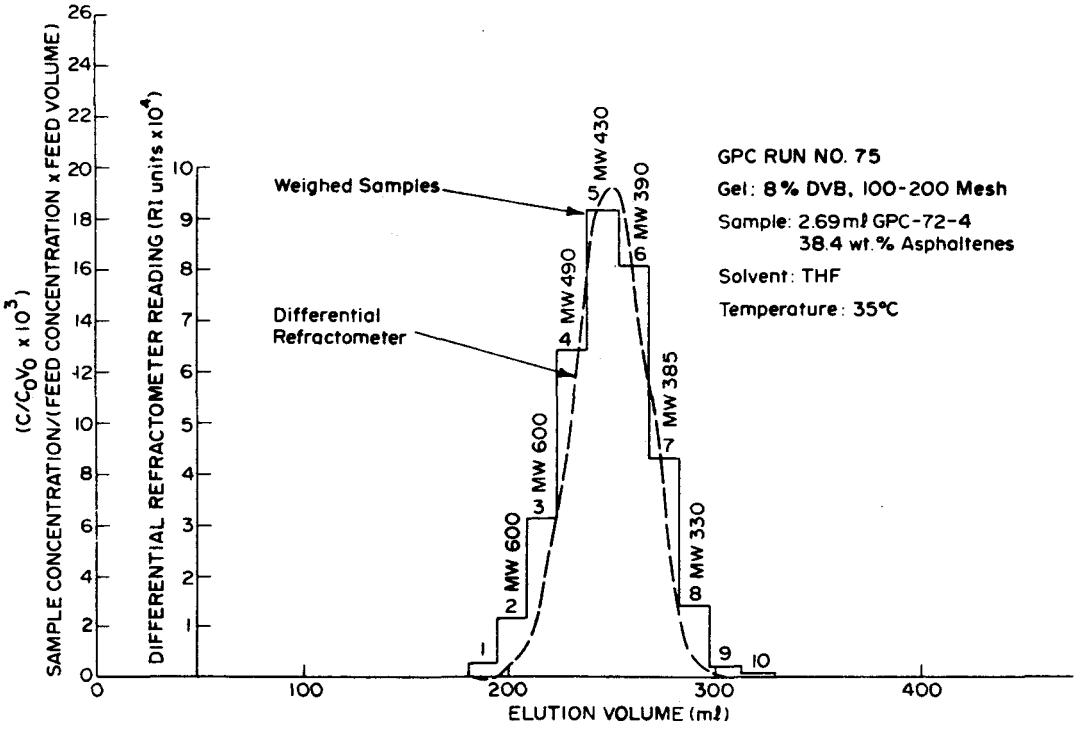

Figure 7. GPC Fractionation of Fraction GPC-72-4 in 25-mm x 100-cm Long Column.

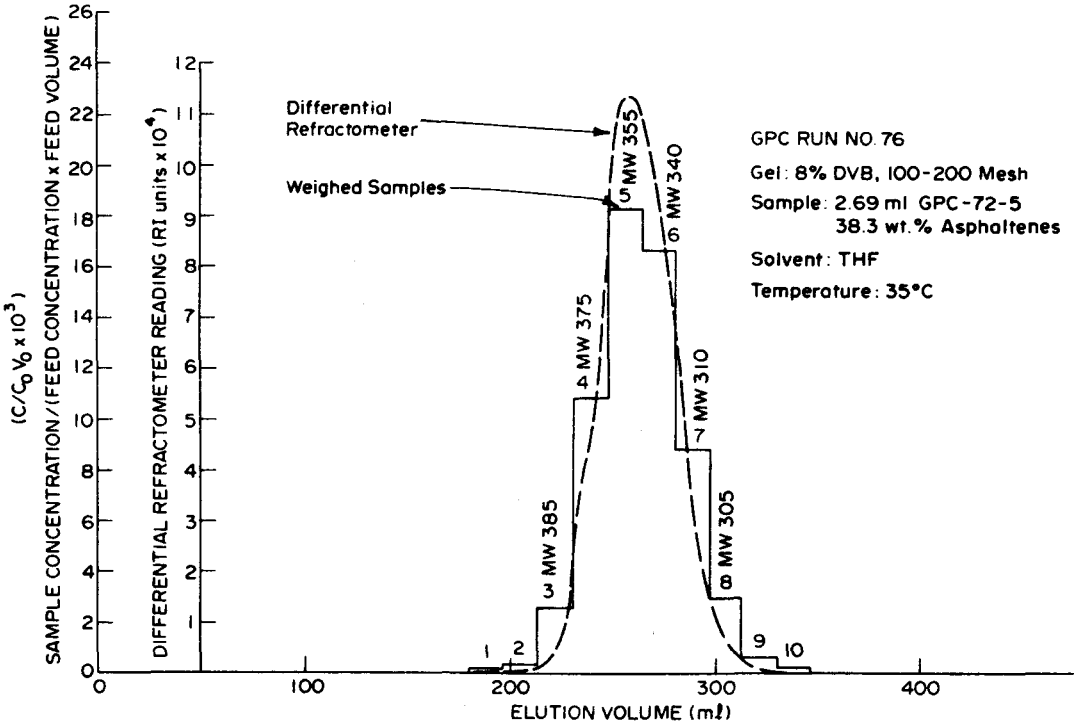

Figure 8. GPC Fractionation of Fraction GPC-72-5 in 25-mm ID x 100-cm Long Column.

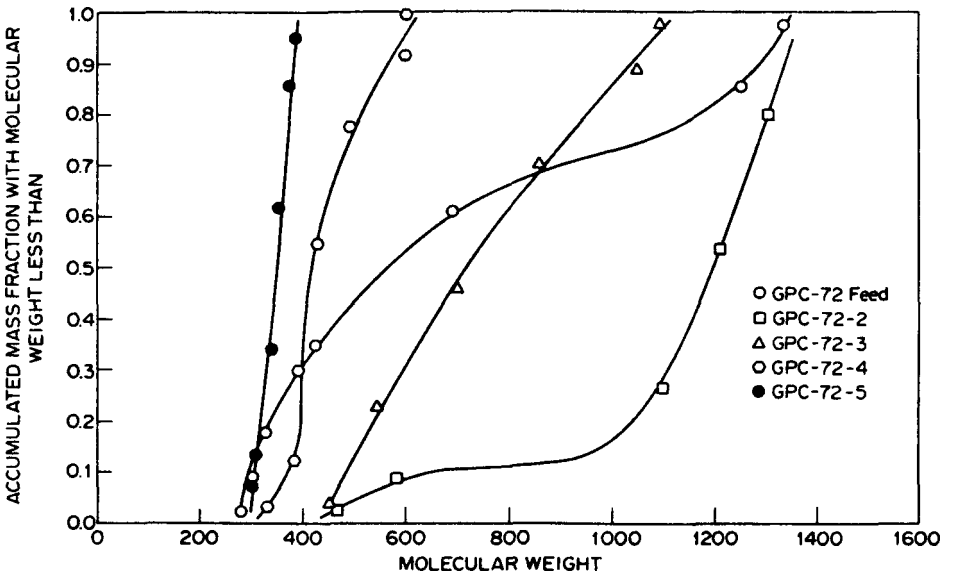

Figure 9. Molecular Weight of Fractions from GPC Run No. 72 and the Distribution of Molecular Weights in Fractions GPC-72-2 Through GPC-72-5 from GPC Run No. 73-76.

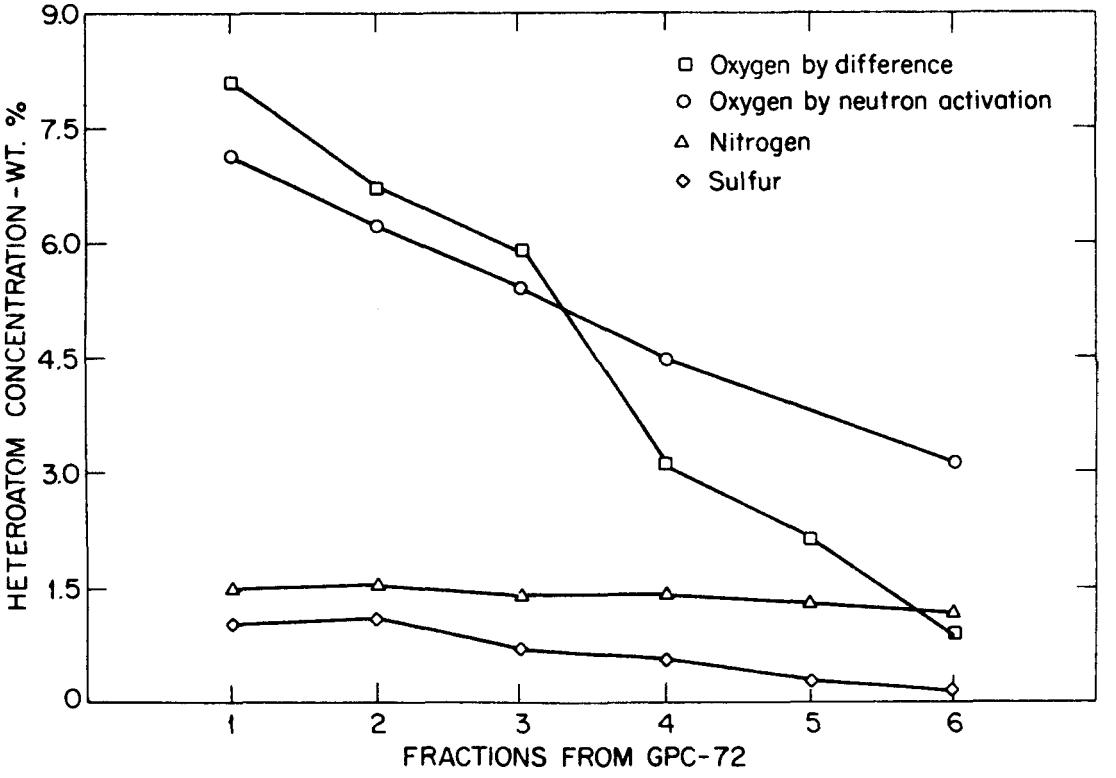

Figure 10. Heteroatom Content of GPC Fractions from Fractionation of Asphaltenes from Hydrocarbon Research, Inc., H-Coal Vacuum Bottoms from an Illinois No. 6, River King Mine Coal.

to 600. Fraction GPC-72-3 shows an even wider range, 455 to 1090, but nearly linear on this type plot. Fraction GPC-72-2 shows over 80% of its mass having a molecular weight over 1000 but strangely has about 10% of its mass being below 600.

Elemental analyses were made on the first six of the seven samples of GPC-72, GPC-72-1 through GPC-72-6. Elemental analyses for carbon, hydrogen, nitrogen, and sulfur were done by Spang Microanalytical Laboratory, Ann Arbor, Michigan. In addition, a preasphaltene fraction, Extract 60(4), (THF-soluble/toluene-insoluble) used in the adsorption work, was also analyzed. These results are presented in Table 5. The oxygen content of these samples was determined independently by neutron activation analysis. Proton nuclear magnetic resonance (PNMR) examinations of the samples were done with a Varian T-60 and T-60A Nuclear Magnetic Resonance Spectrometer. Table 5 gives the results of the PNMR for each fraction as the ratio of the aliphatic hydrogen to aromatic hydrogen present.

Figure 10 graphically shows the percent heteroatoms for the GPC fractions which are in order of decreasing molecular weight. The oxygen content decreases with decreasing molecular weight and in general the oxygen content by difference and oxygen content by neutron activation agree fairly well. The sulfur content decreases to a very low value at low molecular weights while the nitrogen content decreases only slightly. In general the heteroatoms in the material decrease by a factor of almost three going from a molecular weight of over 1000 to a molecular weight of about 300. The aliphatic hydrogen to aromatic hydrogen ratio decreases steadily from the first fraction to the last.

3. Neutron Activation Analysis for Metals
(U. Sen Gupta and J. D. Jones)

Neutron activation was used to measure the metals content of liquefied coal samples used in the experimental program. The analysis was done by two separate procedures, for metals with short half-lives and those with long half-lives (days). For short half-life metals, Na, K, Ca, Mg, Mn, Aℓ, Ti, and V, each sample was irradiated in polyethylene tubes for five minutes and the activity counted for 300 seconds after a wait time of 12 minutes. For metals with long half-lives, Fe, Cr, Ni, Zn, Co, As, Sb, and others, the samples in quartz tubes were irradiated together in a pool for 20 hours. Because of the high radioactivity of the long half-life metals, several weeks had to pass before the samples could be handled for analysis. The samples are currently being analyzed and the results will be reported in a later report.

Results for the short half-life metals from the GPC fractions are presented in Tables 6 and 7. Because of interference from certain metals, absolute quantities for some metals such as potassium, magnesium, and calcium could not be reported in all cases. Where numbers are reported as "less than", the values represent the lowest levels which can be detected because of interference from other radioactive materials.

Table 5. Analysis of Asphaltenes (Toluene Soluble, 75%-Pentane/25%-Toluene-Insoluble) and Preasphaltenes from Hydrocarbon Research, Inc., H-Coal Vacuum Bottoms from an Illinois No. 6, River King Mine Coal.

Fraction	Weight %	Mol. Wt(a)	Weight Percent						Atoms in Average Molecule (d)					$\frac{H_{al}(e)}{H_{ar}}$
			C	H	N	S	O(b)	O(c)	C	H	N	S	O	
Asphaltenes														
GPC-72-1	5.5	1335	82.92	6.49	1.47	1.03	8.09	7.13	92.25	86.64	1.40	.43	6.75	4.6
GPC-72-2	18.7	1250	83.90	6.78	1.51	1.08	6.73	6.22	87.40	84.75	1.35	.42	5.26	3.2
GPC-72-2B(f)		1100	85.32	6.01	1.66	1.06	5.95	4.81	72.81	66.11	1.30	.36	4.09	...
GPC-72-3	29.5	690	85.00	6.99	1.39	0.70	5.92	5.40	48.87	48.23	.69	.15	2.55	2.8
GPC-72-4	23.1	425	87.74	7.19	1.39	0.56	3.12	4.48	31.07	30.56	.42	.07	.83	2.4
GPC-72-5	10.9	330	89.37	6.95	1.29	0.25	2.14	...	24.58	22.94	.30	.026	.44	2.1
GPC-72-6	7.3	305	91.12	6.70	1.17	0.14	0.87	3.15	23.16	20.44	.25	.013	.17	1.9
GPC-72-7	5.0	280	...	...	...	...	...	3.17	...	...	...	...	...	1.6
	100.00													
Preasphaltenes														
Ext. 60(4)		980	83.97	6.19	1.73	1.03	7.08	4.68	68.58	60.66	1.21	.32	4.34	1.8

(a) Number average molecular weight from vapor pressure oxmometry in pyridine at 75°C.

(b) Determined by subtracting the weight percent of other elements from 100.

(c) Measured by neutron activation.

(d) Based on oxygen from difference.

(e) From proton NMR

(f) Fraction GPC-72-2B was the fraction of GPC-72-2 which was insoluble in tetralin.

Table 6. Concentrations of a Number of Metals in Liquefied Coal Extracts of Hydrocarbon Research, Inc. H-Coal Vacuum Bottoms from an Illinois No. 6, River King Mine Coal and U.S. Bureau of Mines Synthoil Centrifuge Residue from a Pittsburgh Seam, Ireland Mine Coal.

Extract or Sample	Vacuum Bottoms	Centrifuge Product	Centrifuge Residue	Pentane Soluble		Pentane Insoluble 75% Pentane-25% Toluene Soluble		75% Pentane-25% Toluene Insoluble Toluene Soluble		Toluene Insoluble THF Soluble		THF Insoluble Cake
Source Extract No.	H-Coal	Synthoil	Synthoil	H-Coal 61(1)	Synthoil 27(1)	H-Coal 61(2)	Synthoil 27(2)	H-Coal 61(3)	Synthoil 27(3)	H-Coal 61(4)	Synthoil 27(4)	H-Coal 60(4)
Metals (ppm)(a)												
Na	---	---	---	45.2	64.3	69.1	237.0	119.1	58.2	2461.2	80	---
K	---	---	---	<34.9	<66.6	<99.8	<195.5	157.4	88.4	<1331.7	<215.4	---
Mg	2258.3	240.1	2921.9	<11.7	34.4	<26.7	<71.7	63.5	<28.0	<259.8	<54.4	6075.0
Ca	8666.7	1053.1	4090.9	<4.1	<12.2	9.9	21.8	16.1	10.8	232.4	36.6	24413.4
Al	21326.9	2320.5	39767.1	54.3	<47.9	455.3	340.1	236.1	102.3	15088.4	415.8	143185.0
Mn	177.2	5.97	69.9	2.8	2.5	2.8	15.4	11.0	9.4	457.0	20.1	513.5
Ti	1089.3	116.7	1258.6	<1.5	4.4	4.5	<9.7	22.6	27.7	398.8	123.6	3169.6
V	54.7	3.42	96.6	<0.12	0.21	1.58	<0.59	7.1	0.33	83.2	1.22	151.1

(a) Values for K, Mg, Ca, Ti and V shown as "less than" indicated values are the upper limits of those metals for the analysis and therefore do not represent precise measurements. This is due to interference and lack of sensitivity.

Table 7. Analysis of Asphaltenes (Toluene-Soluble, 75%-Pentane/25%-Toluene-Insoluble) and Preasphaltenes from Hydrocarbon Research, Inc., H-Coal Vacuum Bottoms from an Illinois No. 6, River King Mine Coal.

Fraction	Weight %	Mol. Wt(a)	Weight Present						Metals (parts per million)(c) (d)							
			C	H	N	S	O(b)	O(c)	Na	K	Mg	Ca	Aℓ	Mn	Ti	V
Asphaltenes Ext. 61(3)									119.1	157.4	63.5	16.1	236.1	11.0	22.6	7.1
GPC-72-1	5.5	1335	82.92	6.49	1.47	1.03	8.09	7.13	39.0	<565.6	<180.7	<41.8	30.0	7.2	52.7	1.3
GPC-72-2	18.7	1250	83.90	6.78	1.51	1.08	6.73	6.22	22.5	<333.7	<130.6	<24.9	24.6	3.7	43.1	1.0
GPC-72-3	29.5	690	85.00	6.99	1.39	0.70	5.92	5.40	15.0	<209.4	<87.6	<23.0	8.5	1.1	16.2	0.38
GPC-72-4	23.1	425	87.74	7.19	1.39	0.56	3.12	4.48	15.7	<231.0	<108.4	<51.7	10.0	0.4	<9.9	0.42
GPC-72-5	10.9	330	89.37	6.95	1.29	0.25	2.14	...	...	...	...	...	...	...	...	...
GPC-72-6	7.3	305	91.12	6.70	1.17	0.14	0.87	3.15	16.5	<189.4	<70.4	<17.3	7.3	<0.3	<8.0	0.11
GPC-72-7	5.0	280	...	...	...	...	...	3.17	18.3	<164.0	<73.1	<18.0	10.9	0.3	<7.3	<.03
	100.0															
Preasphaltenes Ext. 60(4)		980	83.97	6.19	1.73	1.03	7.08	4.68								
Ext. 61(4)									2461.2	<1331.7	<259.8	232.4	15088.4	457.0	398.8	83.2

(a) Number average molecular weight from vapor pressure osmometry in pyridine at 75°C.

(b) Determined by subtracting the weight percent of other elements from 100.

(c) Measured by neutron activation.

(d) Values for K, Mg, Ca, Ti and V shown as "less than" indicated-values are the upper limits of those metals for the analysis and therefore do not represent precise measurements. This is due to interference and lack of sensitivity.

Table 6 contains the concentrations of some short half-life metals in various extracts of liquefied coal material from Hydrocarbon Research, Inc., H-Coal Vacuum Bottoms from an Illinois No. 6, River King Mine Coal and from U.S. Bureau of Mines Synthoil Centrifuge Residue from a Pittsburgh Seam, Ireland Mine Coal. The metals in the extracts can exist as organo-metallic compounds, as submicron sized mineral particles associated with organic molecules or as very very small mineral particles which pass through the filter cake and filter paper used to separate the mineral solids from the extract. In the case of Extract 61(4), the high metal concentrations may be caused by poor initial filtration. The analysis is being repeated on a refiltered sample of the extract.

As expected there is a higher concentration of metals in the higher molecular weight fractions. These fractions also contain the highest levels of heteroatoms which contribute to metal complexes and chelates.

The levels of metals in the GPC fractions are much less than the material from which they originated. A large fraction of the metals are either filtered out or excluded in the GPC separation. This effect can be seen when the levels for sodium, aluminum, manganese and vanadium in Extract 61(3), Table 7, are compared to GPC fractions 72-1 to 72-7. It can also be seen that the degree of reduction is not the same for each element. In fact there is an increase in the titanium levels in GPC fractions 72-1 and 72-2 above that in Extract 61(3). This suggests the existance of titanium complexes.

The data in Table 6 were examined to check the material balance on the metals between starting residue and the individual extracts and to assess the relative enrichments of metals in the individual extracts. The results are given in Tables 8 and 9. As seen in Table 8 there is good agreement between the calculated H-Coal residue based on the weight fraction of extract with the metals concentrations and the H-Coal vacuum bottoms residue. The level of aluminum in the H-Coal vacuum bottoms residue appears to be low by a factor of two when compared to the ratios of aluminum to calcium in the Cake 61(4) and Illinois No. 6 Coal.

There appears to be less interaction between calcium and the liquefied coal extracts than for the other metals as seen in Table 8. Walker et al., found that calcium accumulates as calcium carbonate and is usually found with larger particles in the residue.[3] Consequently, the levels of other metals were ratioed to calcium to determine apparent enrichment of metals in various extracts. The results are tabulated in Table 9. At this point, it is not known whether the enrichment is due to metal complexes or to the extremely small size of certain mineral particles. In either case, enrichment in the asphaltene and preasphaltene fractions, Extracts 61(3) and 61(4), would be expected.

4. Determination of Oxygen in Coal and Coal-Derived Materials (U. Sen Gupta and J. D. Jones)

There is no standard procedure for the determination of oxygen in organic compounds. The Schutze-Unterzaucher method and some of its modifications are widely used.[4] Oxygen in a sample is thermally decom-

Table 8. Concentrations of a Number of Metals in Liquefied Coal Extracts of Hydrocarbon Research Inc., H-Coal Vacuum Bottoms from an Illinois No. 6, River King Mine Coal.

	Wt% Extract in Residue	Aluminum		Calcium		Magnesium	
		PPM in Sample	Distribution in Samples %	PPM in Sample	Distribution in Samples %	PPM in Sample	Distribution in Samples %
H-Coal Vacuum Bottoms Residue		21329.9		8666.7		2258.3	
Extract 61(1)	31.25	54.3	0.035	4.1	0.016	11.7*	0.179
Extract 61(2)	12.60	455.3	0.118	9.9	0.015	26.7*	0.165
Extract 61(3)	13.80	236.1	0.067	16.1	0.028	63.5	0.430
Extract 61(4)	9.45	15088.4	2.931	232.4	0.273	259.8*	1.204
Cake 61(4)	32.90 / 100.00	143185.0	96.849 / 100.000	24413.4	99.670 / 100.000	6075.0	98.022 / 100.000
Calculated H-Coal Residue Based on Extract Values and Weight Fractions		48640.6		8058.6		2039.0	

	Wt% Extract in Residue	Manganese		Titanium		Vanadium	
		PPM in Sample	Distribution in Samples %	PPM in Sample	Distribution in Samples %	PPM in Sample	Distribution in Samples %
H-Coal Vacuum Bottoms Residue		177.2		1089.3		54.70	
Extract 61(1)	31.25	2.8	0.407	1.5*	0.043	0.12*	0.064
Extract 61(2)	12.60	2.8	0.164	4.5	0.052	1.58	0.338
Extract 61(3)	13.80	11.0	0.706	22.6	0.288	7.10	1.666
Extract 61(4)	9.45	457.0	20.099	398.8	3.475	83.20	13.367
Cake 61(4)	32.90 / 100.00	513.5	78.625	3169.6	96.146 / 100.000	151.20	84.571 / 100.000
Calculated H-Coal Residue Based on Extract Values and Weight Fractions		214.87		1084.6		58.82	

*Due to measurement sensitivity, the reported values are the maximum concentrations of the elements and not necessarily the actual concentrations.

Table 9. Concentrations and Enrichments of a Number of Metals in Liquefied Coal Extracts of Hydrocarbon Research Inc., H-Coal Vacuum Bottoms from an Illinois No. 6 River King Mine Coal.

H-Coal	Residue	Wt. Ratio of Element to Calcium in Sample					
		Residue	61(1)	61(2)	61(3)	64(4)	Cake
	ppm						
Aluminum	21329.9	2.4611	13.2439	45.9899	14.6646	937.1670	5.8650
Calcium	8666.7	1.0000	1.0000	1.0000	1.0000	1.0000	1.0000
Magnesium	2258.3	0.2606	2.8537	2.6970	3.9441	16.1366	0.2488
Manganese	177.2	0.0204	0.6829	0.2828	0.6832	28.3851	0.0210
Sodium	*	*	11.0	6.9798	7.3975	152.8696	*
Titanium	1089.3	0.1257	0.3659	0.4545	1.4037	24.7702	0.1298
Vanadium	54.70	0.0063	0.0292	0.1596	0.4410	5.1677	0.0062
	Wt. Ratio Element to Calcium in Coal Ash**		Wt. Ratio of Element to Calcium in Sample / Wt. Ratio of Element to Calcium in Residue				
Aluminum	5.1837		5.381	18.686	5.958	380.791	2.383
Calcium	1.000		1.000	1.000	1.000	1.000	1.000
Magnesium	0.2178		10.950	10.349	15.135	61.921	0.955
Manganese	-		33.475	13.863	33.490	1391.426	1.029
Sodium	0.4353						
Titanium	0.3247		2.911	3.616	11.167	197.058	1.033
Vanadium	-		4.634	25.333	70.000	820,270	0.984

*Not Measured

**Mineral Analysis of Ash, Wt% (Monterey No. 1 Coal, Illinois No. 6 Seam)

Sodium Oxide, Na_2O	1.3
Potassium oxide, K_2O	1.8
Lime, CaO	3.1
Magnesia, MgO	0.8
Ferric Oxide, Fe_2O_3	18.2
Titania, TiO_2	1.2
Phosphorous pentoxide, P_2O_5	0.3
Silica, SiO_2	47.3
Alumina, Al_2O_3	21.7
Sulfur trioxide	4.1
Undetermined	0.2
	100.0

posed in a stream of nitrogen and passed over carbon at 1000-1120°C to form CO which is determined by treatment with I_2O_5. The procedure is destructive of the sample but does give satisfactory accuracy and precision for determining total oxygen in samples. The procedure takes approximately one-half hour per sample. A common convention is to determine oxygen by difference from measured values of carbon, hydrogen, nitrogen, and sulfur in a sample.

Neutron activation analysis has been found to be a versatile and accurate non-destructive method for oxygen determination. For coal liquids, where the oxygen content may range from 1 to 10% by weight, 100-300 mg of sample are required for adequate sensitivity.

a. Previous Work

Coleman and Perkin determined the oxygen content of beryllium metal by neutron activation.[5,6] Oxygen in the range of 0.01 to 2% was determined and as little as 0.001% oxygen detected. Veal and Cook described an oxygen analysis technique for compounds containing no boron.[7] An accuracy of ± 17% at an oxygen level of 1% was reported with a sensitivity of 0.032% oxygen. Steele and Meinke analyzed samples containing 10 mg or more of oxygen to within ± 10% accuracy with fast neutrons.[8]

b. Method

Oxygen occurs in nature as the three isotopes of mass numbers 16, 17, and 18. Only the isotope of mass 16 oxygen is present in sufficient abundance (99.76%) and is of importance for neutron activation analysis.

Fast neutrons (14 m.e.v.) are best suited for the oxygen determinations. Oxygen undergoes a (n,p) reaction

$$O^{16} + n + 9.62 \text{ m.e.v.} \rightarrow N^{16} + p$$

The threshold value for the reaction is 9.62 m.e.v. and consequently slow neutraons are unable to activate oxygen. Measurement of N^{16} radioactivity constitutes the basis of the method.

The radioactive product N^{16} has a half-life of 7.2 seconds and decays with the emission of beta-particles and γ-rays of predominately 6.1 and 7.1 m.e.v. energy. This combination of parameters makes the method for oxygen unique. The short half-life provides for rapid saturation during irradiation with 15-30 seconds being sufficient. On the other hand, counting must commence as soon as possible and at a known time after irradiation to maximize sensitivity and accuracy of the method.

Scintillation crystals were used as detectors in the early measurements of oxygen via the (n,p) reaction. Unfortunately, the crystal detectors do not provide sufficient discrimination from other isotopes which can be produced by 14 m.e.v. neutrons. By using detectors which

respond to energies greater than 5 m.e.v., most of the radioactivity produced from other elements is eliminated. The method then becomes remarkably free from interferences except from fluorine which produces the same N^{16} isotope via a (n,α) reaction and from large quantities of boron and uranium. Although all these elements may occur in coal, they are generally not at levels where interference is a problem. Anders and Briden suggested that an energy window from 4.5 to 7.5 m.e.v. using a 7.6-cm wide x 7.6-cm high NaI crystal with a 1-cm thick plastic beta-shield be used as a detector.[9] This system absorbs beta particles and eliminates all γ-energy other than the 6.1 and 7.1 m.e.v. α-energy from N^{16}. This detector system is now accepted for oxygen determinations and avoids interferences from all elements except fluorine, boron and uranium.

c. Procedure

The general procedure is to compare the γ activity of samples with that from a known oxygen content sample irradiated and counted in the same identical way. Calibration curves are prepared for the measured activity of known irradiated oxygen compounds as a function of the mass of sample present for a given irradiation time and counting procedure.

Standard samples and samples to be analyzed were weighed and sealed in polyethylene vials before irradiation at the Phoenix Memorial Laboratory at the University of Michigan. Precaution must be taken to avoid direct hand contact with the vials and to prepare samples and to make measurements in a dry atmosphere. Coal liquids and especially asphaltene samples are difficult to handle because of their physical nature. Semi-solid samples were dissolved in a small quantity of THF and transferred to the vials and dried to constant weight before sealing.

d. Calibration

Water, sodium oxalate and oxalic acid contain large fractions of oxygen and were used as calibration compounds. Sodium oxalate and oxalic acid were found satisfactory and are recommended as standards for oxygen determinations. Three different masses of the two standards were irradiated and the γ activity counted in the same manner. An irradiation time of 15 seconds is sufficient. After irradiation, the vial is immediately transferred to the detector. Timing is critical for accuracy. An ND (Nuclear Data) 4420 model multichannel computer analyzer was used to measure the activity. The analyzer is programmed to count the γ activity over three successive 15 second periods to wait 25 seconds and to count the activity over a final 15 second period. The net count is taken as the difference between the counts during the first and last 15 second period.

Since the activity is a function of the neution flux, it is important to maintain a source of constant strength. The neutron flux was constant during the experiments and measured at 8.73×10^{11} neutrons/cm^2 sec.

Figures 11 and 12 give the counts over a 15 second interval plotted versus the time at the end of each counting period for different weights

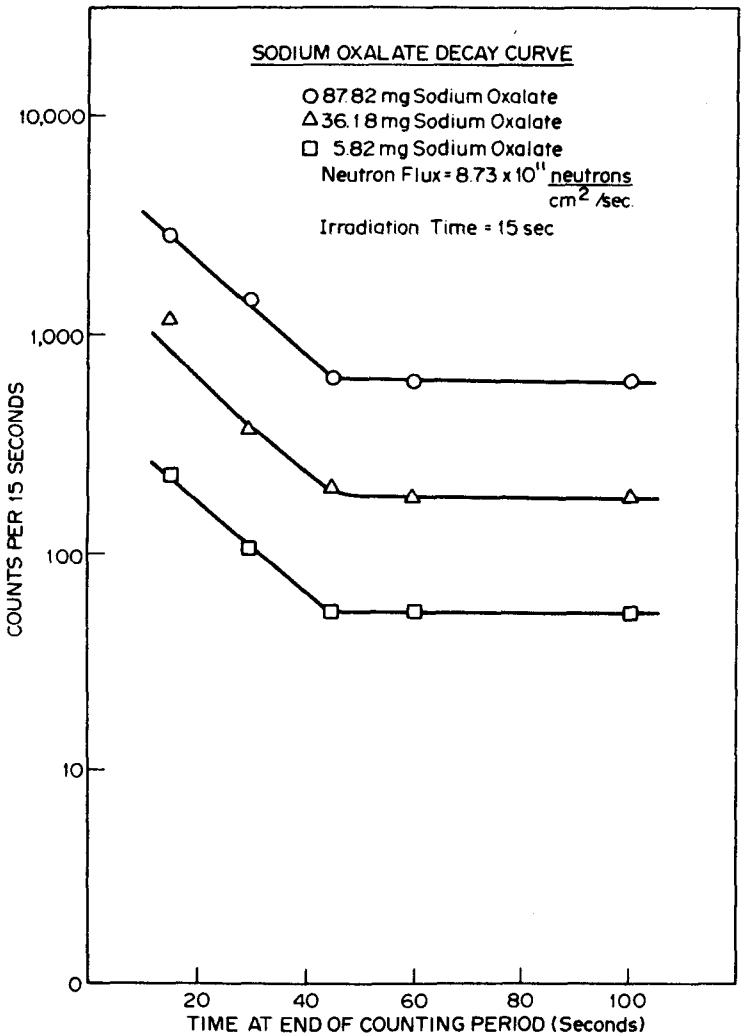

Figure 11. Radioactivity of Sodium Oxalate after Irradiation with Fast Neutrons.

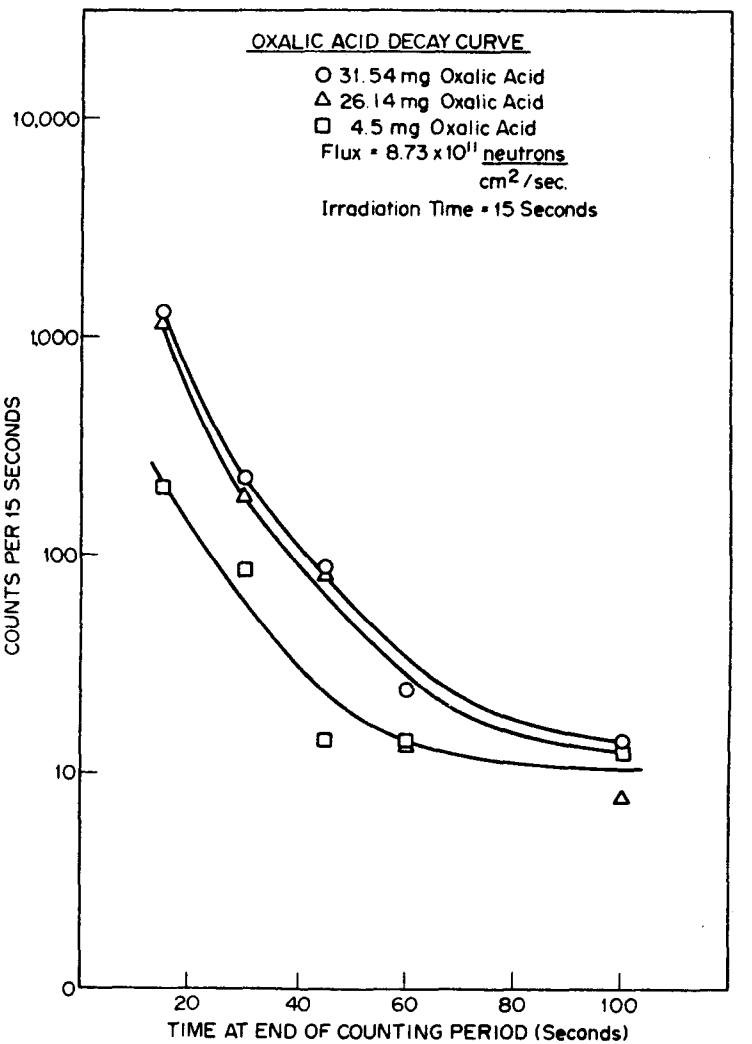

Figure 12. Radioactivity of Oxalic Acid after Irradiation with Fast Neutrons.

of sodium oxalate and oxalic acid, respectively. Figure 13 gives a cross plot of net counts as defined above versus the sample weights. From the three figures it is apparent that both irradiation and counting timing are critical to calibration and measurement accuracy. The net counts per mg oxygen from Figure 13 are:

	Net Counts/mg Oxygen 10-Second Irradiation	Net Counts/mg Oxygen 15-Second Irradiation
Oxalic Acid	55.18	85.78
Sodium Oxalate	55.56	82.88

These values can be used to determine the oxygen content of weighed irradiated samples.

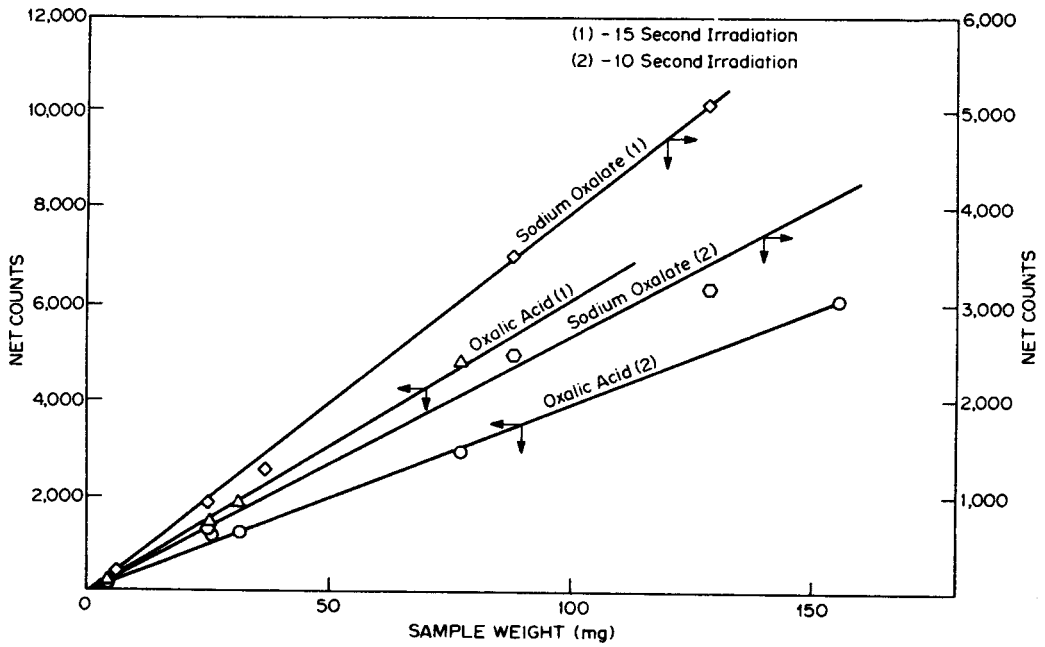

Figure 13. Calibration Curves for Sodium Oxalate and Oxalic Acid.

5. Acid-Base-Neutral Separations

A number of experiments were conducted during the year to assess different methods for separating asphaltenes and preasphaltenes into acidic, basic and neutral fractions. The acidic and basic fractions play a dominant role in the colloid behavior of liquefied coal. The individual efforts of the researchers are reported separately.

a. H-Coal Separations
(D. Greminger and J. A. McKeen)

Dry HCl gas was bubbled through a disposable pipette into a solution of Extract 41(3) asphaltenes and toluene. The HCl was generated from concentrated H_2SO_4 and NaCl in a standard gas generator. The reaction flask was vented into a beaker of water to absorb the excess HCl.

The reaction began immediately. A black solid precipitated on the side and bottom of the reaction flask. HCl addition was continued for two hours. Often HCl-nitrogen base adducts are gummy solids, but this precipitate was quite brittle. Some solids remained on the vessel walls and could not be scraped off.

Filtration of the precipitate was rapid. The precipitate was quite crystalline for asphaltene material and dried rapidly.

The toluene soluble portion after HCl addition had a blue-green color. After standing in a sealed jar for some time, solids deposited on the side of the jar.

The HCl-base adduct was neutralized with NaOH to recover the basic portion. A mixture of NaOH, HCl-base adduct, toluene, and water was dispersed for 1-1/2 hours in an ultrasonic bath. After 15 minutes, four layers were observed. The top layer was a dark brown toluene layer indicating that much of the basic asphaltenes was in the toluene solution. The next layer was a light brown floc layer. Below this was a darker brown frothy transitional zone between the floc and the cloudy white (due to NaOH) water phase on the bottom.

After standing five days, only three phases were left:

1. A dark brown toluene layer,
2. Light brown floc layer at the interface,
3. Pale yellow water phase.

The pale yellow color of the water phase means some of the nitrogen bases are water soluble to a small degree. The water was still basic as shown by a phenolphthalene indicator test.

The three phase mixture was then filtered. It was a slow process. The mixture was filtered before separating the organic and water phases to reduce the handling of the floc which again clung to the glassware. The amount of floc was small, not enough to readily measure. Samples of the toluene-base solution and the toluene-acid-neutral solution were vacuum dried to determine the solution concentrations.

The results for two experiments are presented in Figures 14 and 15. In the first run a considerable amount of toluene insoluble material remained after the first NaOH neutralization and toluene addition. After separation of the toluene phase, the aqueous phase, containing the residual solid material, was concentrated by evaporation. The NaOH neutralization and toluene addition were repeated yielding a second portion of

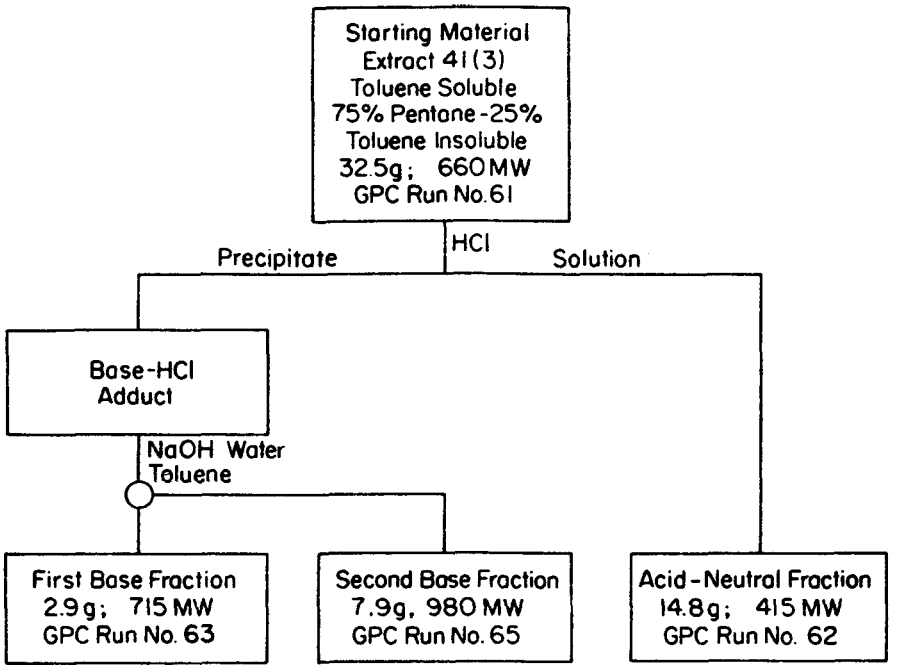

Figure 14. Run 1, Acid-Base Separation of Toluene Soluble, 75%-Pentane/25%-Toluene-Insoluble, Extract 41(3), Hydrocarbon Research, Inc., H-Coal Vacuum Bottoms from Illinois No. 6, River King Mine Coal.

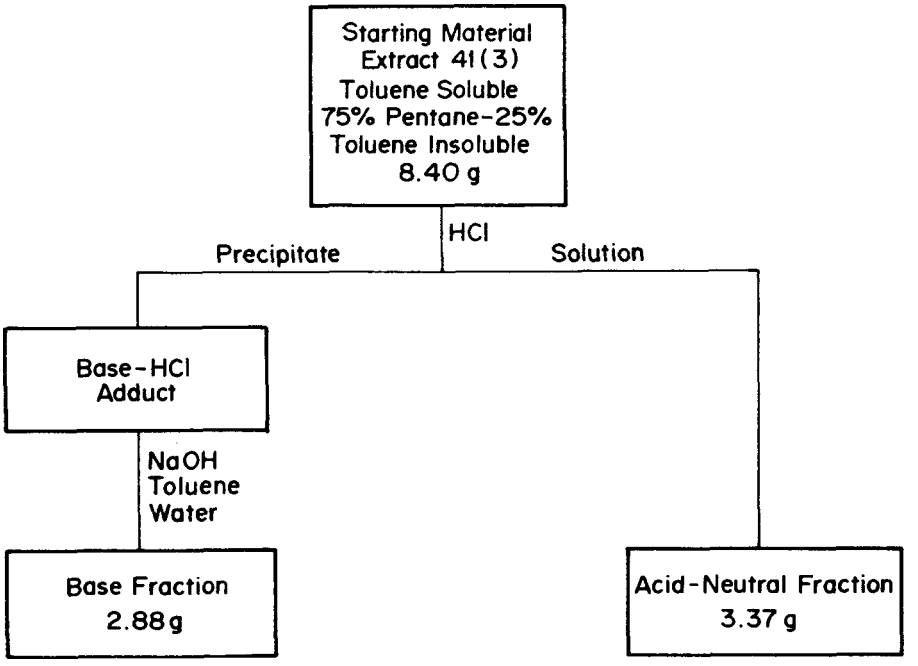

Figure 15. Run 2, Acid-Base Separation of Toluene Soluble, 75%-Pentane/25%-Toluene-Insoluble, Extract 41(3), Hydrocarbon Research, Inc., H-Coal Vacuum Bottoms from Illinois No. 6, River King Mine Coal.

toluene soluble bases. The two portions were analyzed separately. After the second toluene addition a small amount of toluene insoluble material remained. The starting material, the acidic-neutral fraction and the two basic fractions were fractionated by GPC. The results are given in Figure 16.

The mass losses in the two experiments were 21 and 25%, respectively. The procedure has potential for a preparative scale acid-base separations, but additional refinement is necessary to account for and to control mass losses.

One problem was discovered; when drying HCl containing samples in a vacuum oven, care should be taken to keep the samples separate from pyridine solvent samples as pyridine hydrochloride will form in the oven.

An experiment was conducted to determine if HCl could disrupt the hydrogen bonding between the acid-base pairs of toluene insoluble preasphaltenes, Extract 41(4), in toluene and render some material soluble. The basic components would form an HCl adduct and precipitate while the acidic and neutral portions would become solubilized.

Dry HCl was added as before to an ultrasonically dispersed toluene suspension of preasphaltenes for a period of 1-1/2 hours. The suspension settled to give a blue green solution, as opposed to a brown opaque solution with asphaltenes. The precipitate on the bottom was black. The precipitate did not adhere to the walls and filtered without problems. About 4% of the preasphaltenes were made soluble by this procedure.

An experiment was conducted to determine if acid-base separation of asphaltenes could be obtained by making the nitrogen bases water soluble as a citric acid adduct.

100 ml of toluene-asphaltene solution was extracted three times with 100 ml of 0.5M aqueous citric acid solution. In each case a brown floc formed almost immediately. Initially the solids were in the water phase, but upon standing migrated to the water-toluene interface. The solids were not toluene soluble but seemed to prefer the organic phase. It was easy to separate the solids from the water phase, but no definite interface existed between the floc and the toluene solution.

During all the separations, the solids accumulated on the separatory funnel sides as a scum.

The water phase was a light straw color, indicating that very little of the bases present had been made water soluble. No concentration measurements were attempted as the concentrations would be too low to leave a measureable mass when dried.

The floc-organic phase was then filtered. The filtrate was solids free, but filtration was slow. The floc compressed greatly, leaving a thin almost impervious layer on the filter paper. Not enough solids were present to be removed from the filter paper and measured.

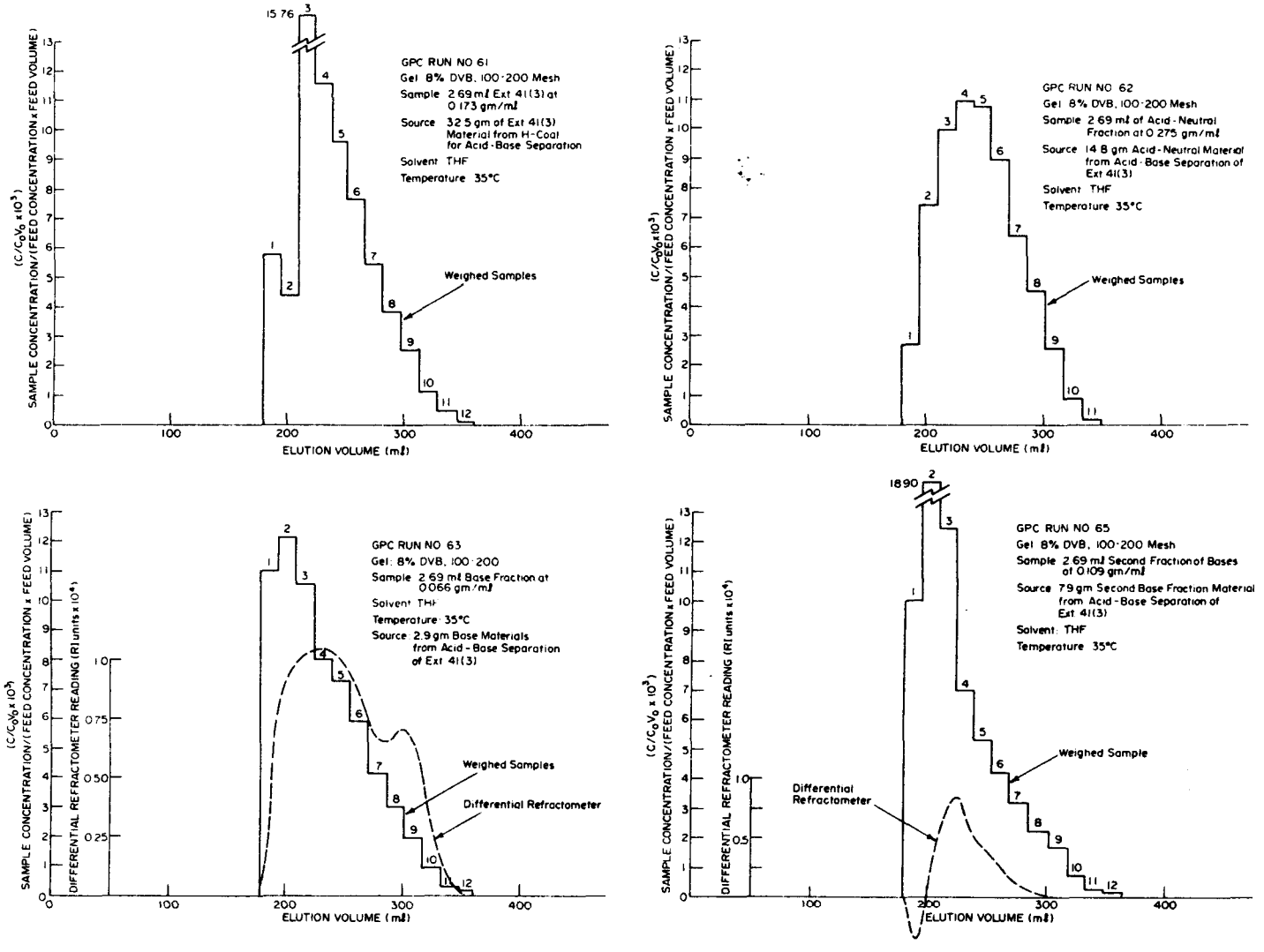

Figure 16. Comparison of GPC Fractionated Samples of the Starting Material, the Basic Fractions and the Acid-Neutral Fraction from the Acid-Base Separation of Toluene Soluble, 75%-Pentane/25%-Toluene-Insoluble Extract, Ext. 41(3), Hydrocarbon Research Inc., H-Coal Vacuum Bottoms from Illinois No. 6, River King Mine Coal - Run 1.

Citric acid extraction of nitrogen bases is not an effective means of separation.

Methods and techniques to effectively separate asphaltenes and preasphaltenes into their acidic and basic components will be sought. It is particularly important for the preasphaltenes because they contain a higher amount of heteroatoms which contribute to intermolecular association and to adsorption on solid surfaces present. Burk has used methyl iodide to form base adducts of THF soluble preasphaltenes.[10] Although it is difficult to reverse the process and recover the basic portion, this technique may be useful for preparative scale separations.

b. SYNTHOIL Separations
(L. Moore)

Benzene solutions of oils, resins, and asphaltenes were prepared by stirring solids from the U.S. Bureau of Mines SYNTHOIL process with refluxing benzene for a period of twenty-four hours. Benzene-insoluble materials were removed by filtration prior to chemical manipulations. Hydrogen chloride gas was bubbled through the filtered benzene solution yielding a tar-like precipitate, following the general procedure of Schweighardt and coworkers.[11] Bubbling was continued until there was no evidence of further precipitate formation.

The precipitate was collected on a glass frit, and washed with several portions of benzene. It was then freed of HCl by shaking with an excess of dilute sodium hydroxide solution. The basic solution was extracted with benzene and the benzene extract dried over anhydrous sodium sulfate. The solvent was removed by rotary-evaporator, yielding a brown, viscous oil.

The material that had remained in benzene after treatment with HCl was further extracted with several portions of distilled water. The aqueous extracts were found to be slightly acidic. These were rendered basic and extracted as previously described. The solvent was removed, yielding an amber oil. Following the water extraction, the benzene solution was extracted with 25% sodium hydroxide. The sodium hydroxide extract was acidified with dilute hydrochloric acid. The solution was extracted with benzene and the extract dried over potassium carbonate. The solvent was removed, yielding a dark brown oil with the distinctive odor of phenol. The benzene solution was washed with small portions of water to remove residual sodium hydroxide. The solution was dried over anhydrous sodium sulfate and then stripped of solvent. The remaining oil was extracted with hexane. A small portion of the oil remained insoluble, however. To this, carbon tetrachloride was added yielding a carbon tetrachloride-soluble fraction and an insoluble solid. Acid, basic and neutral fractions were further treated with glacial acetic acid after their separation into solubility classes. Acetic acid extracts were neutralized with sodium hydroxide and extracted with benzene. These extracts were washed with water and dried over anhydrous sodium sulfate. A total of thirteen fractions were collected. A flow diagram summarizing the extraction sequence is presented in Table 10.

Table 10. Extraction Sequence for Separating Benzene Soluble Centrifuge Residue from the U.S. Bureau of Mines SYNTHOIL Liquefaction of Pittsburgh Seam, Ireland Mine Coal into Acidic, Basic and Neutral Fractions.

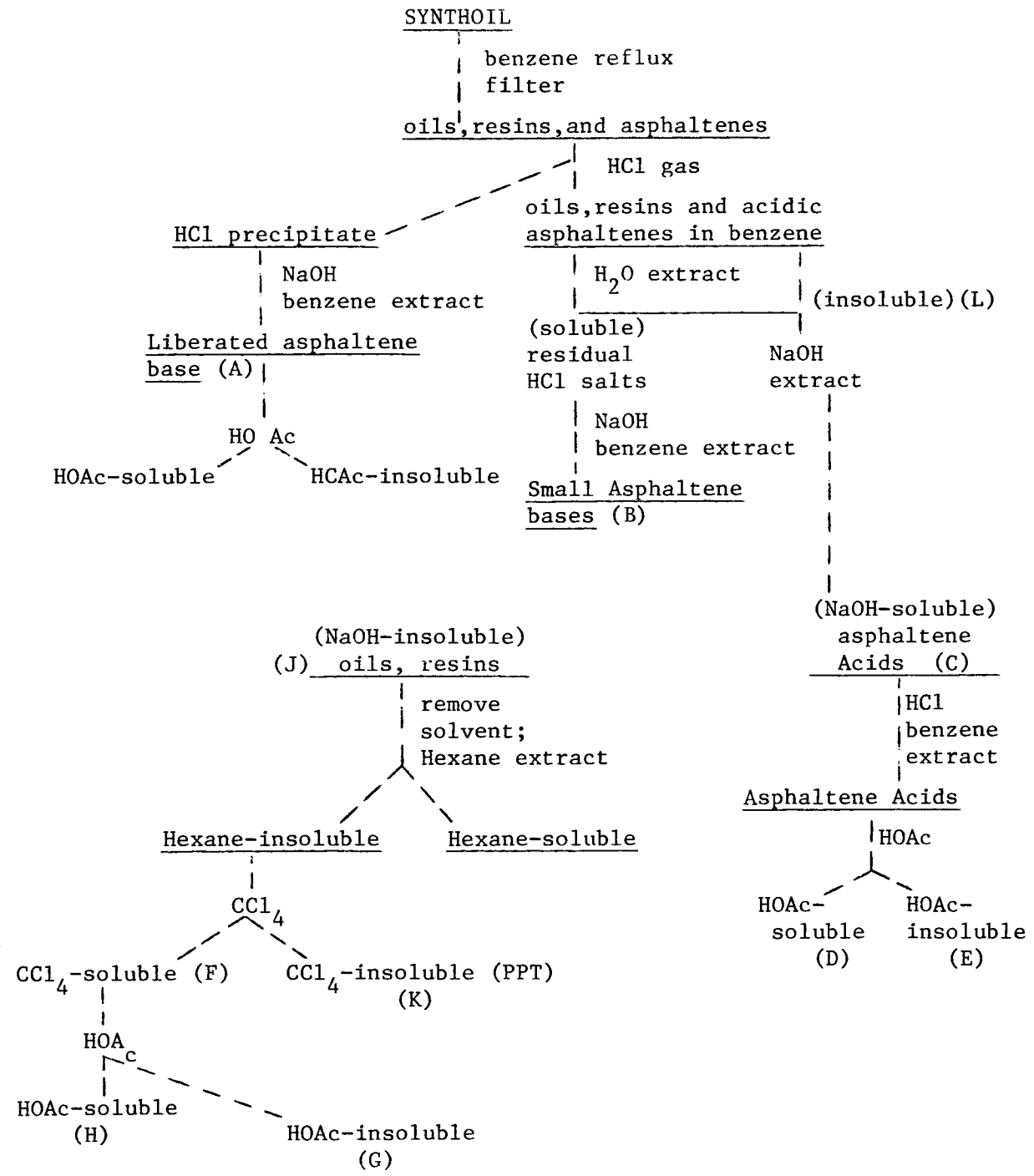

The chemical separation of oils, resins, and asphaltenes achieves a gross physical separation by chemical class. Acidic asphaltenes dissolve substantially in aqueous base, while asphaltene bases may be dissolved in suitable acids. Such separations will make the task of further analysis by complimentary methods much easier. For this reason chemical separation of coal derived materials stands as perhaps the most logical first step in the separation scheme.

Infrared and proton nuclear magnetic resonance studies of chemically separated oils, resins, and asphaltenes have been carried out. The IR spectra were obtained using a Perkin-Elmer model 237B spectrograph. ^{1}H NMR spectra were recorded using a Varian Associates T-60A spectrometer. The chemical shifts given for NMR results are in ppm relative to tetramethylsilane.

(1) Experimental: ^{1}H NMR

The ratios of aliphatic to aromatic protons and benzyl to alkyl protons were determined by ^{1}H NMR integration methods. The results are presented in Figures 17a-17ℓ and summarized in Table 11. Materials classed chemically neutral, e.g., oils and resins, were found to be relatively high in alkyl content but very low in aromatic and, consequently, benzyl hydrogen content. Chemical shifts indicative of functional groups, i.e., phenol OH, amine NH, etc. were not observed. These groups are either not present, as suggested by other experimenters, or in concentrations too dilute to be detected.[11] Unsaturation in these compounds also could not be confirmed, unambiguously, based on NMR results.

Asphaltene acids and bases were found to be much higher in aromatic, and benzylic hydrogen content than oils and resins. Surprisingly, the ratio of benzylic to alkyl protons for these compounds is greater than, or equal to, 1 on the average. For straight-chain alkyl benzenes this ratio is no greater than 0.66 (ignoring methylbenzenes). Alkyl benzenes, then, may be tentatively ruled out as possible asphaltene structures. Fused ring systems on the other hand, tend to have benzyl to alkyl ratios which are in the range of observed values. Added to the fact that fused ring systems are common among the constituents, or related petroleum nitrogen- and oxygen-containing compounds, similar structures for asphaltenes seem plausible.[12] Another possible explanation for benzylic/non-benzylic hydrogen ratios is the possible presence of α,ω-diarylalkane structures. A 1,4-diarylbutane, for example, would have a benzylic/non-benzylic ratio of 1.

(2) Infrared Spectra

Samples for infrared analysis were observed as neat, capillary films between sodium chloride plates.

Asphaltene acid fractions showed strong, broad bands at 3350 cm^{-1} (O-H stretch). The IR bands observed at 3030 and 2900 cm^{-1} suggest aromatic and aliphatic C-H stretch, respectively. The absence of carbonyl absorption in the 1695 to 1865 cm^{-1} region is good evidence that phenols, and not carboxylic acids, are responsible for the acidic properties of

Table 11. Summary ^{1}H NMR Results for the Acidic, Basic and Neutral Fractions from the Extraction Sequence.

Chemical Class	^{1}H NMR	R aliph/arom	R benz/alk
base	A	1.58	0.81
base	---	2.39	0.94
base	B	3.46	1.64
acid	C	2.04	1.12
acid	D	1.87	1.05
acid	E	2.39	0.77
neutral	F	3.14	0.47
neutral	G	3.64	0.60
neutral	H	3.52	0.53
neutral	I	2.87	---

Key To Spectra

^{1}H NMR Spectrum		Description
IR	NMR	
1	A	Neutralized HCl precipitate - asphaltene base
2	B	H_2O extract - small asphaltene bases
3	C	NaOH extract - asphaltene acids
4	D	Acetic acid extract of NaOH solubles
-	E	Acetic acid insolubles from NaOH extract
5	F	CCl_4 extract - neutral oils and resins
6	G	Acetic acid extract of CCl_4 solubles slightly soluble materials
-	H	Acetic acid extract of F. Very soluble materials
-	I	Acetic acid insolubles from F
7	J	Hexane extract - oils and resins
-	K	Solid precipitate - carbenes?
-	L	Benzene extract - original oils, resins, and asphaltenes after bases were precipitated

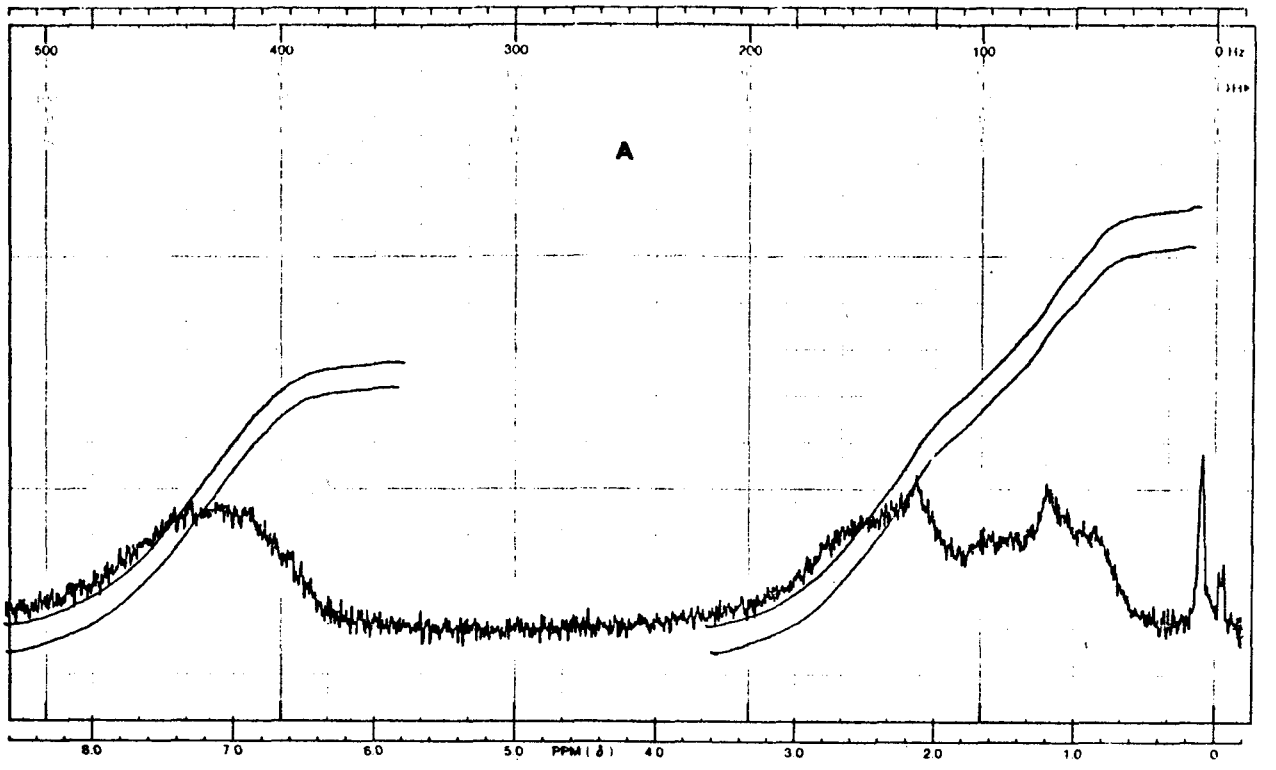

Figure 17a. ^{1}H NMR Results, Spectrum A.

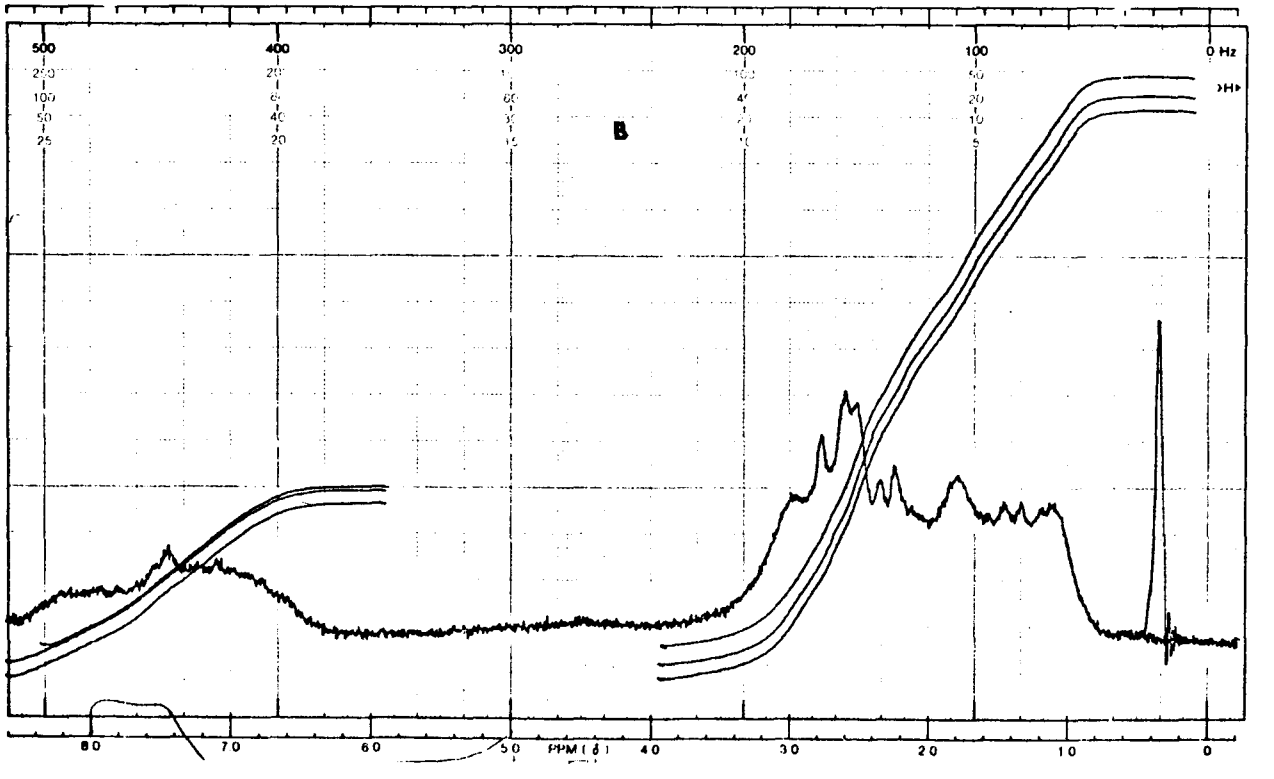

Figure 17b. ^{1}H NMR Results, Spectrum B.

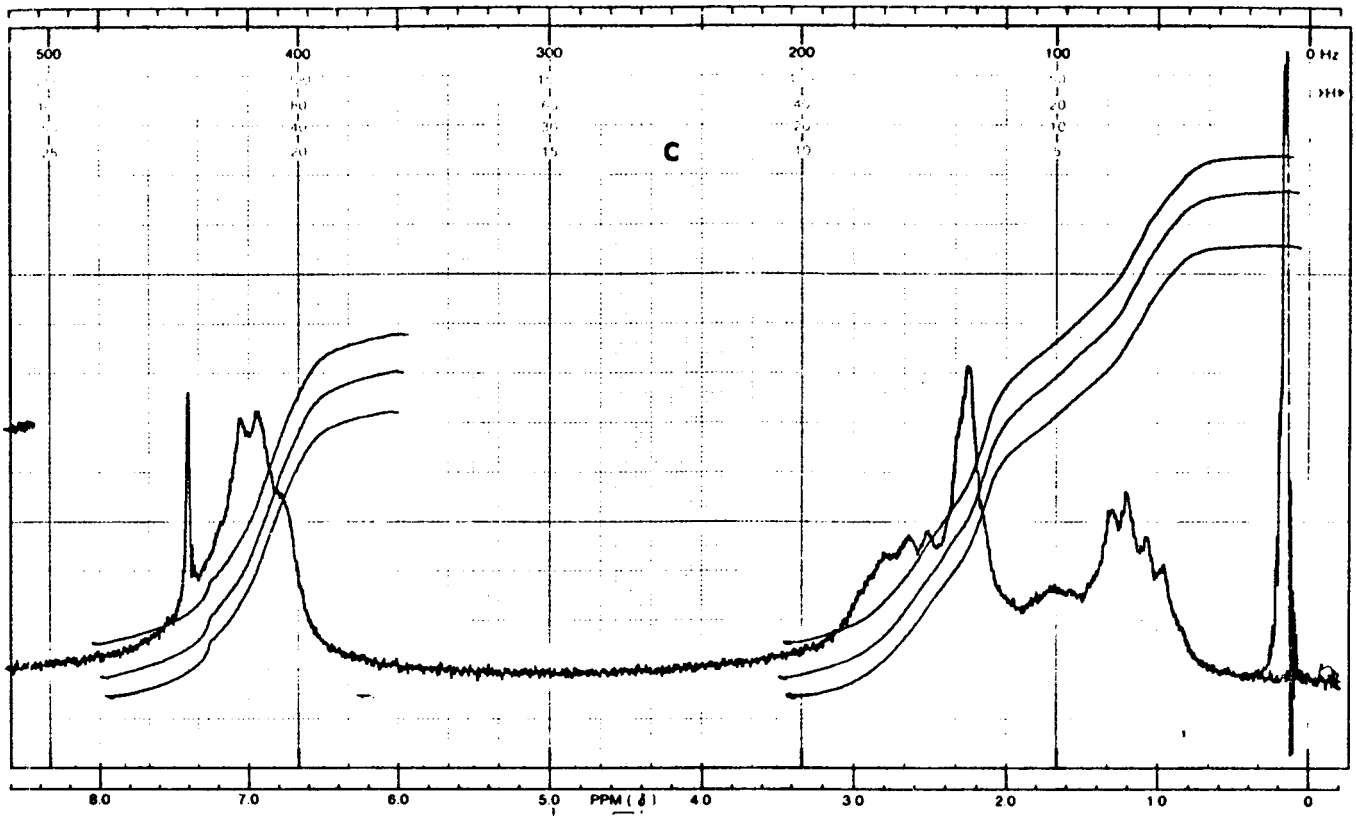

Figure 17c. ^{1}H NMR Results, Spectrum C.

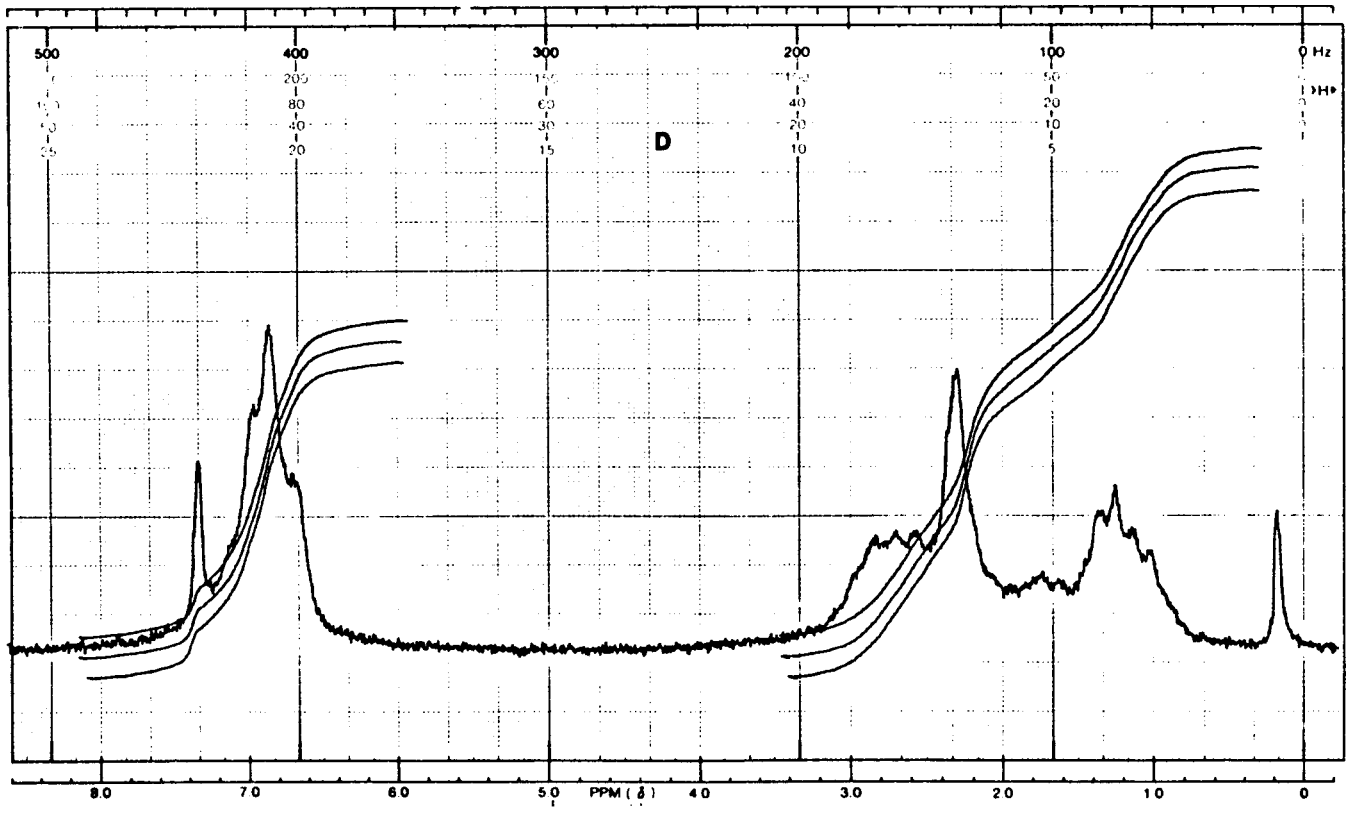

Figure 17d. ^{1}H NMR Results, Spectrum D.

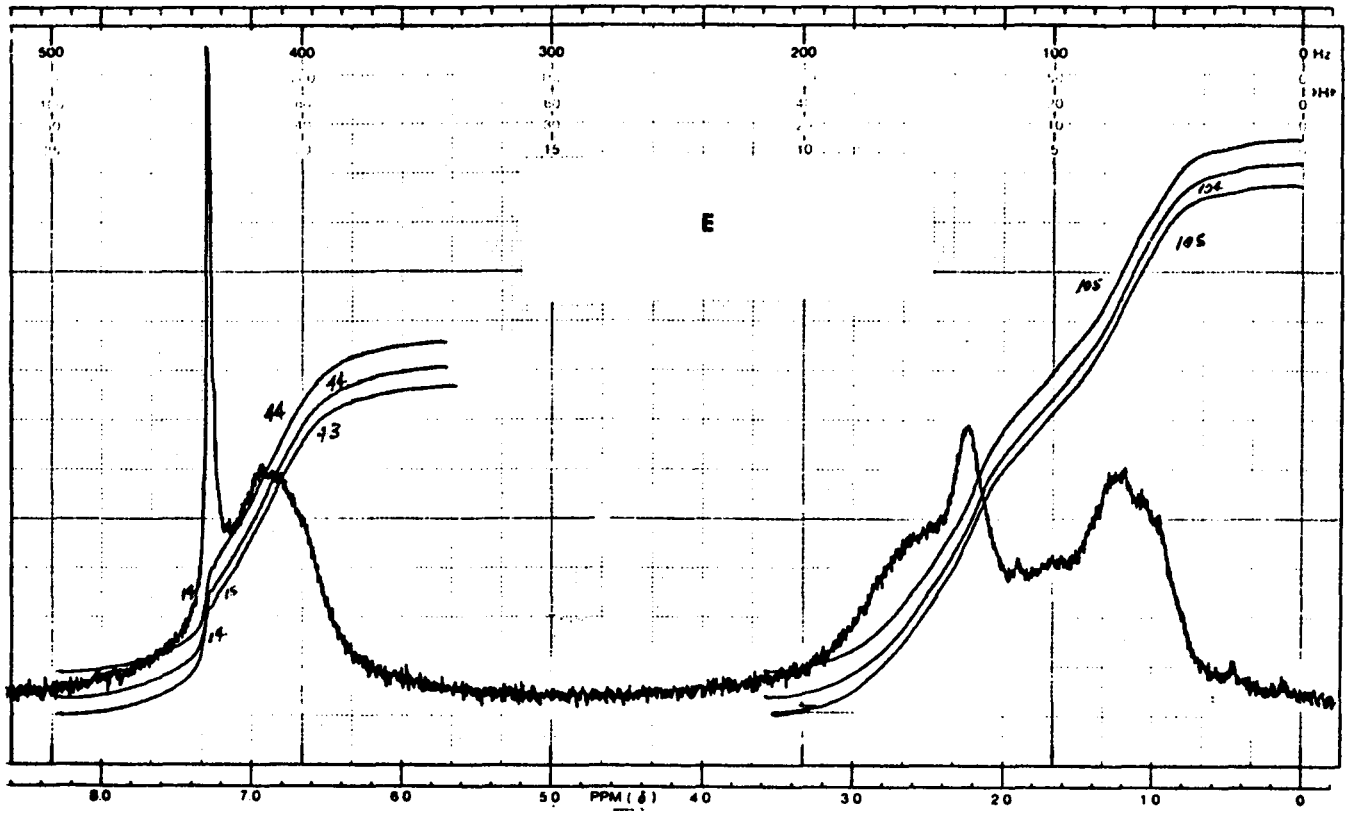

Figure 17e. ^{1}H NMR Results, Spectrum E.

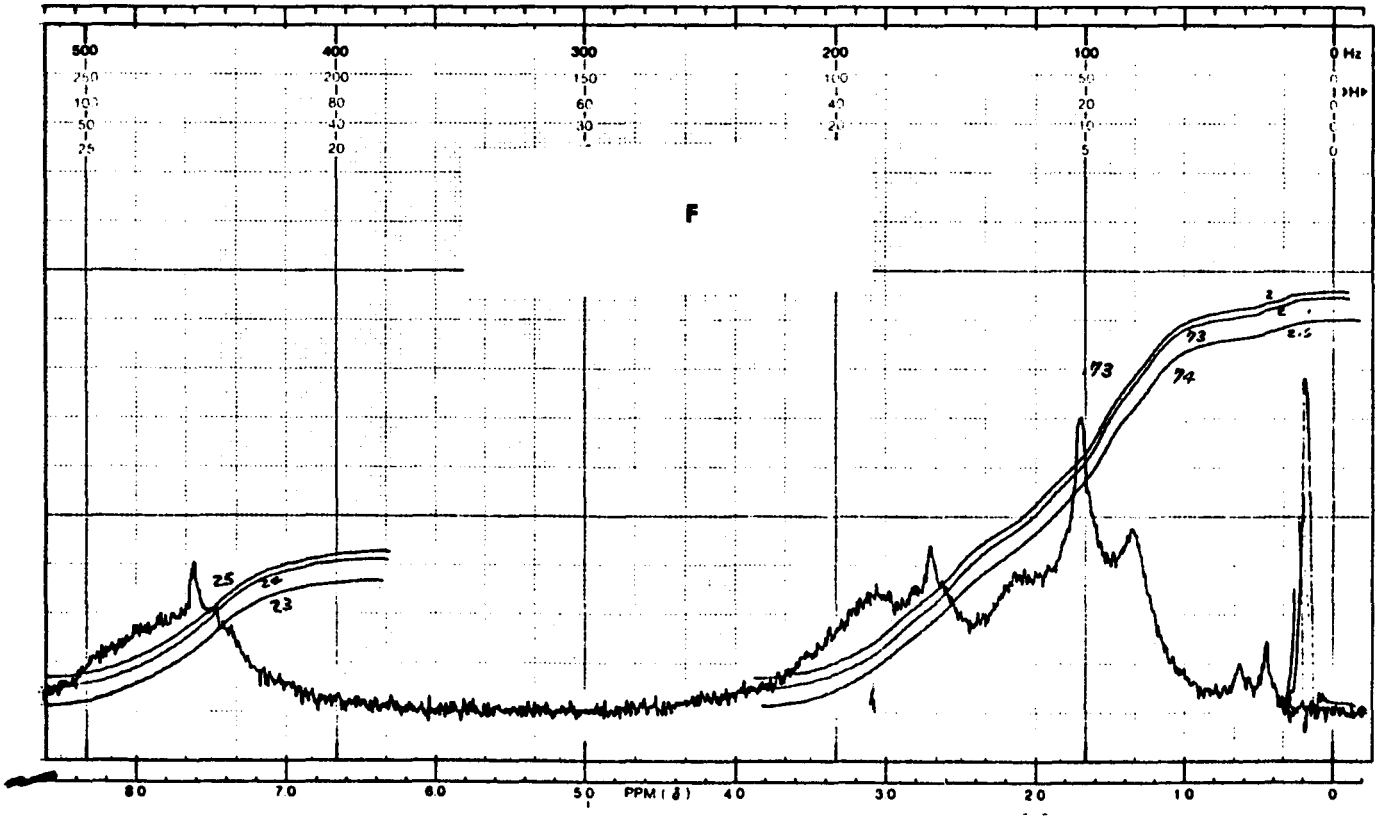

Figure 17f. ^{1}H NMR Results, Spectrum F.

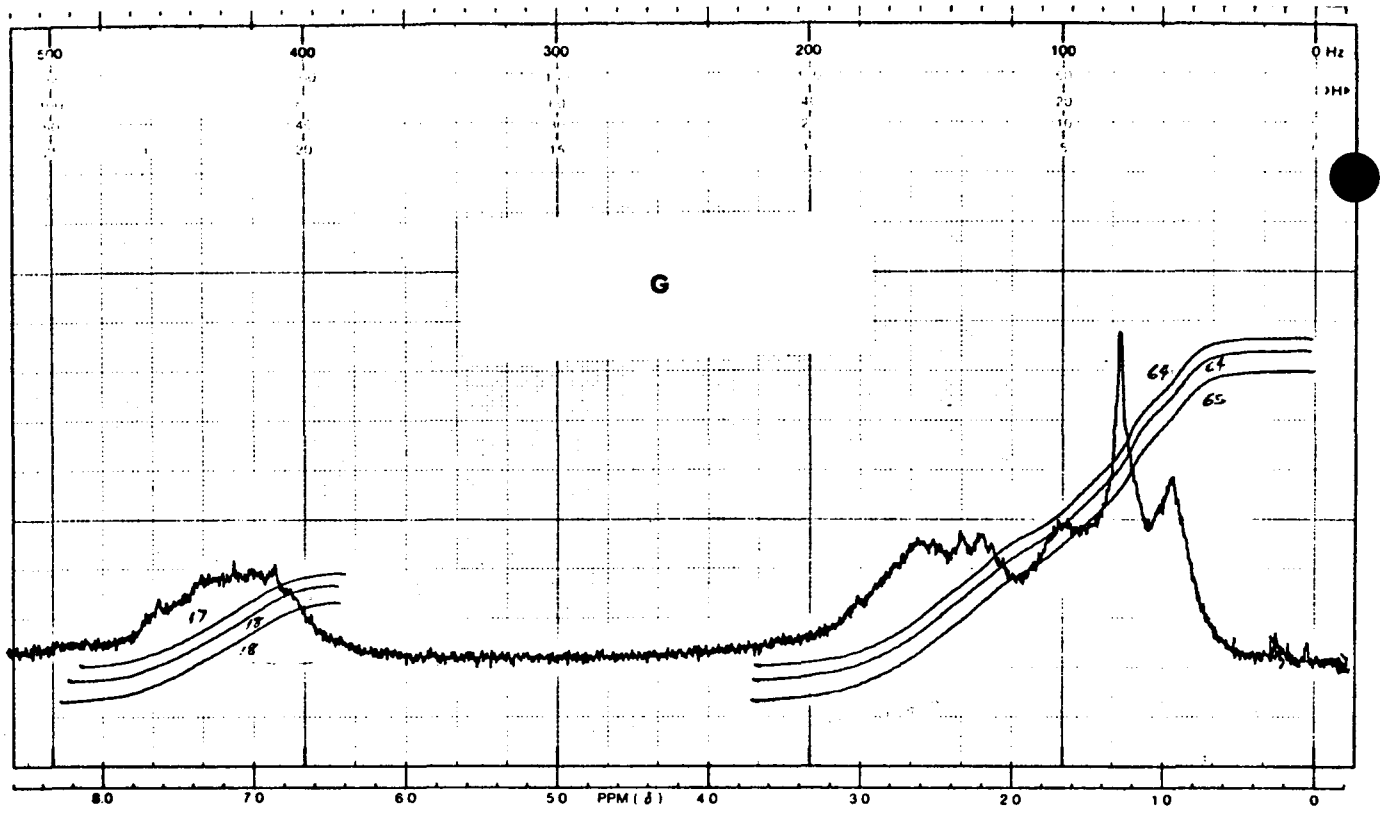

Figure 17g. ^{1}H NMR Results, Spectrum G.

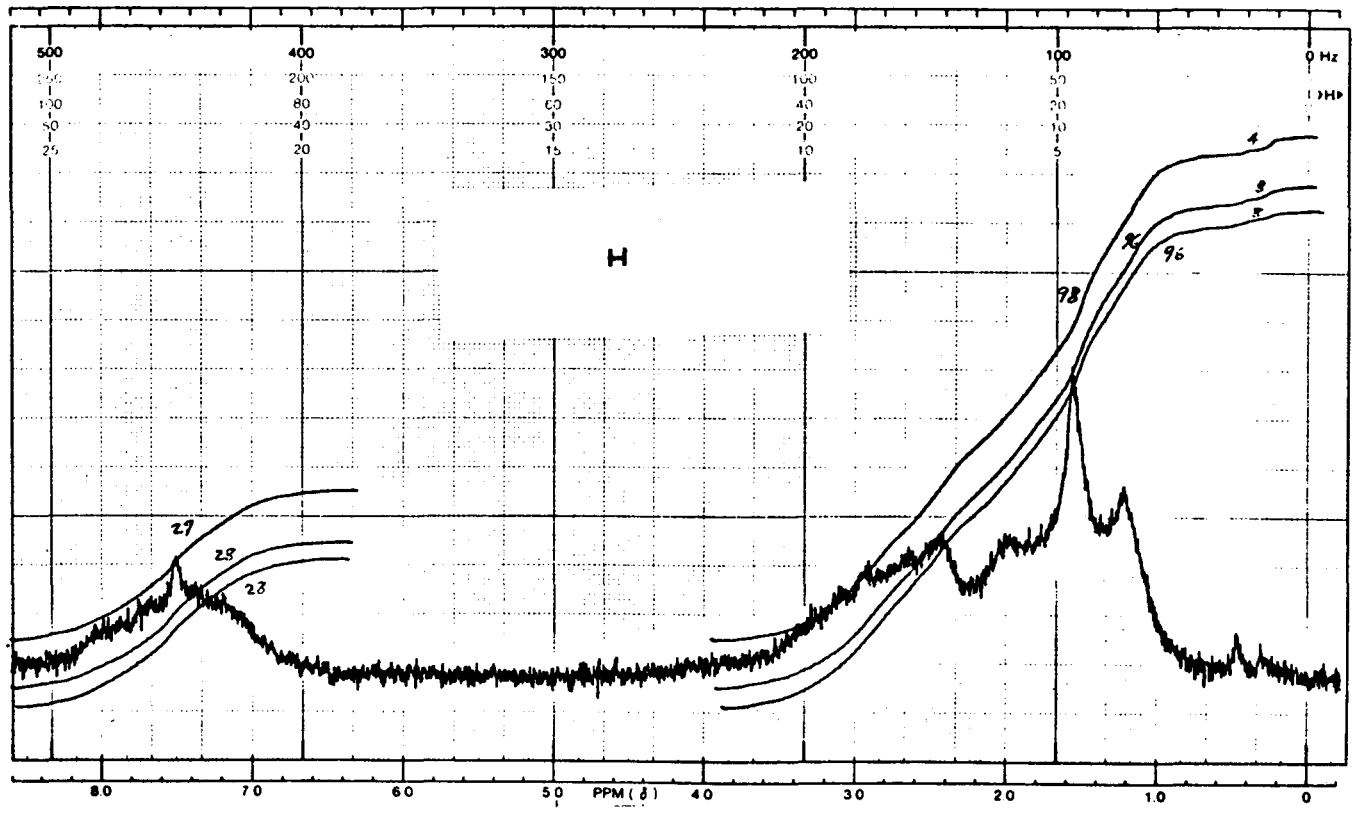

Figure 17h. ^{1}H NMR Results, Spectrum H.

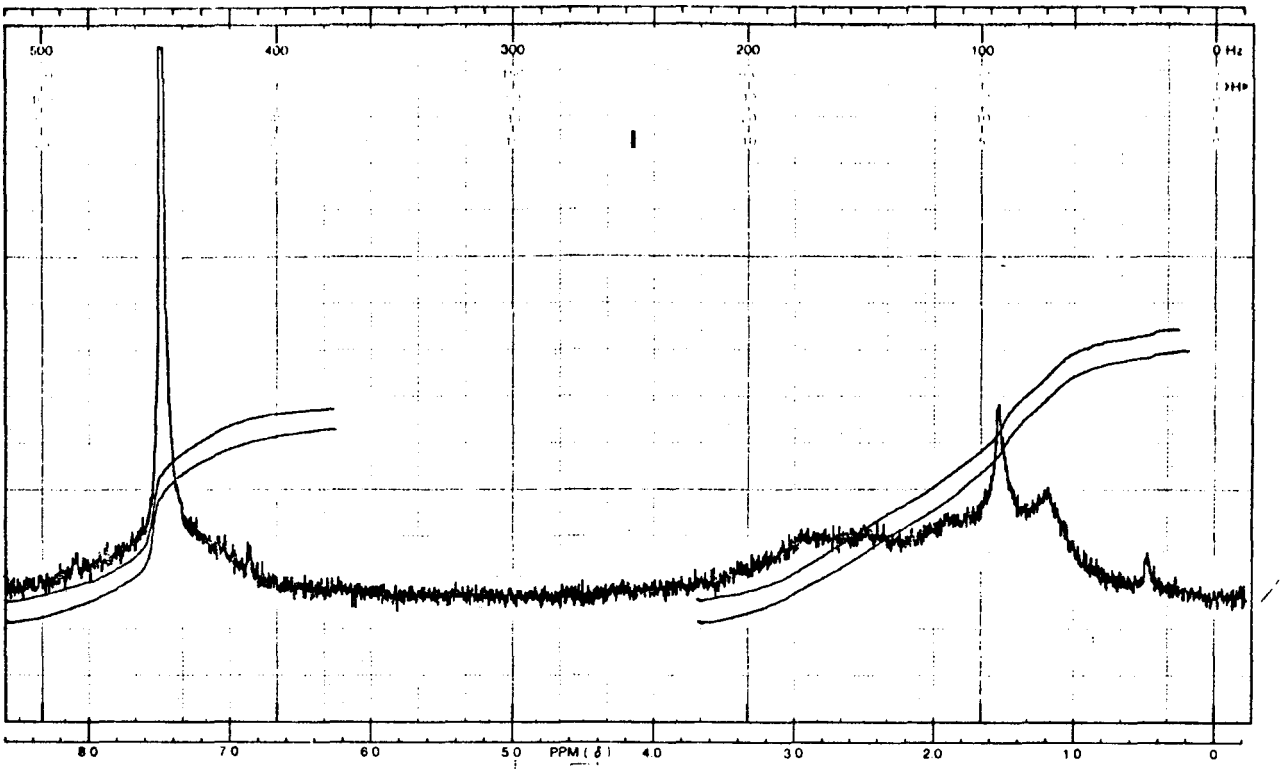

Figure 17i. ^{1}H NMR Results, Spectrum I.

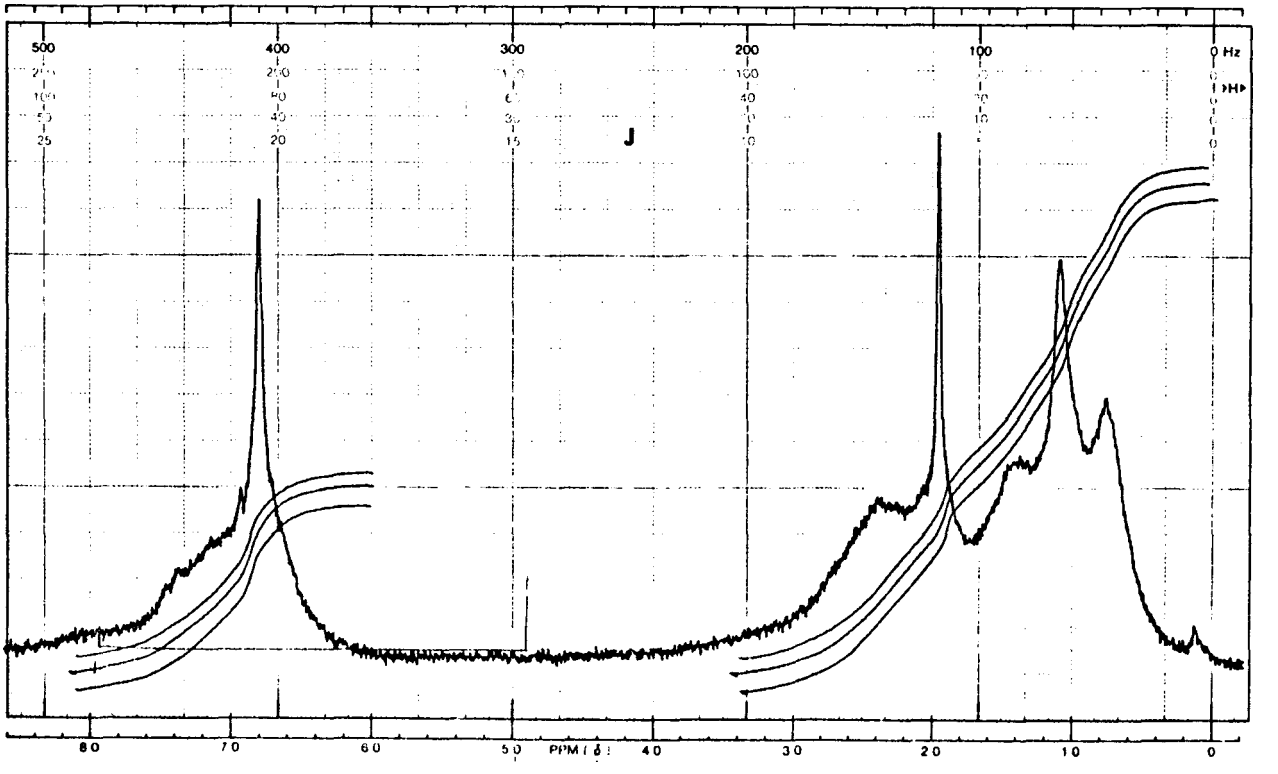

Figure 17j. ^{1}H NMR Results, Spectrum J.

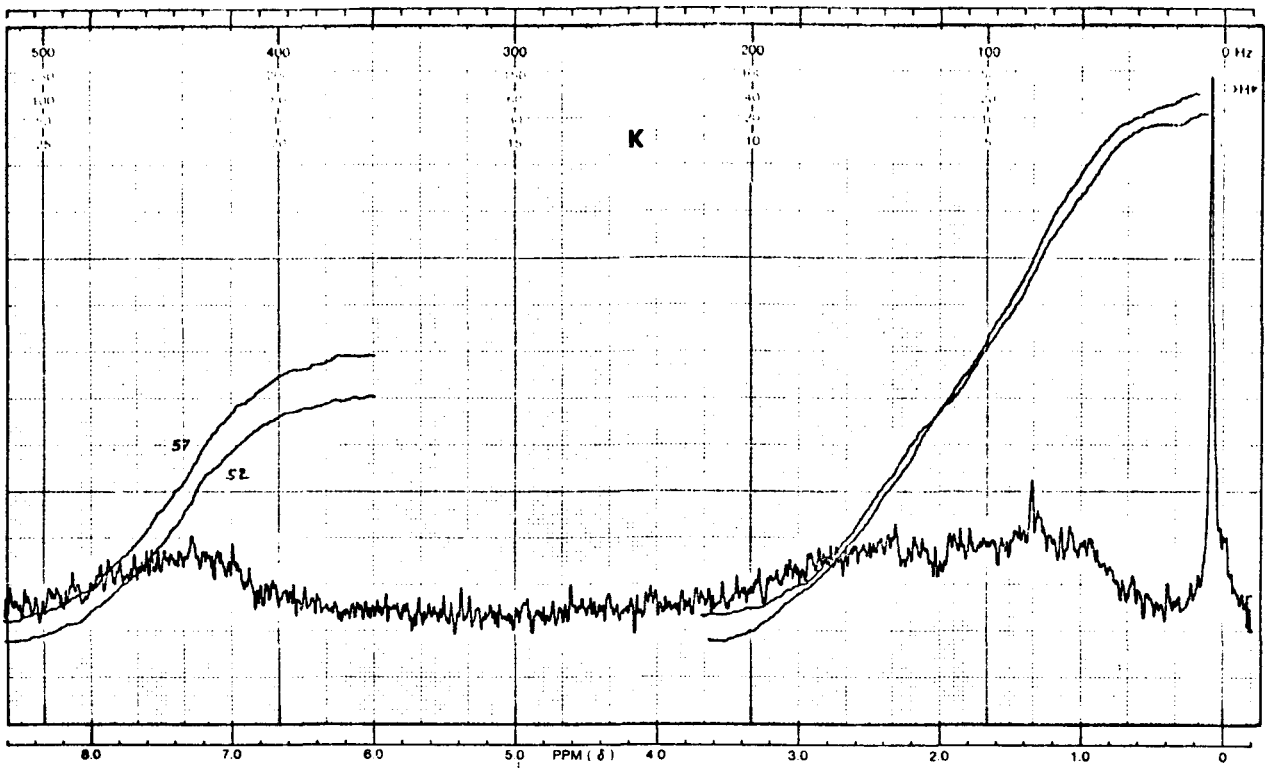

Figure 17k. ^{1}H NMR Results, Spectrum K.

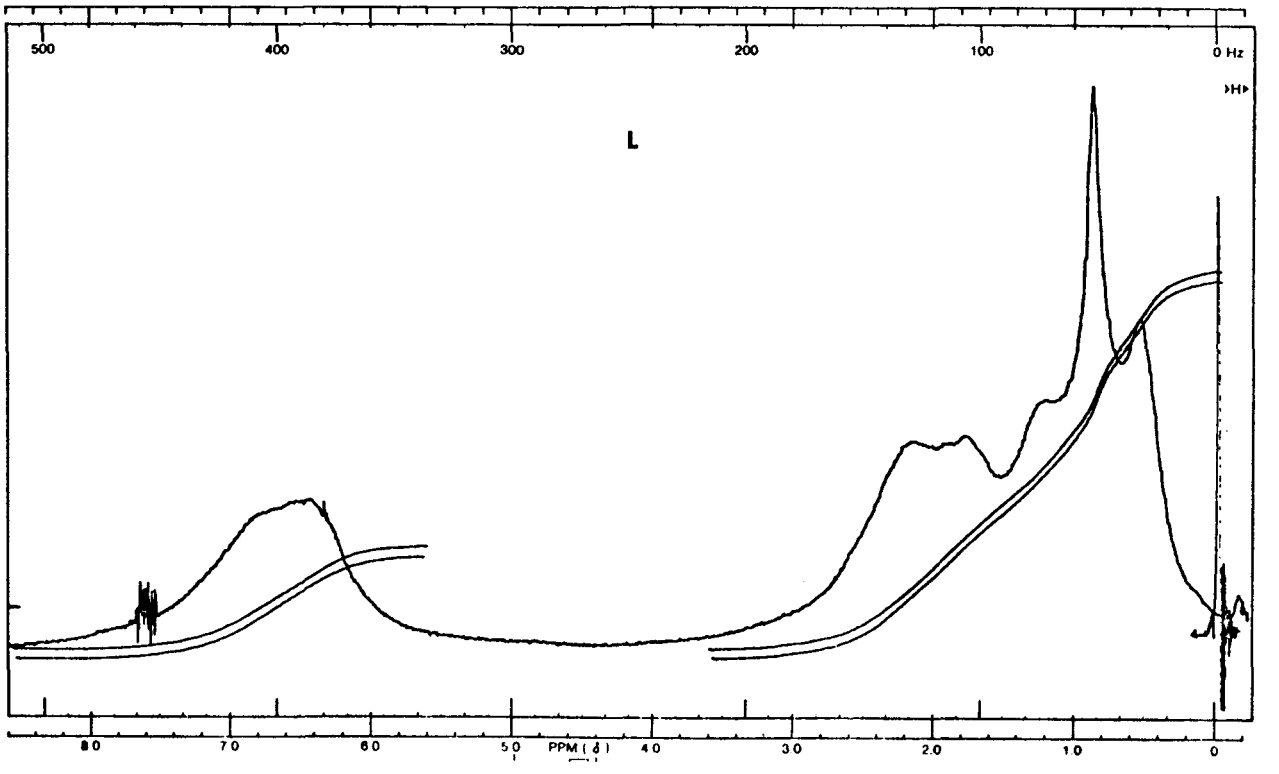

Figure 17ℓ. ^{1}H NMR Results, Spectrum L.

these fractions. Further evidence for phenols can be seen in the region between 1160 and 1300 cm^{-1}, where a broad band, characteristic of aromatic C-O stretch is observed. Other bands observed in this spectrum were assigned to benzene ring vibrations. The basic asphaltene fractions are, in many ways, as interesting spectrally as their acid counterparts. Weak IR absorption bands at 3300 cm^{-1} indicate N-H stretch. The region between 1250 and 1350 cm^{-1} shows a series of very weak bands which may belong to the aromatic C-N stretch vibration. However, this cannot be said with certainty. The remaining spectral assignments are essentially the same as for the asphaltene acid fractions.

Both carbon tetrachloride and n-hexane extracts appear to have identical spectra. Only aromatic and aliphatic C-H stretch can be assigned with any confidence. The shoulder at 3300 cm^{-1} may be due to impurities in the sample or to small quantities of primary or secondary amines actually present in the neutral fractions. IR spectra, taken of similar material at a different time, seem to support the contamination idea however, as very little absorption above 3100 cm^{-1} can be seen.

(3) Conclusions

The infrared and nuclear magnetic resonance spectra of oils, resins, and asphaltenes show undeniable trends. Yet, at this time, nothing definite can be said concerning the identity of the structures which give rise to these spectra. As our ability to fractionate coal-derived materials becomes increasingly sophisticated, however, we can expect that IR and NMR will play a major role in the elucidation of coal structure.

c. H-Coal Asphaltene Separations
(W. B. Bedwell)

A series of experiments was performed in an attempt to determine the acid-base character of asphaltenes.

In general these processes involved the introduction of a strong acid into a solution of asphaltenes in toluene or THF. This acid reacted with basic functional groups to form asphaltene salts. These salts were then separated from the acid-neutral portion by taking advantage of their reduced solubility in toluene.

This insoluble adduct was then treated with NaOH to reverse the acid reaction and regenerate the basic asphaltenes. These regenerated bases were exposed to toluene so that they might be dissolved, as expected. In all cases, a significant amount of this material was not soluble in toluene. The filtration at this point was always very slow.

Experiments D, E, and F, Figures 18-20, were conducted using toluene as the solvent for the acid reaction. In these three cases, as with previous attempts, the once soluble asphaltenes were found to be 10 - 20%-insoluble in toluene. This material was filtered out by vacuum filtration and the soluble portion was treated with acid.

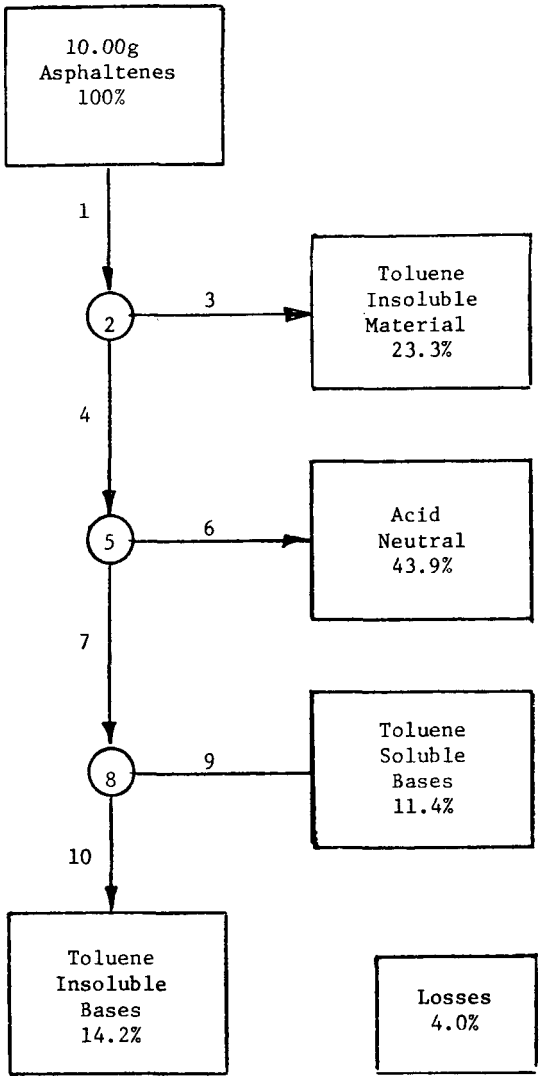

1. Stir sample in ~250 ml toluene (overnight).
2. Filter to remove toluene insoluble material.
3. Dry solids to recover Toluene Insoluble Material.
4. Bubble HCl through toluene solution for 1.5 hours.
5. Filter to remove precipitated bases.
6. Evaporate toluene to recover Acid Neutral portion.
7. Stir solids with ~200 ml 0.25 M NaOH solution and ~400 ml toluene (overnight).
8. Filter to remove toluene insoluble bases.
9. Separate toluene layer from aqueous layer. Evaporate toluene to recover Toluene Soluble Bases.
10. Wash solids with H_2O and dry to recover Toluene Insoluble Bases.

Percentage of total recovered: 96.8%

Figure 18. Experiment D, Acid-Base Separation of Toluene-Soluble, 75%-Pentane/25%-Toluene-Insoluble Asphaltenes from Extract 43(3), Hydrocarbon Research, Inc., H-Coal Vacuum Bottoms from Illinois No. 6, River King Mine Coal.

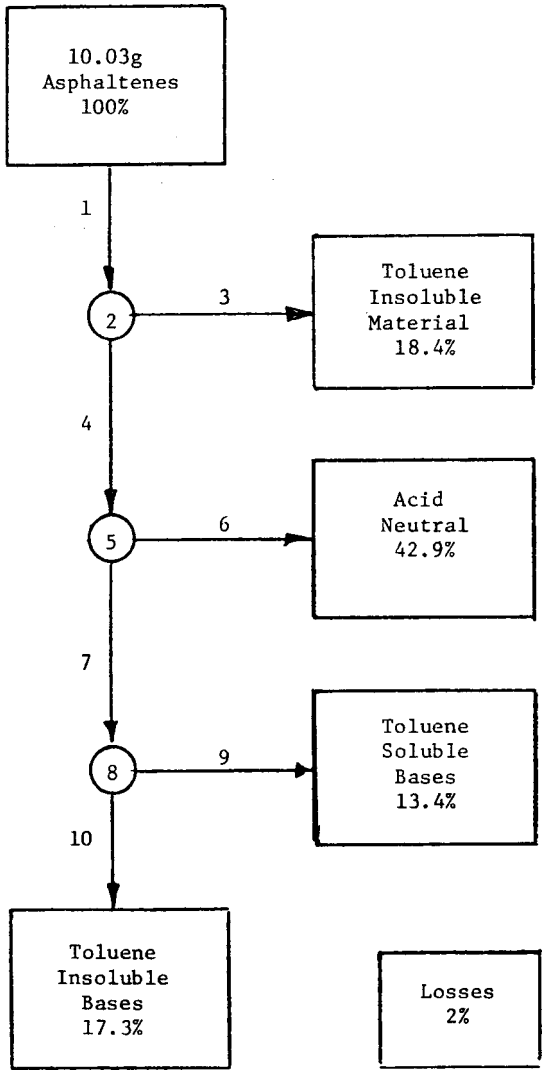

Percentage of total recovered: 94%

1. Stir sample with ~250 ml toluene (overnight).
2. Filter to remove toluene insoluble material.
3. Dry solids to recover Toluene Insoluble Material.
4. Stir toluene solution with ~100 ml 35% perchloric acid (overnight).
5. Filter to remove precipitated bases.
6. Separate toluene layer from aqueous layer. Evaporate toluene to recover Acid Neutral Portion.
7. Stir solids with ~100 ml 0.25 M NaOH and ~300 ml toluene (five hours).
8. Filter to remove toluene insoluble bases.
9. Separate toluene layer from aqueous layer. Evaporate toluene to recover Toluene Soluble Bases.
10. Wash solids with H_2O and dry to recover Toluene Insoluble Bases.

Figure 19. Experiment E, Acid-Base Separation of Toluene-Soluble, 75%-Pentane/25%-Toluene-Insoluble Asphaltenes from Extract 43(3), Hydrocarbon Research, Inc., H-Coal Vacuum Bottoms from Illinois No. 6, River King Mine Coal.

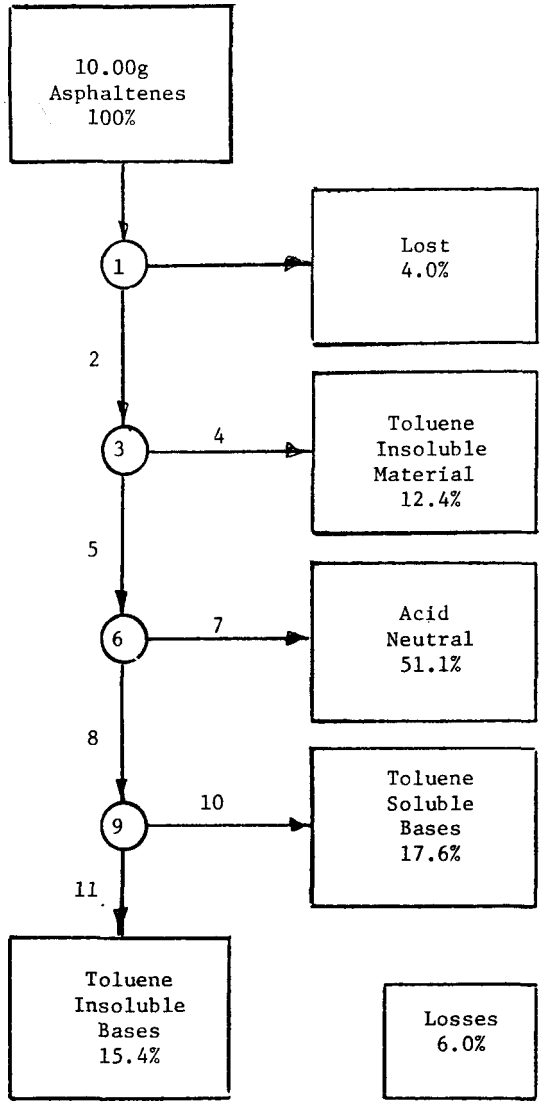

1. Pulverize sample and heat. Weigh to check weight loss.
2. Stir sample with ~200 ml toluene (overnight).
3. Filter to remove toluene insoluble material.
4. Dry solids to recover Toluene Insoluble Material.
5. Bubble HCl through toluene solution for 0.5 hours.
6. Filter to remove precipitated bases.
7. Evaporate toluene to recover Acid-Neutral portion.
8. Stir solids with ~100 ml 0.25 M NaOH (overnight).
9. Filter to remove toluene insoluble bases.
10. Separate toluene layer from aqueous layer. Evaporate toluene to recover Toluene Soluble Bases.
11. Wash solids with H_2O and dry to recover Toluene Insoluble Bases.

Percentage of total recovered: 106.5%

Figure 20. Experiment F, Acid-Base Separation of Toluene-Soluble, 75%-Pentane/25%-Toluene-Insoluble Asphaltenes from Extract 43(3), Hydrocarbon Research, Inc., H-Coal Vacuum Bottoms from Illinois No. 6, River King Mine Coal.

In experiments D and F, HCℓ gas was bubbled through these solutions to precipitate the adduct, while in experiment E the asphaltene solution was stirred with aqueous perchloric acid. The adduct was filtered out in all three cases and treated with NaOH solution and toluene.

This mixture was filtered to collect the toluene insoluble bases. The toluene layer was separated from the aqueous layer and dried to collect the toluene soluble bases. Similarly, the toluene solution containing the acid-neutral material was dried to collect this fraction.

In the interest of characterizing the 10 - 20%-toluene-insoluble material not treated in the previous examples, Experiments C and G, Figures 21 and 22, were performed. The acid reaction was conducted in THF which completely solubilized the sample. Experiment C involved the use of aqueous H_2SO_4 while experiment G utilized HCℓ gas. Unfortunately, with these operations the adduct did not precipitate in THF and some THF is converted to 4-chloro, 1-butanol with HCℓ. After the reaction, the THF was evaporated and toluene added. This mixture was then filtered to separate the solid adduct from the toluene-soluble acid-neutral portion. These portions were then processed as in the previous experiments.

These last two experiments did not appear to break up the initially toluene-insoluble fraction into soluble acidic and basic portions. Rather the toluene-insoluble material seemed to go through the process as a solid and come out with the toluene insoluble bases.

Asphaltenes are very sticky solids and as such are difficult to handle quantitatively. The acid-neutral portion was generally a dark brown sticky glassy substance. The toluene-soluble bases were the same color, but slightly more crystalline. The toluene-insoluble bases were a black brittle solid. The adduct was a black crystalline solid.

Every operation left glassware with some material adhering to the sides. Any of this material which could not be collected was dissolved with pyridine or THF and kept to be included as losses in the material balance. Losses were also monitored by weighing filter paper before and after filtrations.

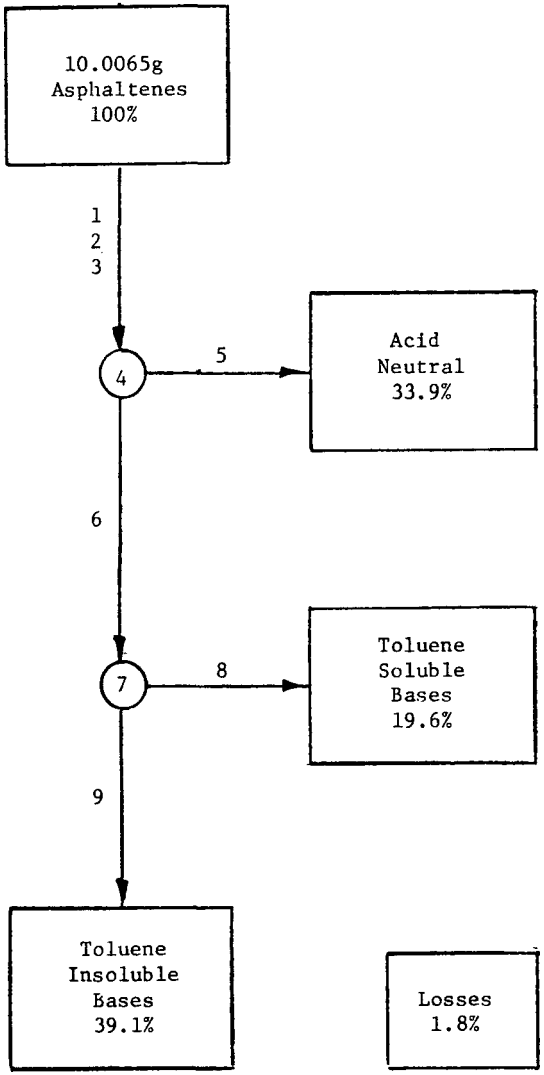

1. Dissolve sample in 300 ml THF.
2. Add ~100 ml 20% H_2SO_4.
3. Evaporate THF and add 400 ml toluene (stir overnight).
4. Filter to remove precipitated bases.
5. Separate toluene layer from aqueous layer. Dry toluene layer to recover Acid-Neutral portion.
6. Stir solids overnight with ~300 ml toluene and ~100 ml 0.25 M NaOH solution.
7. Filter to remove Toluene Insoluble Bases.
8. Separate toluene layer from aqueous layer. Evaporate toluene layer to recover Toluene Soluble Bases.
9. Wash solids with H_2O and dry to recover Toluene Insoluble Bases.

Percentage of total recovered: 94.4%

Figure 21. Experiment C, Acid-Base Separation of Toluene-Soluble, 75%-Pentane/25%-Toluene-Insoluble Asphaltenes from Extract 43(3), Hydrocarbon Research, Inc., H-Coal Vacuum Bottoms from Illinois No. 6, River King Mine Coal.

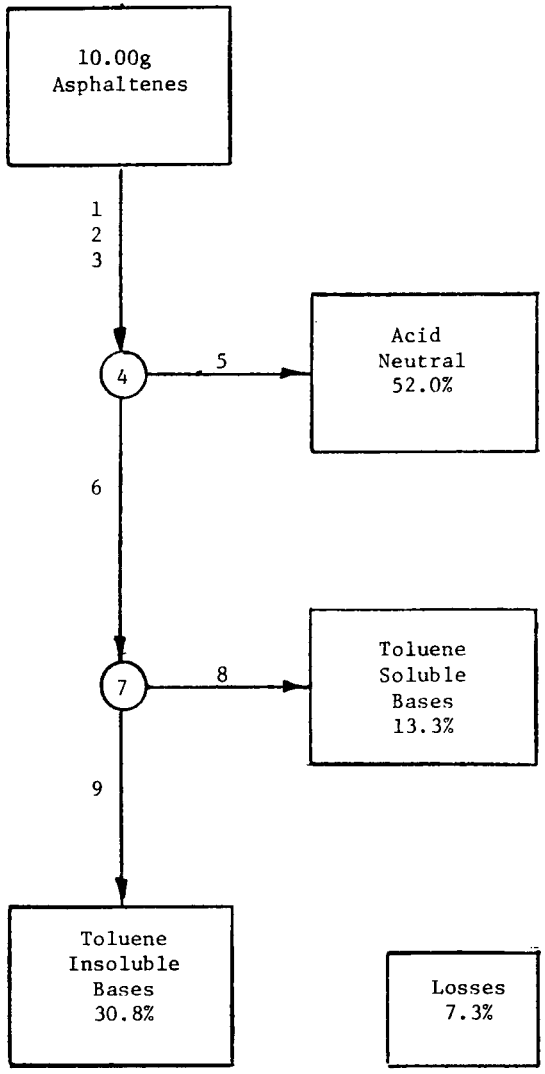

1. Dissolve sample in ~325 ml THF.
2. Bubble HCl through solution for 45 minutes.
3. Evaporate THF and add ~200 ml toluene (stir overnight).
4. Filter to remove precipitated bases.
5. Evaporate toluene to recover Acid-Neutral portion.
6. Stir solids with ~100 ml 0.25 M NaOH and 300 ml toluene (overnight)
7. Filter to remove toluene insoluble bases.
8. Separate toluene layer from aqueous layer. Evaporate toluene to recover Toluene Soluble Bases.
9. Wash solids with H_2O and dry to recover Toluene Insoluble Bases.

Percentage of total recovered: 103.4%

Figure 22. Experiment G, Acid-Base Separation of Toluene-Soluble, 75%-Pentane/25%-Toluene-Insoluble Asphaltenes from Extract 43(3), Hydrocarbon Research, Inc., H-Coal Vacuum Bottoms from Illinois No. 6, River King Mine Coal.

II. SOLIDS SEPARATION - FILTRATION EXPERIMENTS
(J. A. McKeen and J. A. Stirling)

During this year Mr. Stirling completed his Ph.D. research and dissertation which was initiated under an NSF RANN Grant. Mr. McKeen assisted Mr. Stirling in data acquisition and analysis and is presently responsible for the filtration studies.

Filtration studies were done on slurries of H-Coal vacuum still bottoms in oils and resins and on solutions of H-Coal toluene soluble asphaltenes in tetralin. In earlier experiments slurries of H-Coal vacuum still bottoms in tetralin had been filtered and unusual behavior was observed, namely a significant increase in the specific cake resistance as the total asphaltene and preasphaltene concentration in the liquid phase is increased from 10 to 20 wt.%.[1] Slurries of H-Coal vacuum still bottoms in oils and resins were filtered to eliminate the possibility that the tetralin itself may have caused some of the unusual behavior.

A large quantity of oils and resins (defined as the pentane soluble portion of the H-Coal vacuum bottoms) was obtained by extracting the vacuum still bottoms with pentane as described in the above reference. This material served as the bulk suspending media, replacing tetralin, for these filtrations. In each of the slurries the concentration of THF insoluble solids was held constant at 13.8 wt.% and the total concentration of H-Coal asphaltenes and preasphaltenes was varied from run to run. The concentration of THF insoluble solids was held constant by adding extra THF insoluble solids to the slurries in which the quantity of whole H-Coal vacuum still bottoms was insufficient to give the proper amount of THF insoluble solids in the slurry.

The results of this series of filtrations is presented in Figure 23. In this figure the specific filter cake resistance is plotted as a function of total asphaltene and preasphaltene concentration in the liquid phase. The viscosities of the slurries (at 450°F) that were filtered are presented in Figure 24.

In Figure23 it can be seen that there is a significant increase in specific cake resistance as the total asphaltene and preasphaltene concentration is increased from 10 to 20 wt.%. This increase corresponds to similar increases in specific cake resistance observed earlier when tetralin was used as the bulk suspending media for the filtrations. However, the increase in specific cake resistance is less when oils and resins are used as the bulk suspending media. The oils and resins appear to have a moderating effect on the interactions between the asphaltenes and the preasphaltenes in solution and the THF insoluble particles in the built-up filter cake.

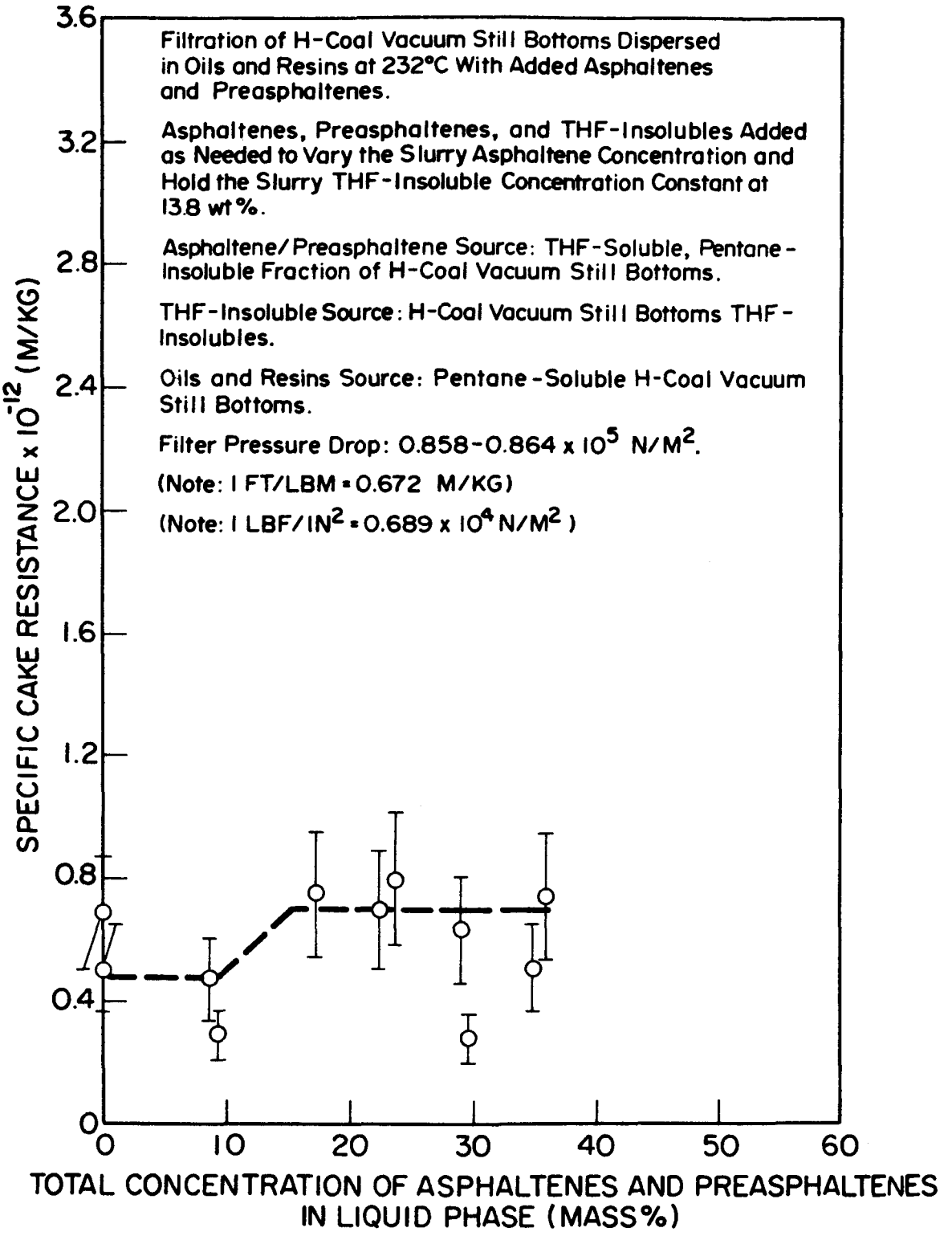

Figure 23. Filtration at 232°C (450°F) of Whole H-Coal Vacuum Still Bottoms Dispersed in H-Coal Pentane-Soluble Oils and Resins with Added H-Coal Asphaltenes and Preasphaltenes.

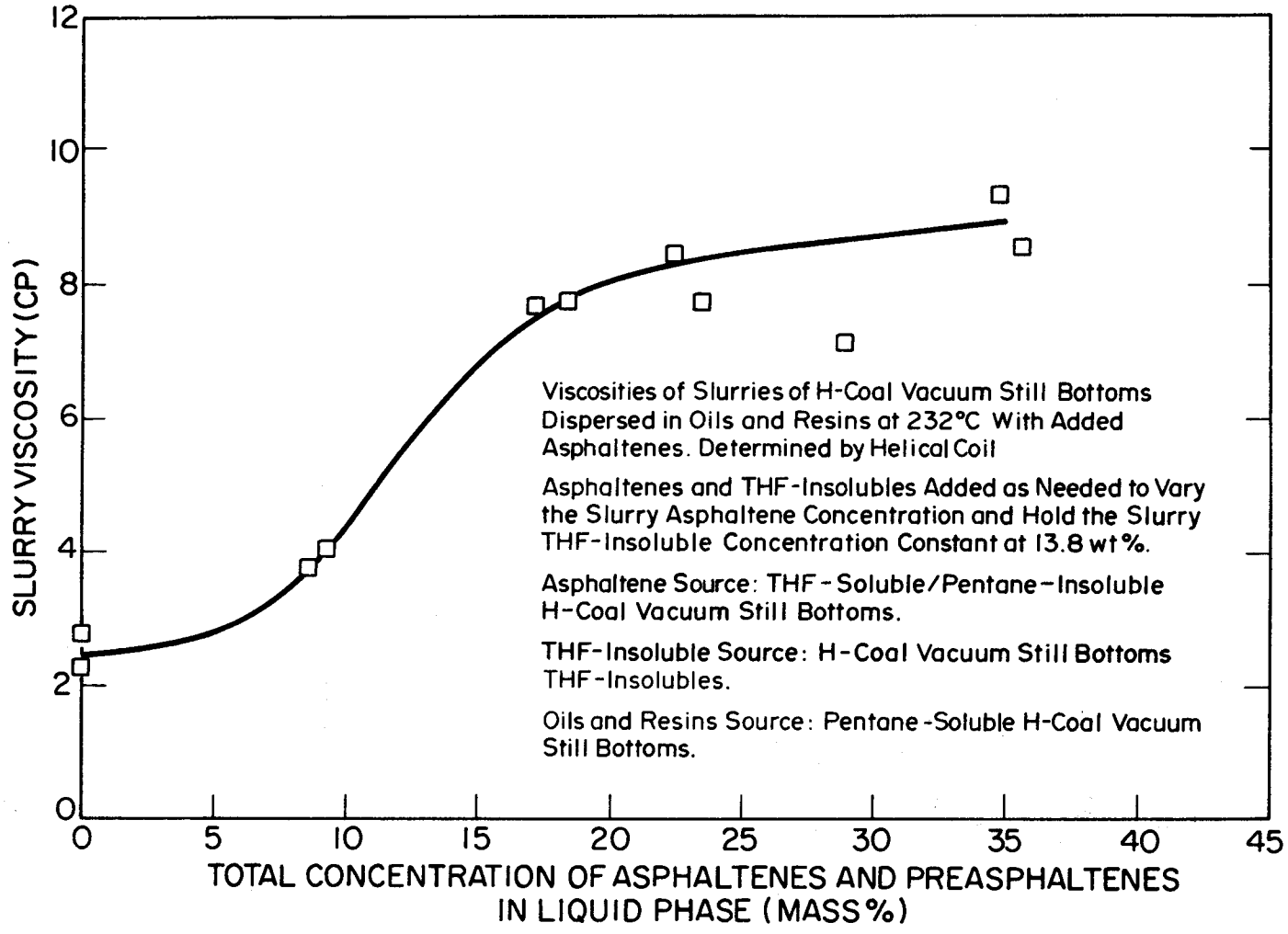

Figure 24. Viscosities at 232°C (450°F) of Slurries of Whole H-Coal Vacuum Still Bottoms Dispersed in H-Coal Pentane-Soluble Oils and Resins with Added H-Coal Asphaltenes and Preasphaltenes.

The viscosity data in Figure 24, which shows an abrupt increase in viscosity when the total concentration of asphaltenes and preasphaltenes is increased from 10 to 20 wt.%, agree with other data taken in our laboratory, indicating that a drastic change in solution behavior takes place in that concentration range. This helps to explain the increase in specific cake resistance observed in the filtrations discussed above.

Filtration studies were also done on solutions of H-Coal toluene soluble asphaltenes in tetralin. A total of nine runs were done, two of which were used to complete the data for Mr. Stirling's thesis. The other seven were run primarily to acquaint Mr. McKeen with the operation of the experimental apparatus and the reduction of the experimental data. Due to Mr. McKeen's inexperience in operating the equipment several of these runs had to be aborted before actual filtration data were taken. From the runs that were completed, it was shown that the presence of asphaltenes in tetralin solution did increase the precoat layer flow resistance, but the additional resistance is small compared to the resistance of mineral solids.

After completion of Mr. Stirling's thesis data the filtration equipment was shut down to undertake equipment modifications and repairs. Repairs made to the equipment included installing new valve stems and seals on about half of the valves and replacing insulation in areas where it had been damaged.

Several equipment modifications were also planned and carried out. The purpose of these modifications is to increase the accuracy of the data taken during an experimental run and to decrease the time needed to complete a run.

The slurry preparation vessel heating system was upgraded by putting it on a separate electrical circuit. This has reduced the time needed for heating the slurry from ambient temperature to 232°C (450°F) from three hours to one hour. In addition, the tubing and piping systems have been further insulated to reduce heat losses.

Other major modifications include the redesign and repiping of the filtrate density and flow rate measuring system and the installation of a filtrate sampling tap. The redesigned filtrate density and flow rate measuring system is shown in Figure 25. The new system works on the same principles as before, but eliminates the need to have the high pressure side of the differential pressure transmitter filled with liquid. This was done by installing a nitrogen gas purge line and a check valve on the high pressure side tubing. The new system enables faster, easier, and more accurate measurements of fluid density and flow rate to be obtained. A photograph of the equipment is shown in Figure 26.

After the equipment modifications and repairs were completed the filtration equipment was calibrated. The calibration procedure consisted of first recalibrating each of the three differential pressure transmitters contained in the filtration equipment. Following this,

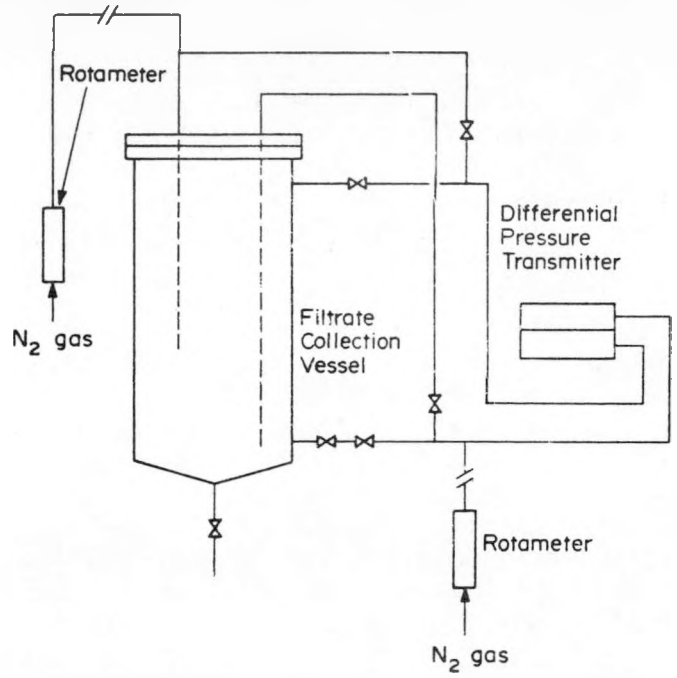

Figure 25. Filtrate Density and Flow Rate Measuring System.

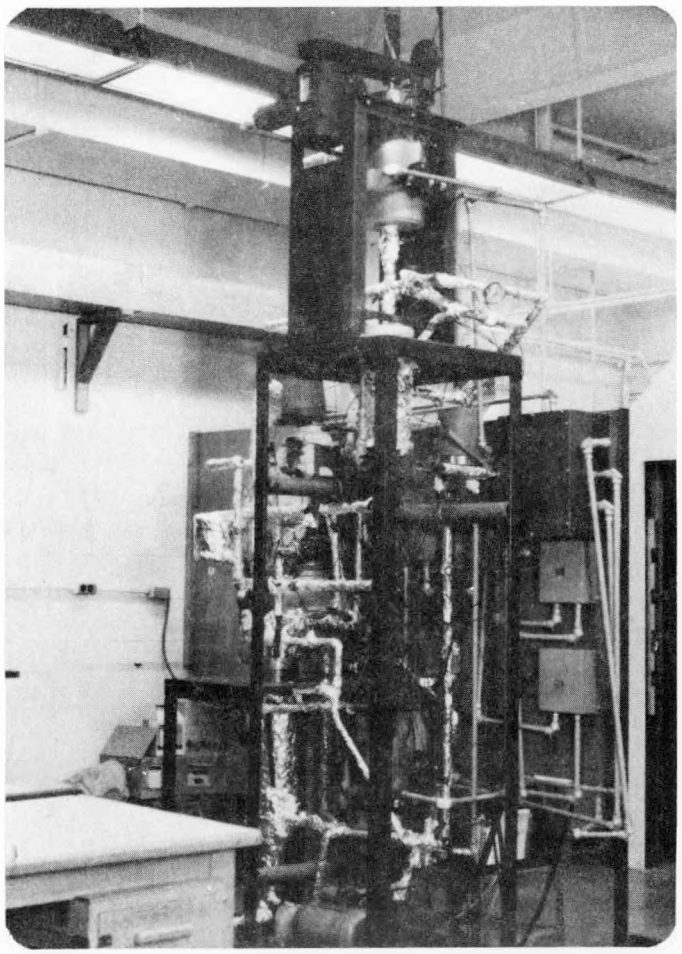

Figure 26. Photograph of Filtration Equipment.

the filtrate flow rate, density, and viscosity measuring systems were calibrated using a liquid, the density and viscosity of which were known over a range of temperatures.

Several static shake-down runs were then completed in order to check the operation of the equipment. One of the procedures tested in these runs was the precoating procedure. A typical precoat, obtained during one of these runs, is shown in Figure 27. Upon completion of these static shake-down runs the filtration equipment will be ready to be used to take experimental data. It's expected that the filtration experimental program will begin in the very near future.

Figure 27. Typical Diatomaceous Earth Precoat Cake.

III. COLLOID CHEMISTRY OF LIQUEFIED COAL SLURRIES

The work during the first year concentrated on asphaltene solubility and on measuring the electrical charge on asphaltenes. In the area of asphaltene solubility, the effort was directed at developing an X-ray method to determine the size and shape of asphaltene and preasphaltene colloid micelles at or near concentrations likely to be found in the solids separation step of a coal liquefaction process. Changes in temperature, addition of solvents or removal of products can change the extent of intermolecular association and hence the micelle size. Micelle depeptization leads to large increases in the size of the kinetic unit and a precipitate can be said to exist.

The electrical charge on or associated with asphaltenes, preasphaltenes, and trace amounts of mineral solids in solution are important to the electrophoresis work. It also is important to understanding the formation of micelles and to adsorption phenomena. A system has been developed to measure the electrical conductivity and the dielectric constant of solutions which contain asphaltenes. Electrophoresis cells have also been constructed to measure the charge on asphaltenes.

A. Asphaltene Solubility
(B. Ho)

The size, shape, and character of the colloid micelles affect all types of solid-liquid separation processes: filtration, settling, vacuum distillation, flocculation, etc. The size and shape of the micelles are functions not only of the sample itself but also of the conditions of preparation such as temperature, solvents, and concentrations. In certain solvents or combinations of solvents, asphaltenes and preasphaltenes exist as peptized micelles. In other solvents they associate without bound and form precipitates which can be observed visually.

Small angle X-ray scattering is a technique to measure the size-configuration of suspensions or colloidal solutions where the kinetic units are in the range of 10-1,000 °A in size. The size is determined from the intensity of the scattered X-rays as a function of scattered angles.

1. General Theory of Small Angle X-ray Scattering

The simplest case is the scattering at an extremely small angle of monochromatic X-rays by a spherical particle which is large compared to the wavelength of the X-ray.

The scattered intensity from a particle of uniform density averaged over all orientations is

$$I(h) = n^2 I_e i(h) \qquad (1)$$

where n is the number of electrons in a particle, I_e is the scattered intensity from a single electron (essentially constant at small angles and equal to $(7.9 \times 10^{-26}\ I_o)/d^2$ where d is the distance to the point of observation from the specimen, I_o is the incident intensity), and i(h) is called the single-particle scattering function; h is defined as $(4\pi\sin\theta)/\lambda$ with λ and 2θ being the beam wavelength and scattering angle, respectively (13).

Beeman et al. have calculated the i(h) for various shapes. A few of their results are given in Table 12.[14]

Table 12. Beeman's Single Particle Scattering Functions For Different Shaped Units.[14]

(1)	Sphere of radius a	$3(\sin(ha)-ha\cos(ha))^2/(h^3a^3)^2$	
(2)	Rod of height 2H, diameter 2a (H >> a)	$Si(2hH)/hH - (\sin^2(hH)/h^2H^2$ where h << 1/a & $Si(x) = \int_o^x (\sin y)/y\ dy$	
(3)	If h is large enough for the rod so that hH >> 1, then	$i(h) \cong \frac{\pi}{2hH} \exp(-h^2a^2/4)$	h << 1/a h >> 1/H
(4)	Disks (H << a)	$(2/h^2a^2)\ 1 - (1/ha)J_1(2Ha)$ where h << 1/H & J_1 is the Bessel function of order 1	
(5)	If h is large enough so that ha >> 1, then	$\frac{2}{(ha)^2} \exp(-h^2H^2/3)$	h << 1/H h >> 1/a

At very small angles Equation (1) can be expressed by the Guinier approximation

$$I(h) = \exp(-h^2R^2/3) \qquad (2)$$

where R is the 'average' radius of gyration of the particle. R is defined as the root mean square of the distances of atoms from the center of gravity of the particle, each distance being modified by a coefficient equal to the atomic number of the atom, a well-defined geometrical parameter considered to be a characteristic of a molecule of any shape. The radius of gyration, R, can be found from the slope of the line through the data in the small angle region when ln i(h) is plotted versus h^2. This measurement is perhaps the most widely used in the application of small-angle techniques.[13] Table 13 lists the radius of

gyration of the standard particles in terms of their physical dimensions.

At the large-angle extremity of the small-angle region, Equation (1) reduces to

$$I(h) = I_e (2\pi \rho^2 S/h^4) \quad (3)$$

where S is the total surface area contained in the volume irradiated. It holds for all particles regardless of shape. Thus it is noted that the scattered intensity is inversely proportional to the fourth power of h at large-angles.

In an actual sample there will be many particles within the irradiated volume, all of which will contribute to the experimentally measured scattering curve.

Table 13. Radius of Gyration R for Various Particle Shapes.[14]

Shape	Dimensions	R^2
Sphere	Radius = a	$3a^2/5$
Ellipsoid of Revolution	Axes 2a, 2a, 2va	$\frac{(2+v^2)a^2}{5}$
Right Circular Cylinder	Diameter = 2a Height = 2va	$\frac{(3+2v^2)a^2}{6}$
Rectangular Prism	Sides a, 2a, 2va	$\frac{(5+4v^2)a^2}{3}$

In the case of widely separated identical particles, as in the case of dilute solution, the total-scattering curve is just the sum of all the single-particle curve (i.e., $I_{total} = \Sigma I_{individual\ particles}$).

As the concentration of particles increases, interference between the individual scattered waves occurs and the scattering curve becomes distorted. Or if there is a distribution of sizes in solution, then the larger kinetic units in solution intensify and consequently skew the data to indicate a larger "average" particle then actually exists. Very comprehensive treatments of this subject are given by Guinier, Beeman, and Pilz.[14,15,16] Very often, fairly good approximation methods for interpretation of data can be used.

2. General Interpretation Procedures

The central problem of the small-angle scattering technique is the determination of the particle size-configuration of the sample which produces the scattering. In principle, one has only to compare the

experimental data (i.e., the measured scattered intensity) with the appropriate formula to find the radius of gyration, the shape, etc. In practice, however, there are certain corrections which must be made to the data before the basic equations can be used to solve the structure, such as the slit correction for the collimated X-ray beam.

All the single-particle scattering functions are derived assuming perfect collimation of the incident and scattered X-rays. In an actual experiment, an angular divergence exists for the incident ray because of the finite size of the collimating apertures. Moreover, in a counter detector the scattered intensity is integrated over a range of scattering angles because of the size of the detector aperture. Hence an error is induced which cannot be tolerated. A correction must be made before the interpretation can be made. The correction is usually very complex. A computer program written by Hendricks and Schmidt has been developed that will easily correct the slit contribution.[17]

The background scattering from the cell windows and solvent also gives an apparent contribution to the measured scattered intensity and should be subtracted out.

After all the necessary corrections have been made, the radius of gyration can be determined from the slope of a ln I(h) vs h^2 plot.

Cases will arise in practice where the ln I(h) vs h^2 plot will not be a straight line due to polydispersity effect or interparticle interference effect. In such cases, either the Jellinch, Solomon and Fankucher approximation[18] or the tail analysis[13] can be used to get the radius of gyration, and subsequently, the particle size-configuration. For the first method, a tangent at the greatest angle of scattering is drawn. This tangent intersects the axis of ordinates at a value K_1. The values corresponding to this target are then subtracted from the original curve and a new corrected curve not containing the contribution of this fraction is obtained. In a similar manner the next tangent of minimum slope is drawn to the new curve with its intercept K_2. The procedure is repeated until the final points yield a straight line of intercept K_6. In this way, six lines are obtained, with successively larger slopes, and intercepts K_1, $K_2 \ldots K_6$. From these slopes, we can obtain a size distribution range for the whole specimen.

The second method is based on the fact that all particles scatter as $1/h^4$ regardless of shape in the region of large scattering angles. If the particles are spherical, there will be a smooth transition from the Gaussian behavior at small angle directly to the inverse fourth-power dependence. A $1/h^2$ transition region indicates the presence of flat platelets or disks. A 1/h transition indicates the presence of needlelike rod where $h \simeq 1/a$ and where 2a is the rod diameter.

3. Experimental Equipment

A Rigaku-Denki small angle unit equipped with a proportional counter, automatic step-scanner and digital print-out is available from the Material and Metallurgical Engineering Department on a shared basis to measure the scattered intensity.

The use of pulse-height discriminator in conjunction with Ni-filtered Cu radiation will provide very distinct monochromatic scattering data. Over 99% of the recorded radiation is in the K α lines.

A Cu-target Norelco X-ray diffraction tube with the Beryllium-mica window operating at a focal line size of 0.04 x 8 mm, 54 KV and 25 ma, and a wavelength of 1.5418 A is used.

The design of the sample cell is primarily based on the requirement of a very thin window so that the attenuation of the monochromatic X-ray beam would be as small as possible. Stainless steel 304, which is normally used for slit construction is an excellent wall material for the cell too. The entrance ane exit windows of the cell should have a high transmission and low scattering at small angles. Three materials are generally used today: beryllium, mica, and mylar. Mica is chosen to be the cell window material as it has about the lowest scattering intensity at small angles among the three, and it can be cleaved to give transmission of the order of 90% or more. Sintered beryllium sheet, while giving a high value of transmission, gives rise to a strong scattering at small angles, and should be avoided. Mylar sheet, though also giving extremely high values of transmission, contributes a large background scattering which will induce a much worse slit error than mica.[13] Further, mica is highly durable.

The slit opening for the cell windows are 2 mm x 18 mm and the windows are 0.06 mm thick mica. The sample holder and cell descriptions are given in Figure 28.

4. Review of Pertinent Literature

In recent years, more and more investigations to study the colloidal nature of petroleum asphaltics by small angle X-ray scattering have begun, though this technique has long been used to study the size and shape of proteins and polymers in solution.

The following section serves to give a general overview of how the technique can be applied in various fields of research specifically for particle size and shape determination in solution of the range from 10 - 1000 Å.

Hight, Higdon, and Schmidt made an investigation with sodium montmorillonite clay particles in suspension at concentrations of 1/2 and 2%.[19] Unlike other techniques, small angle X-ray scattering gives a direct measurement of the platelet thickness, in this case about 9 Å. The small angle X-ray scattering apparatus consisted of a standard North American Philips copper target X-ray tube, a slit collimation system, balanced filters and Geiger counter detector.[20] The collimator employed four slits, of adjustable width, 1 cm in height and with 50 cm between neighboring slits. The sample holders were made of sheet aluminum. They varied in thickness from 0.5 mm to 1 mm with 3/16 in. by 1-1/4 in. cut-outs to provide room for the suspension. The sample was contained within the cut-out volume by wrapping the holder with Saran Wrap which became the X-ray window. The same authors later studied some bentonite clay systems in which there were interactions between the clay platelets.[21]

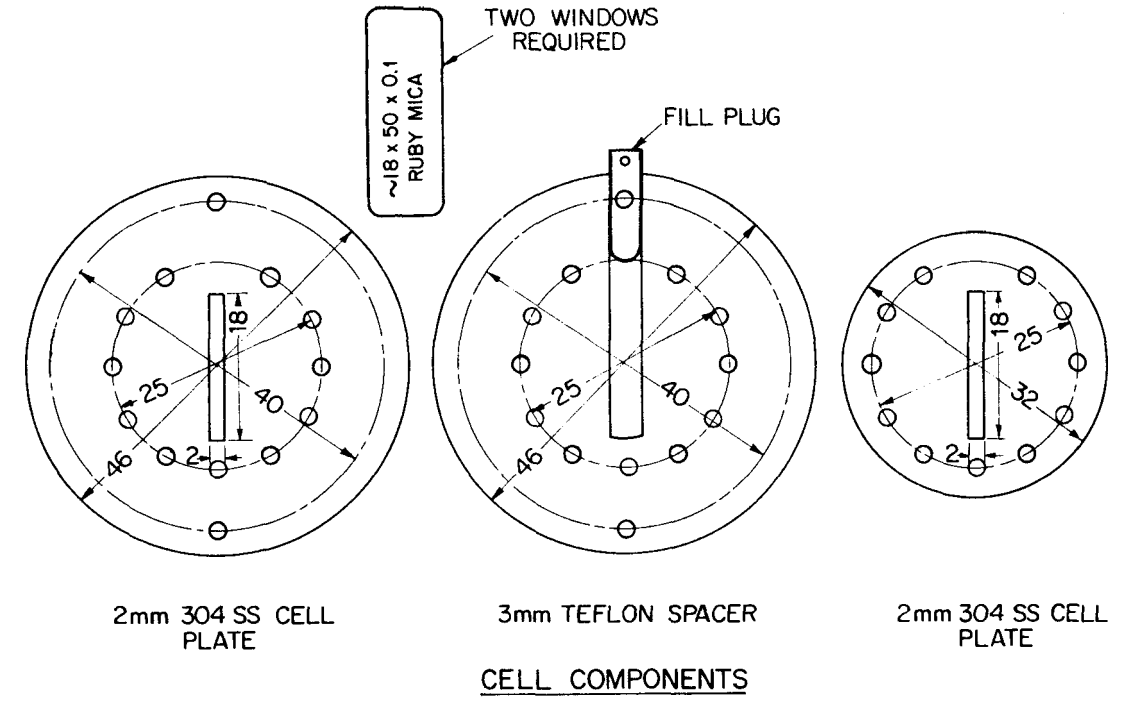

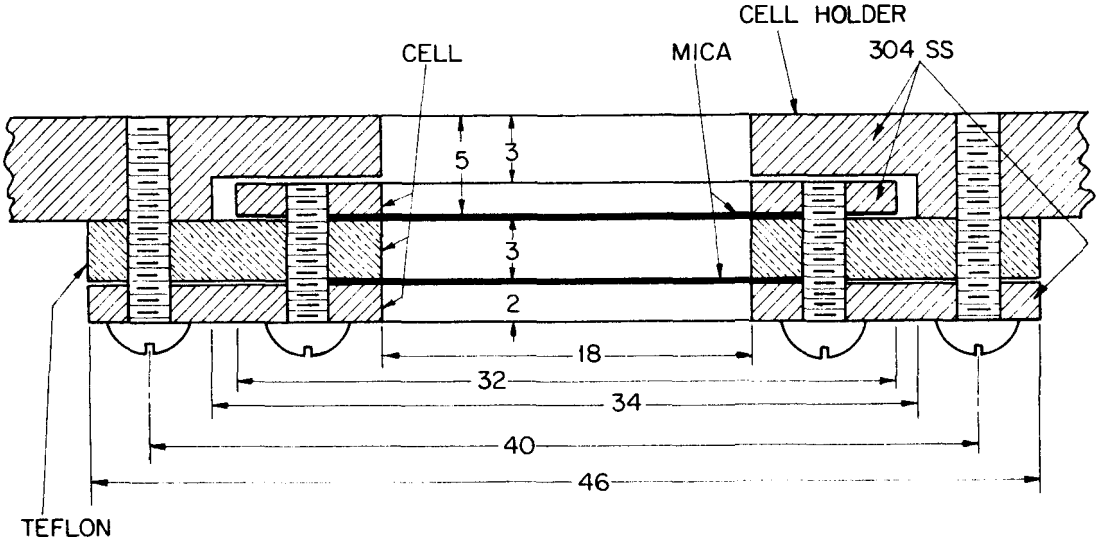

Figure 28. Component Parts and Cross-Section of Small Angle X-Ray Scattering Cell.

Reiss-Husson and Luzzati developed an interpretation method of absolute small angle X-ray scattering by micellar solutions of soaps and detergents in water.[22] Their method would lead to a determination of the concentration ranges in which the micelles may be assumed to be monodispersed. When the structures are independent on concentration, the micelle size and shape can be determined more directly.

When lysozyme from white of hen's eggs was dispersed in 0.15 M aqueous saline solution in six concentrations ranging from 1.01 to 4.95% at pH $\approx$ 5.7, contained in a cell with parallel windows of mica for transmission of the direct and scattered X-ray beams, Luzzati, Witz, and Nicolaieff[23] found that the radius of gyration was about 15.2 Å as compared to Ritland, Kaesberg, and Beeman's results of 16.0 Å for lysozyme in aqueous solution.[24] This shows the adaptibility of the technique for the study of the large molecules of biochemistry.

Siegel found that the polar, more heavily scattering ends, are in the interior of the micelle of the aerosol di - (2-ethylhexyl) sodium sulfoccinate in n-dodecane for the concentration range 6% - 75%.[25] The sample holder consisted of an aluminum plate 1.5 mm thick with a rectangular aperture which was covered with 0.001 in. polystyrene windows.

A number of interesting measurements of so-called spherical viruses have been published by Beeman and his co-workers using four-slit collimation arrangement similar to that of Hight, Higdon, and Schmidt discussed earlier.[14] The sample solution to be studied was placed in a Lucite sample holder about 1 mm thick, with film. They found that the southern bean mosaic virus had a spherical diameter of 286 Å. In the case of tobacco necrosis virus, a spherical shape with a diameter of 280 Å was obtained. The measurements of tomato bushy stunt virus led to a spherical particle of 310 Å diameter.

Fournet studied a solution of colloidal silver and obtained a curve of log I vs h^2 which had a long linear part; from this the radius of gyration was easily determined to be 50 Å.[15] The results of this experiment were confirmed by a measurement with the electron microscope. The micelle appeared as approximately spherical particles with a rather uniform diameter of about 120 Å. The sphere of radius of gyration of 50 Å has a diameter of 130 Å.

Dwiggins made a small angle X-ray scattering study of the colloidal nature of petroleum using a flat sample cell whose windows were 0.0064 cm thick Mylar film. Radii of gyration were determined for several whole crude oils, for crude oils diluted with solvents, and for oil at different temperatures. No large temperature effect was detected.[26]

Yen et al., extended X-ray studies into the small angle region on petroleum asphaltics using known weights (ca. 0.5 g) of the specimen packed in a rectangular cell of known dimensions (1.38-cm x 0.4-cm x 0.2-cm) made of brass plate. No binders or adhesives were used. A new band was found at sin θ/λ equal to 0.015, corresponding to a Bragg equivalent distance (diameter of the particle) of approximately 50 Å.[27,28]

B. Determination of Asphaltene Charge by Electrophoretic Measurements
(L. Hachigian and D. B. McAlpine)

Asphaltenes from crude oil and liquefied coal are known to possess some electrical charge. The exact cause for the charge is not clearly understood with both positive and negative values of the charge reported. Asphaltenes can take on the charge of adsorbed metal ions. Asphaltenes can also exist as free radial species during coal dissolution and subsequent chemical changes.

Precipitation of petroleum asphaltenes while flowing through porous media have been observed.[29] This is believed to be associated with neutralization of the electric double-layer surrounding an asphaltene colloid micelle by the streaming potential produced when charge compounds flow through porous media. It is also possible for two or more micelles to be forced together into a larger kinetic unit by drag forces when asphaltene micelles flow between extremely small particles. Precipitation of coal derived asphaltenes during filtration could have a significant influence on specific cake resistance and/or slurry viscosity.

Preckshot et al., measured the mobility of crude oil between closely spaced platinum electrodes.[29] Since deposition occurred on the positive electrode, they concluded that the asphaltene charge was negative. Csanyi and Bassi performed a similar experiment and found that 13 of 15 asphalts deposited onto the negative electrode.[30] The other two deposited onto the positive electrode. Wright and Minesinger performed experiments by suspending finely ground asphalts between electrodes and observed with a microscope that the particles in nitromethane migrated toward the negative electrode.[31]

In a previous study Addington did a preliminary experiment to determine the charge associated with coal derived asphaltenes. The asphaltene solution was prepared by adding 1.708 g of a 25%-pentane/75%-benzene-insoluble, 100%-benzene-soluble asphaltene obtained from the liquefaction of a Pittsburgh Seam, Ireland Mine Coal in the SYNTHOIL process to 100 ml of tetralin.[32] Platinum electrodes, spaced 3 mm apart, where placed into the solution with a voltage difference of 170 volts DC. After five days, there were deposits on both electrodes, but the positive electrode had considerably more.

In a few experiments conducted at Oak Ridge National Laboratory, dendritic deposition of coal derived asphaltenes was observed to deposit on the electrodes and form a bridge between electrodes.[33]

1. Equipment and Procedure for Measuring Electrical Charge

An experimental cell was constructed which could be disassembled so each electrode could be weighted separately at the conclusion of each run. The electrodes were made of 1/2 in. diameter, 304 stainless steel disks with 304 stainless steel lead wires. Each disk was press-fitted into a recess in a small, thin piece of teflon and the electrodes kept 1/16 in. apart with 1/16 in. teflon spacers. The cell was held together

with two No. 2/56 machine screws through the spacers and electrode holders. Photographs of the disassembled and assembled cell are shown in Figures 29 and 30.

A 125-325 volt DC regulated power supply was used and a milliampere or microampere meter inserted in the line as appropriate. The experiments were carried out in a 4 oz. glass bottle. Before each experiment, the faces of the electrodes were polished and each electrode was weighed. The wires were then pushed through a cork stopper which fits into the bottle and the cell placed with respect to the cork so the cell would be in the proper position. An asphaltene solution of known concentration was then added to the empty bottle, the cell put into position and the power supply leads attached to the electrode lead wires. The voltage was adjusted and maintained for the duration of the experiment. In the latest series of runs the experiment was continued until the current was reduced to one-half the initial value. At the completion of the experiment, the power supply was turned off, the cell was removed from the bottle and the solvent allowed to drain and evaporate. The cell was then disassembled and each electrode weighed.

In a number of runs the equipment was operated for a period of time, stopped, the electrodes weighed and cleaned and the experiment continued. This was done to determine the cause of the conductivity drop. In most cases the conductivity returned to approximately the starting value. In a few cases it increased beyond the original starting value. Apparently the drop of conductivity is related to the resistance of the material deposited on the electrode.

2. Experimental Results

Four experiments were performed with asphaltenes obtained from batch extraction 41(3). 15 experiments were performed with asphaltenes from batch extraction 61(3) and 11 experiments were performed with preasphaltenes from batch extraction 61(4). The source material was vacuum still bottoms from the Hydrocarbon Research, Inc. H-Coal process liquefaction of an Illinois No. 6, River King Mine Coal. The asphaltenes were 75%-pentane/25%-toluene-insoluble, 100%-toluene-soluble. The preasphaltenes are toluene-insoluble, THF-soluble. The earlier results on Ext. 41(3) are presented in Table 14 and the more recent results on Ext. 61(3) and 61(4) are given in Table 15. As discussed in Section I-B-4, the extracts contain some metals either as complexes or colloid size mineral particles. A photograph of the two electrodes after an experiment with pyridine as the solvent is shown in Figure 31.

The results in Table 15 are asphaltenes and preasphaltenes with five different solvents. More work is needed to sort out relative effects but a few observations can be made. The solvent affects the results significantly. Pyridine, THF, and m-cresol are good solvents and each participates in hydrogen bonding, pyridine being a strong base, THF as a weak base and m-cresol a weak acid. Benzene and tetralin are not particularly good solvents for asphaltenes and some micellization of the asphaltenes and preasphaltenes is expected. The electrical conductivity of pyridine

Table 14. Measurement of Electrical Charge on Asphaltenes Obtained from the Vacuum Still Bottoms from the Hydrocarbon Research, Inc. H-Coal Process Liquefaction of an Illinois No. 6 River King Mine Coal.

Run	1	2	3	4
Solvent	Tetralin	Tetralin	Pyridine	Pyridine
Asphaltene Concentration g/liter	50	50	50	50
Voltage, DC	200	300	300	300
Temperature, °C	~25	45	~25	~25
Duration, Days	5	6	6	3
Deposition:				
+ electrode, g	0.0006	0.0010	0.0818	0.0534
- electrode, g	0.0008	0.0060	0.0084	0.0005

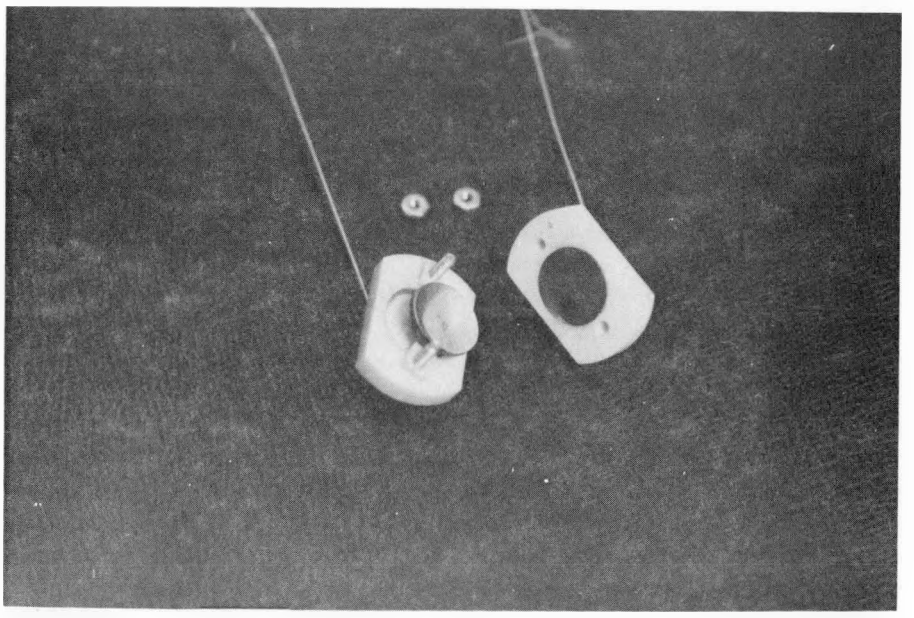

Figure 29. Photograph of the Cell Used to Measure the Charge on Asphaltenes-Cell Disassembled.

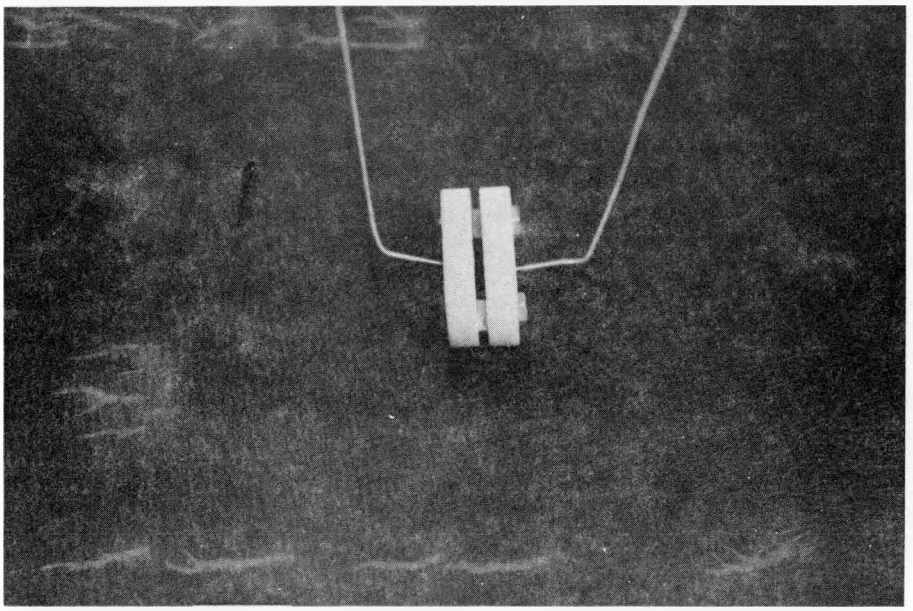

Figure 30. Photograph of the Cell Used to Measure the Charge on Asphaltenes-Cell Assembled.

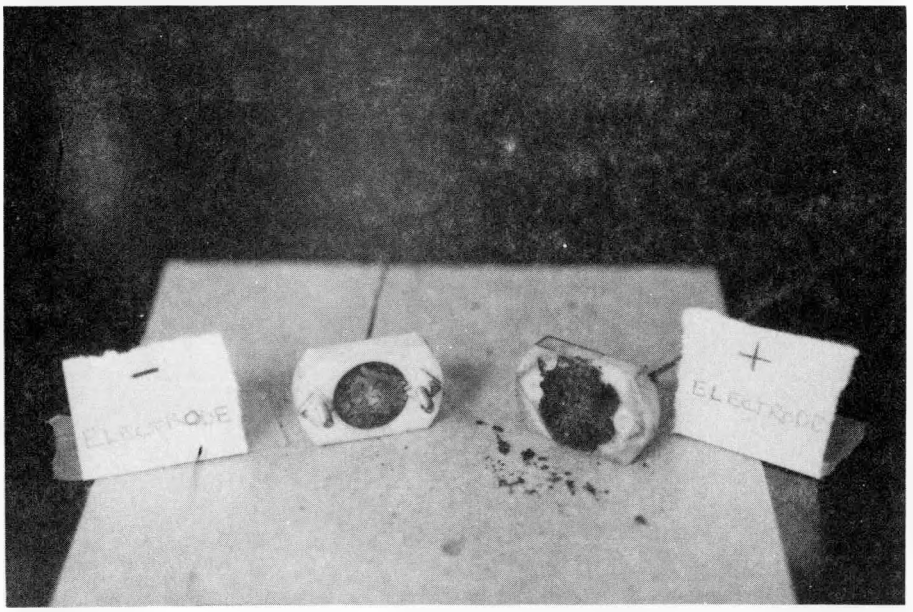

Figure 31. Photograph of the Electrodes After an Experiment with Pyridine as the Solvent.

Table 15. Electrodeposition of Material from Liquefied Coal Extracts of Hydrocarbon Research, Inc., H-Coal Vacuum Bottoms from an Illinois No. 6, River King Mine Coal Dissolved in Five Solvents.

Solvent	Run	Extract*	Concentration gm/l	Voltage dc	Current ma		Ambient or Bath Temperature °C	Run Time hours	Deposition from 50 ml	
					start	end			positive electrode g	negative electrode g
Pyridine	8	61(3)	45.0	300	9.0	4.5	27	3.75	0.0020	0.0005
Pyridine	9	61(3)	46.4	300	10.5	5.0	28	2.00	0.0044	0.0001
Pyridine	32	61(3)	43.1	300	10.0	5.0	28	3.00	0.0056	0.0004
Pyridine	42-1	61(3)	44.3	300	13.0	7.5	100	2.80	0.0230	0.0005
Pyridine	42-2	61(3)**		300	14.5	7.5	100	3.00	0.0219	0.0005
Pyridine	13	64(4)	47.0	200	24.0	18.0	29	0.50	0.0041	0.0006
Pyridine	38-1	61(4)	50.2	300	34.0	20.0	27	0.25	0.0125	0.0050
Pyridine	38-2	61(4)**		300	22.0	15.0	27	0.60	0.0128	0.0009
Pyridine	41-1	61(4)	52.6	200	28.0	24.0	100	0.50	0.0198	0.0007
THF	15	61(3)	34.2	300	2.5	1.5	28	31.0	0.0018	0.0001
THF	18-1	61(3)	44.2	300	2.0	0.7	28	76.0	0.0071	0.0004
THF	18-2	61(3)**		300	2.25	1.0	53	7.5	0.0085	0.0009
THF	20-1	61(3)	50.7	300	2.5	1.0	53	24.0	0.0069	0.0005
THF	20-2	61(3)**		300	1.75	1.0	25	24.0	0.0034	0.0003
THF	50	61(3)	60.3	300	3.25	1.0	25	359.5	0.0046	0.0017
THF	16	61(4)	51.5	300	6.0	2.0	28	0.75	0.0090	0.0013
THF	19-1	61(4)	47.3	300	5.0	1.5	27	0.85	0.0089	0.0025
THF	19-2	61(4)**		300	4.5	2.0	53	0.50	0.0019	0.0071
THF	36-1	61(4)	53.8	300	6.5	2.0	27	0.60	0.0081	0.0014
THF	36-2	61(4)**		300	7.0	3.5	53	0.75	0.0019	0.0050
THF	39-1	61(4)		300	6.0	1.0	52	1.25	0.0078	0.0052
THF	39-2	61(4)**		300	5.0	2.0	52	2.00	0.0033	0.0069
m-Cresol	57	61(3)	34.0	300	12.5	5.5	100	5.25	0.0118	0.0002
m-Cresol	58	61(4)	25.0	300	9.5	5.5	100	5.25	0.0146	0.0005
Benzene	31	61(3)	43.7	300	0.0006	0.0002	26	27.25	0.0007	0.0014
Benzene	49	61(3)	44.1	300	0.0008	0.0002	60	37.50	0.0036	0.0063
Tetralin	11	61(3)	59.8	300	0.0006	0.0002	28	21.5	0.0003	0.0007
Tetralin	14	61(3)	54.1	300	0.0078	0.0006	140	7.5	0.0014	0.0046
Tetralin	37-1	61(3)	45.4	300	0.0086	0.0044	140	19.0	0.0017	0.0018
Tetralin	37-2	61(3)**		300	0.0100	0.0054	140	32.0	0.0041	0.0057
Tetralin	45-1	61(3)	41.0	300	0.0090	0.0054	140	16.0	0.0100	0.0151
Tetralin	45-2	61(3)**		300	0.0110	0.0076	140	19.5	0.0006	0.0013
Tetralin	12	61(4)	27.6	300	0.0032	0.0020	140	6.25	0.0016	0.0035
Tetralin	17	61(4)	28.0	300	0.0038	0.0022	140	7.5	0.0018	0.0039
Tetralin	46-1	61(4)	20.4	300	0.0024	0.0014	140	15.5	0.0049	0.0091
Tetralin	46-2	61(4)**		300	0.0020	0.0006	140	21.5	0.0008	0.0048

*Extract 61(3) was toluene soluble, 75% pentane-25% toluene insoluble
Extract 61(4) was THF soluble, toluene insoluble

**Electrodes were cleaned after Run __-1 and run continued with same liquid.

and m-cresol is higher than that of THF and much, much higher than that of benzene and tetralin. The presence of asphaltenes and preasphaltenes in solution increases the conductivity.

Some deposition of material occurs on both electrodes. Much more material deposits on the positive electrode (negative charge) with pyridine and m-cresol but the opposite is true for benzene and tetralin where more material deposits on the negative electrode (positive charge). The amount of deposition for a given voltage and run time depends most significantly on the solvent strength and secondarily on the electrical conductivity of the solvent. The amount of deposition is dependent upon the degree of colloid peptization, being greatest in stronger hydrogen bonding solvents at elevated temperatures.

Asphaltenes in THF give results similar to pyridine and m-cresol, but behave differently with preasphaltenes. With preasphaltenes in THF, the initial deposition is primarily on the positive electrode. After the electrodes are cleaned, placed in the residual solution and the experiment continued, subsequent deposition is highest on the negative electrode with only minor changes in the starting currents.

The apparent loss of solution electrical conductance during the period of a run is associated with the build-up of solids on the electrodes. After cleaning the conductivity of the residual solution is approximately the same as the starting material and occasionally it is higher.

C. Electrical Conductivity of Solvents Containing Asphaltenes and Preasphaltenes (D. McAlpine)

Electrical conductivity measuring equipment has been set up to measure the electrical conductivity and dielectric constants of solvents and of solvents with additions of asphaltenes, preasphaltenes, and oils and resins either individually or in combination. The set up and procedure are in accordance with ASTM standards. A Balsbaugh Model LRC-1 Liquid Reference Cell and Keithley Model 610C Electrometer are used for conductivity measurements. The cell and a Radiometer MM2 RLC meter will be used for dielectric measurements.

The cell has been calibrated and some preliminary measurements of the electrical conductivity of asphaltenes in benzene have been made.

This work will be continued next quarter to provide basic data for streaming potential measurements in the adsorption work which is presently being done.

IV. ADSORPTION CHARACTERISTICS OF ASPHALTENES
(D. V. Addington)

Significant progress on the adsorption phase of this project was made during the last year. Preliminary work, necessary before getting to the experimental adsorption work, was accomplished. Among this work was a characterization of the chosen adsorbent solids. Coal derived asphaltenes were extracted and then separated by gel permeation chromatography. These asphaltenes were then characterized by elemental analysis, molecular weight, and NMR. Linear elution adsorption chromatography was used in conjunction with model compounds and asphaltene fractions to examine the forces of attraction for adsorption onto alumina and silica gel.

After this preliminary work was completed, the two basic phases of the adsorption work were started. The first phase, the measurement of batch equilibrium adsorption isotherms, has been completed except for work with acidic and basic asphaltene samples. The second phase, the adsorption in the flow system along with streaming potential measurements, is progressing well and partially complete.

The adsorbent solids chosen for the experimental program have been characterized by surface area and density. Also, the surface area was measured as a function of pore diameter for six of the solids, which may be of importance in the later work. Particle size analyses of several of the solids have been completed. This preliminary work is necessary before any of the adsorption data can be properly analyzed.

The separability of coal derived asphaltenes and several model compounds was examined on water deactivated alumina and silica gel. The linear elution adsorption chromatography (LEAC) method developed by Snyder was used to compare the general separability of some coal derived fractions.[34,35] Since the adsorption mechanism for most organic compounds is predominately the adsorption of functional groups at specific sites, the effect of such functional groups and heteroatoms was of interest. Several two and three ring aromatic compounds with various functional groups were obtained and their retention volumes measured on a standard Alcoa F-20 Alumina plus silica gel. Coal derived asphaltene fractions were also run to determine their retention volumes. The results are more qualitative than quantitative but some general conclusions can be drawn.

In some of the early equilibrium isotherms, there appeared to be more adsorption of higher molecular weight material. The solvent extracts have a rather wide molecular weight range and were not considered to be of a homogenous nature. Therefore the third fraction from the extraction procedure was further separated by gel permeation chromatographic in a larger column. The toluene-soluble, 75%-pentane/25%-toluene-insoluble asphaltenes from the H-Coal vaccum still bottoms from the liquefaction of an Illinois No. 6, River King Mine Coal which had been fractionated in the 10.16-cm ID x 122-cm long GPC column were characterized by elemental analysis, molecular weight, and proton NMR. Samples of the

2nd, 3rd, 4th, and 5th fractions from the GPC runs were further separated in a 25 mm ID x 100-cm long column and the molecular weight distribution determined for each sample. Results of these analyses are found elsewhere in this report. The 2nd-5th fractions are the ones of major interest in the adsorption work.

The narrow molecular weight fractions from the 10.16-cm ID x 122-cm long GPC fractionation were used to study the effect of asphaltene molecular weight, temperature, solvent, and solid adsorbent on asphaltene adsorption. Five asphaltene fractions and one preasphaltene fraction were used to assess the effect of molecular weight on adsorption. The effect of temperature range on asphaltene adsorption was investigated from 30° to 180°C using tetralin as a solvent. The effect of solvent properties was studied by using pyridine, tetrahydrofuran, tetralin, toluene, and nitrobenzene as solvents. Finally seven solids, solids present in coal liquefaction processes and two laboratory standards, were used as adsorbents to show any effect of surface area, pore size, and surface properties.

Results of the study of adsorption in flow through fixed beds were inconclusive. It was hoped that breakthrough curve from the flow system could be compared to predictions from the equilibrium isotherms. However, there appears to be a significant amount of irreversibly adsorption of a portion of most asphaltene samples. This makes any correlation with the equilibrium isotherms very inaccurate.

Another part of the experimental objective of the flow studies was to examine the streaming potential of flowing asphaltene solution through a fixed bed. This work has been fairly successful. Streaming potential results can be used to draw some conclusions about the adsorption of the asphaltenes and bring about a better understanding of their behavior.

A. Solids Characterization
(D. V. Addington)

Nine solids were originally proposed for the adsorption work and were obtained. These nine were chosen to represent a variety of surfaces which may be of importance as standards or be present in any coal liquefaction process. Two additional solids were later added for the streaming potential measurements.

The solids, listed in Table 16, are: two diatomaceous earths, frequently used as precoat materials in filtration, two standard laboratory adsorbents, a coal liquefaction catalyst, mineral matter from SYNTHOIL and H-Coal process runs, a gasifier char from a Utah High Vol. B Coal, Illinois No. 6 Coal, and refuse from coal beneficiation of a Pittsburgh Seam Coal. The materials represent solids of various mineral composition, surface area, density, and particle size. Characterization of the adsorbent surface in any adsorption process is necessary. Nine of these solids were characterized by true density and surface area. Preliminary

results on some asphaltene adsorption isotherms showed inconsistencies with respect to monolayer coverage of the solids. If this is due to restrictions in the fine pores, then a knowledge of the surface area available for a given pore size would be of value. Six of the solids were analyzed for surface area as a function of pore size.

All solids were pretreated by vacuum drying at 200°C for 24 hours. The densities were determined on a Micromeritics Model 1302 Helium Air Pycnometer. The surface area and surface area/pore diameter distributions were done on a Micromeritics Model 2100 Orr Surface Area/Pore Volume Analyzer. The B.E.T. equation and nitrogen were used for the surface area determinations. The results of the surface area and density measurements are shown in Table 16. Figures 32 through Figure 37 are the surface area distributions for six of the solids.

Table 16. Characteristics of Solids Proposed for Adsorption Experiments.

Adsorbent	Surface Area (m^2/g)	True Density (g/cc)
Celite 503	1.4	2.32
Celite 550	1.0	2.30
Alcoa F-20 Alumina	212	4.09
Aero HDS-1442A Catalyst	296	6.2
Grace 923 Silica Gel	441	2.55
Ext. 8, SYNTHOIL Mineral Matter	8.0	2.43
Ext. 18, H-Coal Mineral Matter	7.9	2.41
Ext. 30, H-Coal Mineral Matter	10.7	2.56
Utah High Vol. B Gasifier Char	136	5.1
Illinois No. 6 Coal	...	...
Ash, Pyrites, and Coal > +2.0 S.G. Pittsburgh Seam, Monogalia Co., W. Va.	...	...

B. Separation By Linear Elution Adsorption Chromatography
(D. V. Addington, C. E. Berry, Jr., K. A. Heringhausen, and J. R. Skelly)

Since the adsorption of organic compounds on solids is strongly affected by the presence of heteroatoms and functional groups, the effect of this factor needs to be considered. One method of determining this effect is to determine the chromatographic separability of the compounds. Several chromatographic techniques have been used in the separation of multicomponent mixtures. Physical separation of heavy end mixtures like coal liquids appears possible only by elution chromatography from a solid

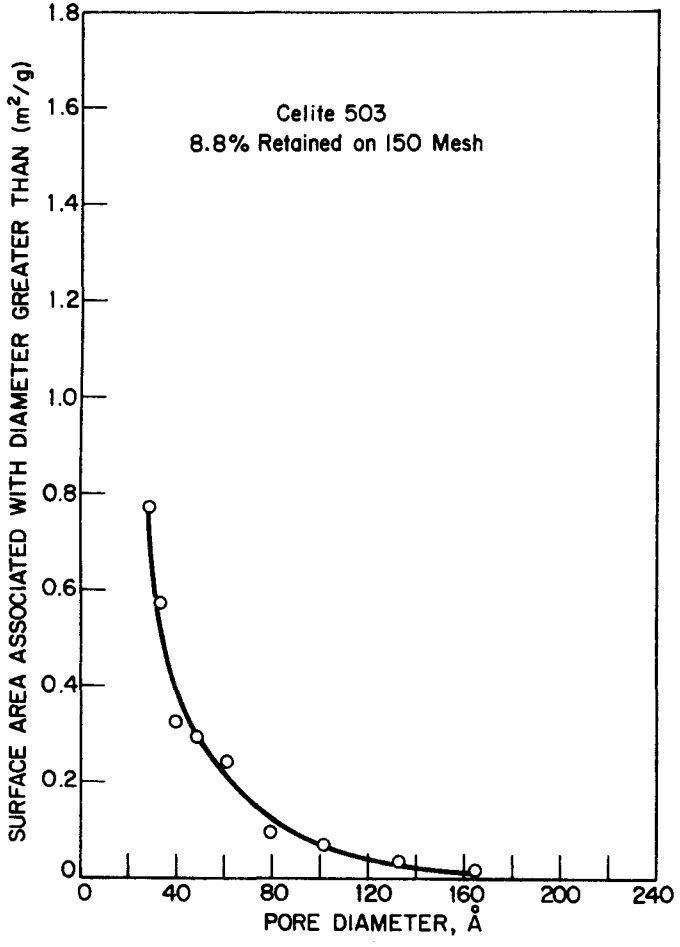

Figure 32. Pore Size Distribution Celite 503, Diatomaceous Earth.

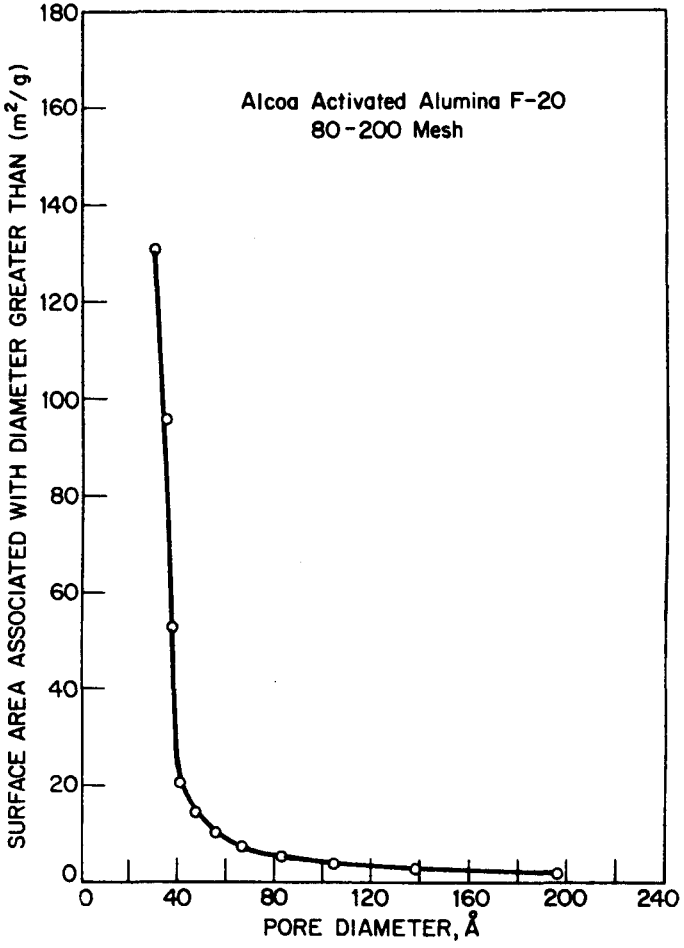

Figure 33. Pore Size Distribution Alcoa F-20 Activated Alumina.

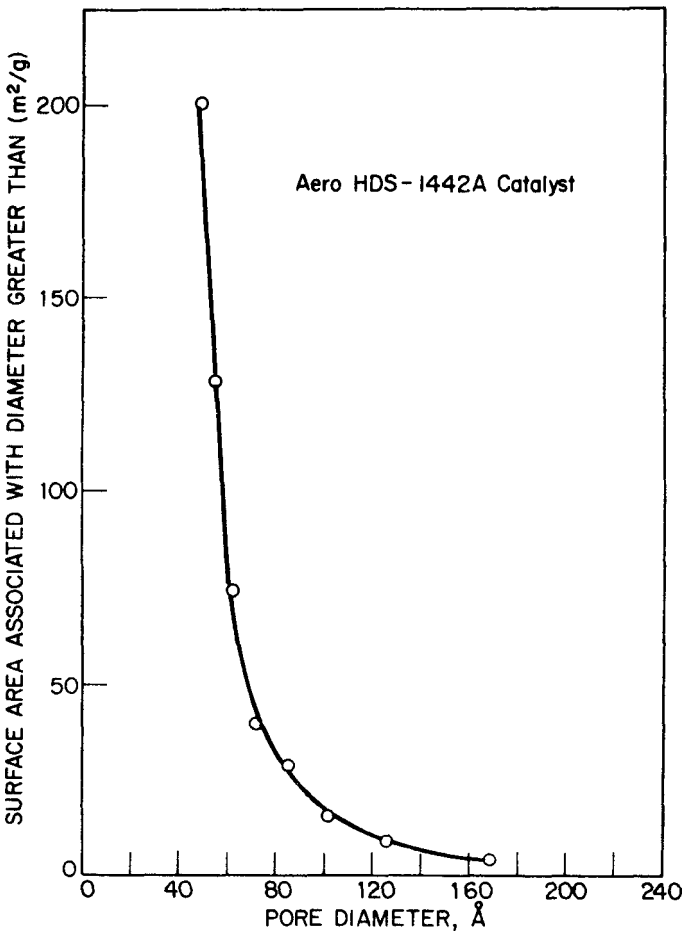

Figure 34. Pore Size Distribution of Aero HDS-1442A Catalyst.

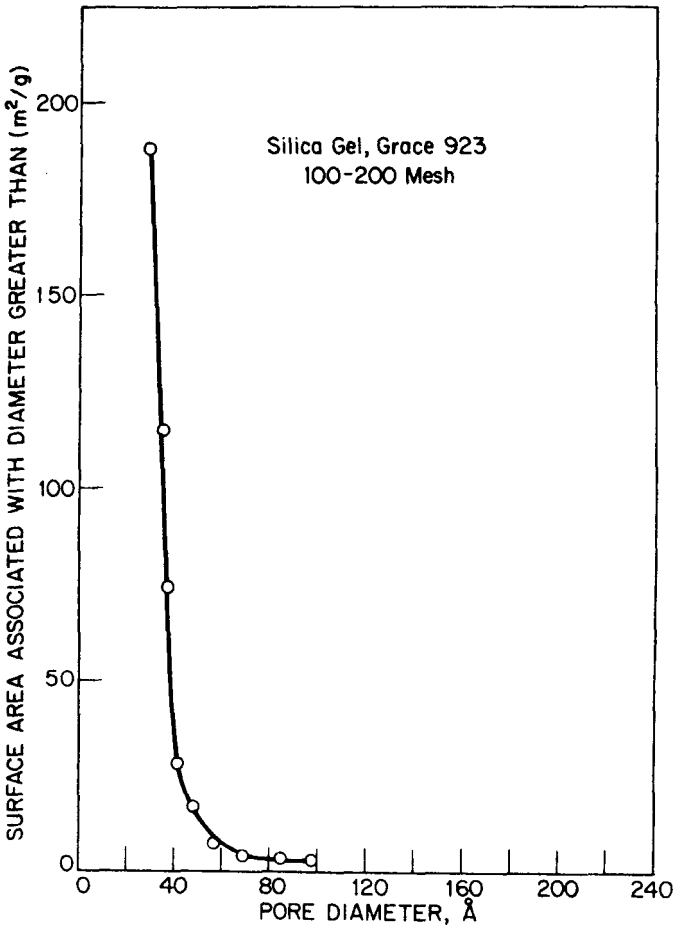

Figure 35. Pore Size Distribution of Grace 923 Silica Gel, 100-200 Mesh.

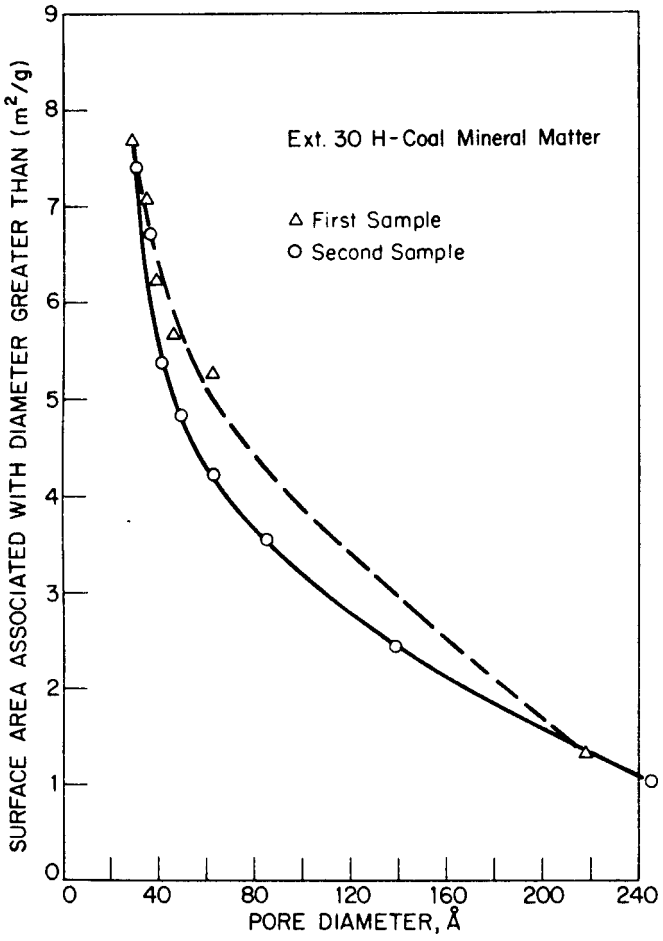

Figure 36. Pore Size Distribution H-Coal Mineral Matter from Illinois No. 6 Coal, River King Mine.

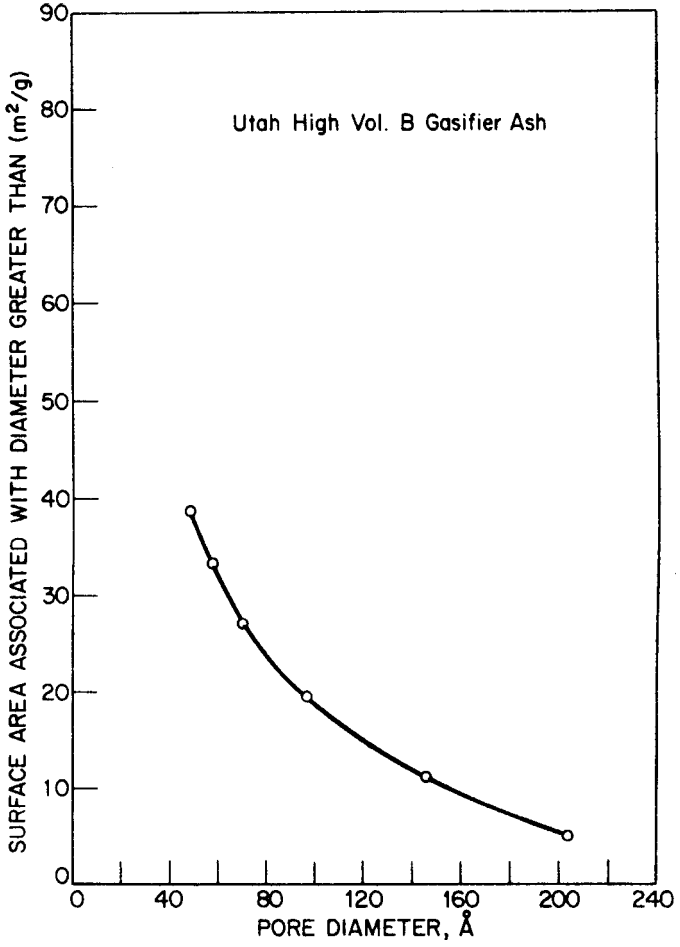

Figure 37. Pore Size Distribution Gasifier Ash from Brigham Young University Entrained Flow Gasifier.

stationary phase. Snyder et al., have developed one technique called linear elution adsorption chromatography (LEAC).[34] By working in the linear region of the adsorption isotherm, it is possible to give a quantitative description of multi-component chromatographic separations. By restricting the adsorption to the linear region, it is possible to gain some information on intramolecular forces and configuration in the adsorbed state.

LEAC is based on the measurement of a retention volume, R, defined as the eluent volume required to elute 50 wt. % of the solute through the column. This retention volume is standardized per weight of adsorbent solid present by subtracting the void volume and dividing by the weight of the solid adsorbent.

The model equation for LEAC is:

$$\log \underline{R}^\circ = \log V_a + \alpha[\sum^{i} Q_i^\circ + \sum^{i} q_i - \varepsilon^\circ \sum^{i} \delta_i] \qquad (3)$$

where, $\underline{R}^\circ$ = Retention volume/unit weight

V_a = Adsorbed volume for solid

α = Activity function for solid

Q_i = Solute structure group factor

q_i = Solute geometry factor

δ_i = Solute size factor

ε° = Eluent polarity or eluting power

The retention volume, $\underline{R}^\circ$, is proportional to an energy of adsorption and is equivalent to the log retention volume in gas chromatography and R_m of paper chromatography. The constants V_a and α are characteristic of the solid adsorbent and have been characterized for Alcoa F-20 alumina as a function of the water deactivated state of the alumina. The contribution to the adsorption by each solute structural group is given by a Q_i valve. The q_i term is added when the geometry of the molecule affects the $\underline{R}^\circ$ valve. The eluent polarity parameter is defined as zero for n-pentane and increases for more polar solvents (benzene 0.32). The molar volume of the solute is calculated by summing the contributions for each individual solute atom δ_i.

For the present work Alcoa F-20 Alumina and Grace 923 Silica Gel were used as the solid adsorbents. Both are widely used as standard laboratory adsorbents.

Silica gel, silica and silicic acid all refer to the same adsorbent. Quartz is quite similar. The adsorptive properties of these materials depend on the hydroxyl groups attached to surface silicon atoms and to the amount of physically adsorbed water which effectively blocks the underlying active surface.[36] Three types of surface hydroxyls exist. They are: 1, "bound", 2, "reactive", and 3, free:

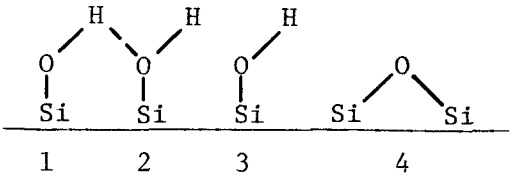

The relative strengths of the hydroxyls are:

$$1 < 3 < 2$$

Physically adsorbed water can be removed without altering the hydoxyls by heating the silica gel to between 150 and 250°C. By adding back a definite amount of water, the adsorbent activity can be controlled. Prolonged heating above 250°C will produce surface siloxane groups, group 4 above, which are less active and nonspecific to polar, nonpolar, saturated and unsaturated molecules. Silica gel is commonly called an acidic adsorbent. Its surface hydroxyls exhibit a weak acidity, but the acidic characteristics often observed is attributable to acidic impurities.

Crystalline forms are controlled by preparation method and activation temperature. Less is known about the surface characteristics of alumina. The existance and role of surface hydroxyls is less clear.[36] The activity of alumina increases above 200°C and continues to increase with temperature until 1000°C where active low-temperature aluminas transform into inactive α-alumina.

The active adsorption sites are believed to be exposed aluminum atoms or strained Al-O bonds. The addition of fixed amounts of water to alumina heated above 400°C gives good control over the activity. Alumina is normally considered a "basic" adsorbent although both acidic and basic sites are present. The acidic sites adsorb most polar and unsaturated molecules and the basic sites adsorb acids strongly.

1. Alumina Results

The alumina was calcined and then deactivated with 2.5 wt. % water. The alumina was packed by vibrating and tamping in an Altex 252-00 6-mm ID x 250-mm long analytical column, nominal volume 6.0 ml. Mallinckrodt analytical reagent benzene was used as the solvent and contained in an air tight system, purged with nitrogen. The sample was injected with an Altex 201-56 slider injection valve with sample volume of 0.0387 ml. The elution breakthroughs were observed by the response of an Altex Model 153 UV Detector (313 nm wavelength) on a strip chart recorder. Before each injection the column was wetted with solvent and the UV detector was stabilized. The column loading for all experimental runs was set at 6×10^{-5} g. solute/g. alumina.

The UV detector response was integrated as a function of elution volume and the 50% solute removal determined from this integration. For the pure components the UV response should be directly proportional to

the mass eluted. For the model compounds, all UV curves appeared nearly symmetrical indicating that the adsorption was in the linear region. In previous work in this project it was found that the UV characteristics of several liquefied coal fractions varied widely because of the rather wide molecular weight distribution.[2] The UV response to the coal derived fractions should give some indication of the mass present but will not be directly proportional the the mass present. Therefore, the breakthrough curves of the coal fractions are more qualitative than quantitative in nature.

Twenty-two various compounds and coal derived fractions which were tested are listed in Table 17. Elution curves for several of the solutes are shown in Figure 38.

Figure 38a shows two representative breakthrough curves for those model compounds which contain no heteroatoms. All these hydrocarbons had very low retention volumes which means a very low energy of adsorption. The figure also shows the curve for dibenzothiophene, one of the model compounds containing sulfur. Evidently, the sulfur atom in the compound has very little affinity for the alumina surface.

Several of the curves for oxygen containing compounds are shown in Figure 38b. The oxygen atom in these compounds clearly is attracted to the alumina surface and shows a stronger adsorptive capacity than the aromatic ring systems. Dibenzofuran seems particularly unusual to have such a low retention volume, a fact which remains unexplained at this time. Xanthene with its oxygen in a six member ring system shows the strongest adsorption of the oxygen containing compounds tested. It should be noted that the 9-hydroxyfluorene was almost completely ionized on the alumina surface. This is in agreement with what has been observed elsewhere.[37]

Four breakthrough curves for nitrogen containing compounds are shown in Figure 38c. The basic pyridine like nitrogen compounds showed the strongest adsorption with 5,6-benzoquinoline being stronger than acridine probably because of molecular geometry. The pyrrole like nitrogen compounds showed a weaker adsorption but still stronger than most of the oxygen compounds. It is interesting to note that the two compounds with two heteroatoms each, phenothiazine and phenoxazine, showed approximately the same retention volume. This retention volume was actually less than that of the similar carbazole. It would appear that the adsorption configuration for these two compounds would be with the nitrogen adsorbed on the surface and the sulfur and oxygen in the bulk solution.

The elution curves for three coal derived fractions are shown in Figure 38d. The oil fraction was the pentane-solubles from H-Coal vacuum still bottoms from the liquefaction of an Illinois No. 6, River King Mine Coal. The asphaltenes were a toluene-soluble, 25%-toluene/75%-pentane-insoluble fraction from the same extraction. These asphaltenes were then separated into an acidic-neutral and a basic fraction by the method of Sternberg.[11] This procedure is explained in another section of this report. Little adsorption would have been expected for the oils and this

Table 17. Retention Volume For 50 Weight Percent Solute Elution With Benzene of Model Compounds Adsorbed on 2.5 Weight Percent Water Deactivated Alcoa F-20 Alumina.

	Model Compound	Formula	Structure	Retention Volume (ml/g)in Benzene
1.	9-Phenylanthracene	$C_{20}H_{14}$	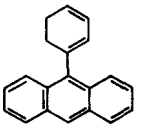	.206
2.	9, 10 Dihydroanthracene	$C_{14}H_{12}$	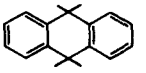	.216
3.	Anthracene	$C_{14}H_{10}$	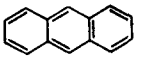	.224
4.	Dibenzofuran	$C_{12}H_8O$	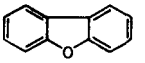	.224, .206
5.	Phenanthrene	$C_{14}H_{10}$	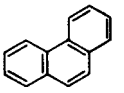	.234
6.	9-Methylanthracene	$C_{15}H_{12}$	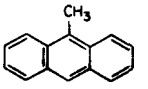	.287
7.	Dibenzothiophene	$C_{12}H_8S$	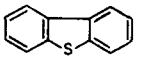	.310
8.	Ext. 41(1) Oils	...		.437
9.	Acidic-Neutral Asphaltenes 41(3)	...		1.32
10.	9-Fluorenone	$C_{13}H_8O$	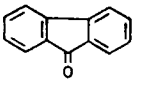	1.48
11.	9-Anthraldehyde	$C_{15}H_{10}O$	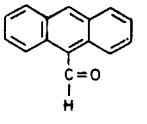	1.49

Table 17. (concluded)

	Model Compound	Formula	Structure	Retention Volume (ml/g)in Benzene
12.	Anthracene-9-Carboxylic Acid	$C_{15}H_{10}O_2$	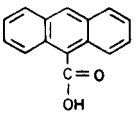	1.85
13.	Anthrone	$C_{14}H_{10}O$	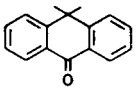	2.04
14.	Phenothiazine	$C_{12}H_9SN$	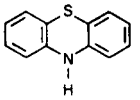	2.19
15.	Phenoxazine	$C_{12}H_9NO$	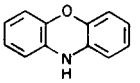	2.28
16.	Carbazole	$C_{12}H_9N$	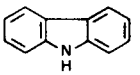	3.05, 2.92
17.	9-Hydroxyfluorene	$C_{13}H_{10}O$	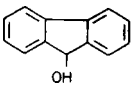	3.29*
18.	Xanthene	$C_{13}H_{10}O$	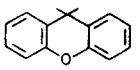	3.68
19.	Acridine	$C_{13}H_9N$	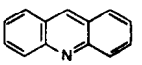	4.42
20.	Basic Asphaltenes 41(3)	...		4.49
21.	5, 6 Benzoquinoline	$C_{13}H_9N$	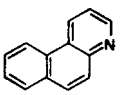	6.42
22.	α,α' Hexamethylene-bisquinoline		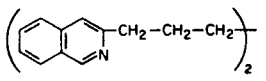	42.6

*Significant ionization of the phenolic group on the alumina

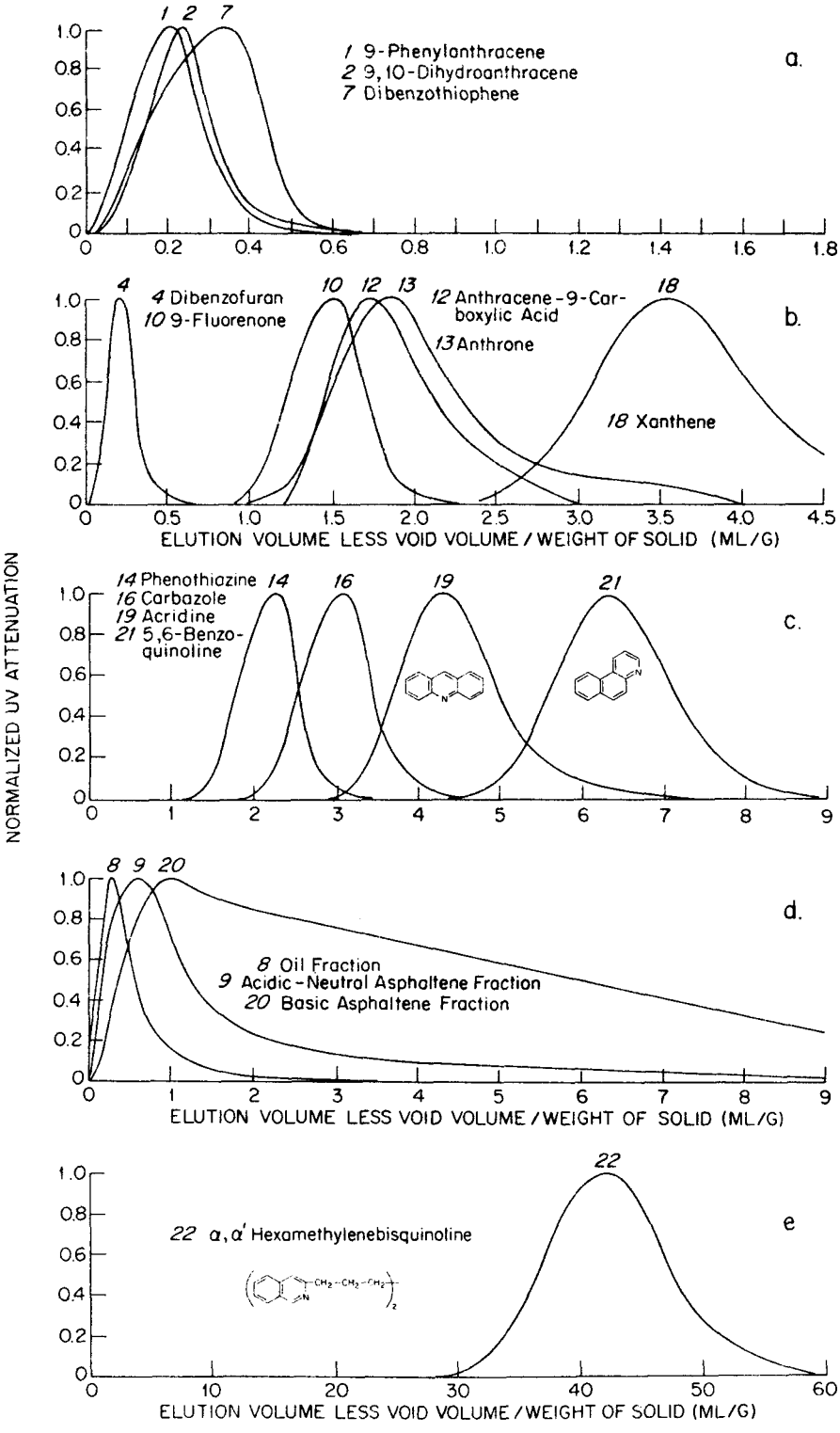

Figure 38. Normalized Elution Adsorption Curves for Model Organic Compounds Adsorbed onto 2.5 Weight Percent Water Deactivated Alcoa F-20 Alumina at 25°C.

result was observed. The acidic-neutral and basic asphaltene fractions both showed peaks quite early with very definite tailing. These mixtures act as if they are not all in the linear adsorption range. Each mixture contains a number of compounds. The functional groups are clearly different. As explained earlier the UV response is not directly proportional to mass but does give some indications of the elution breakthrough. Knowing the acidic nature of the alumina surface, the stronger adsorption of the basic fraction is not too surprising. However, it is surprising that a large percentage of the asphaltenes came through the column so rapidly. This may imply that the heteroatoms are interior to the molecules or are sterically hindered to prevent strong adsorption to the alumina surface.

Figure 38e shows the breakthrough curve for a bifunctional model compound synthesized in the Chemistry Department. The compound, α,α'-hexamethylenebisquinoline has its two nitrogens located such that adsorption at two sites is quite conceivable. From the large value of retention volume, it would appear that such a phenomena is occurring. For the molecule to desorb, the bonds at two sites would have to be broken. When the first nitrogen is desorbed, it may have a good chance of readsorbing before the other nitrogen is desorbed. From the proposed model of coal asphaltenes, such flexible bifunctional molecules are quite possible. This phenomena might be one of the reasons for the many reports of asphaltenes being irreversibly adsorbed.

From this phase of the adsorption work, it appears that the basic portion of asphaltenes are the most strongly adsorbed. The asphaltenes may consist of materials with widely differing adsorption characteristics so further separation may be needed.

2. Silica Gel Results

The adsorption of selected compounds in benzene, chloroform and THF onto 4%-water-deactivated Grace 923 Silica Gel was measured by the LEAC procedure. The results are presented in Table 18. A calibration figure, Figure 39, was prepared giving the retention volume of xanthene as a fraction of the percent water deactivation of the silica gel. Runs with xanthene provide a check on the degree of deactivation.

As expected, the adsorption of the nitrogen bases, acridine, and 5,6-benzoquinoline are much greater for silica gel than alumina.

The important of the solvent is shown in Table 18 for 9-hydroxyfluorene, xanthene and 5,6-benzoquinoline. THF and chloroform, hydrogen bonding solvents, compete with the solutes for the active sites. THF is stronger than chloroform.

Table 18. Eluent Volume For 50 Weight Percent Solute Elution with Benzene of Model Compounds Adsorbed on 4-Weight-Percent-Water-Deactivated Grace 923 Silica Gel.

	Model Compound	Formula	Structure	Retention Volume (ml/g)in Benzene	Chloroform	THF
1.	Anthracene	$C_{14}H_{10}$	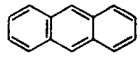	0.322		
2.	Dibenzofuran	$C_{12}H_8O$	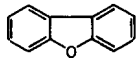	0.307		
3.	Dibenzothiophene	$C_{12}H_8S$	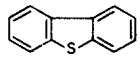	0.362		
4.	9-Fluorenone	$C_{13}H_8O$	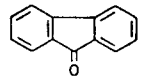	3.320		
5.	9-Anthraldehyde	$C_{15}H_{10}O$	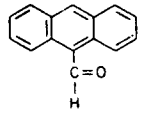	2.379		
6.	Phenothiazine	$C_{12}H_9SN$	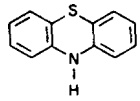	0.862		
7.	Phenoxazine	$C_{12}H_9NO$	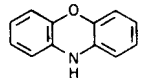	1.199		
8.	Carbazole	$C_{12}H_9N$	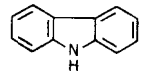	1.054		
9.	9-Hydroxyfluorene	$C_{13}H_{10}O$	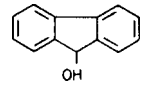	14.208	2.	0.22
10.	Xanthene	$C_{13}H_{10}O$	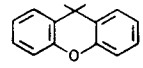	7.272	0.53	0.257

Table 18. (concluded)

	Model Compound	Formula	Structure	Retention Volume (ml/g) in Benzene	Chloroform	THF
11.	Acridine	$C_{13}H_9N$	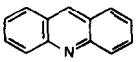	32.050	4.6	0.764
12.	5, 6 Benzoquinoline	$C_{13}H_9N$	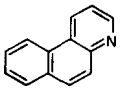	53.917		
13.	Anthrone	$C_{14}H_{10}O$	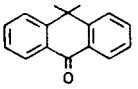	1.765		
14.	Anthracene-9-Carboxylic Acid	$C_{15}H_{10}O_2$	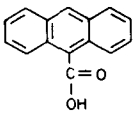	7.829		
15.	9-Phenylanthracene	$C_{20}H_{14}$	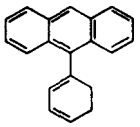	0.234		
16.	9, 10 Dihydroanthracene	$C_{14}H_{12}$	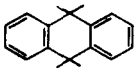	0.237		
17.	9-Methylanthracene	$C_{15}H_{12}$	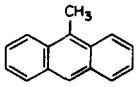	0.303		
18.	Phenanthrene	$C_{14}H_{10}$	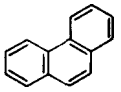	0.257		
19.	Phenol	C_6H_5OH			4.26	0.111

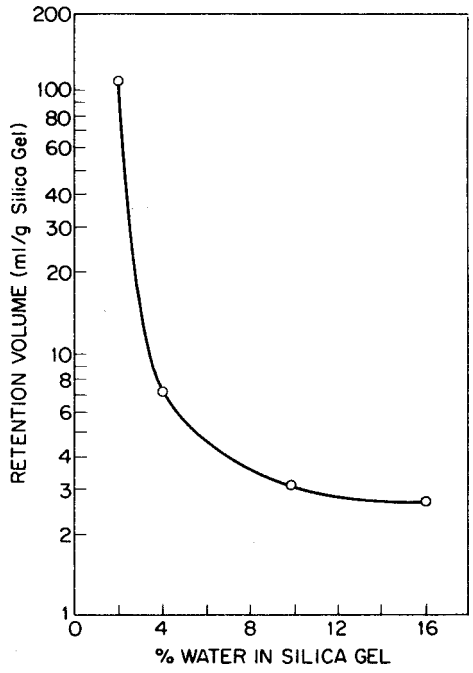

Figure 39. Effect of the Amount of Water Deactivation on the Adsorption of Xanthene on Grace 923 Silica Gel.

C. Equilibrium Adsorption Isotherms
(D. V. Addington)

The objective of this portion of the work was to determine the effect of several major variables on the amount of asphaltene adsorption. The major variables under study were the type and molecular weight of the asphaltenes, temperature, solvent, and solid adsorbent.

Since it appears that the asphaltene fractions are not totally adsorbed reversibly, it is somewhat improper to talk of an "equilibrium" isotherm. In this work the equilibrium asphaltene concentration is the solution concentration at the final steady state conditions.

1. Experimental Procedure

The experimental equipment for the batch adsorption work was basically very simple. Temperature control for the adsorption study was maintained in a constant temperature bath by a Polyscience Model 73 Immersion Circulator. Water was used as the bath fluid for the 30° and 80°C runs and peanut oil was used for the 130° and 180°C runs.

Previously, 20 ml asphaltene solutions were contained in a 50 ml bottom flask and a chain stirrer was used to mix the solution with the added solid adsorbents. This system had several experimental problems and weaknesses and a better procedure was developed.

The new procedure gives better mixing and reduces the quantity of asphaltenes required. A scintillation vial of 22-mm ID (nominal volume 24 ml) with a tin foil lined cap was used to hold the asphaltene solution. The adsorbent was added to the solution, the vial was tightly capped, and the solids and solution were mixed by rotating the vial. An extension clamp, inserted into an adjustable speed T-Line Model 102 Laboratory Stirrer, was used to hold the vial and rotate it to achieve the desired mixing. The stirrer was adjusted so the vial could be submerged in the constant temperature bath at an approximate angle of 45°, to keep the solids well mixed.

The following procedure was used in all the batch adsorption runs. For each isotherm a base asphaltene solution was prepared. This base solution was made by weighing a sufficient amount of solid asphaltenes in a 2 oz. or 4 oz. bottle. Sufficient solvent was added to the bottle to attain the desired concentration and the asphaltenes were allowed time to solubilize. For some solvents and asphaltene samples, the base solution was heated to help this solubilization step. This solution was then vacuum filtered with a 45-mm ID Buchner funnel and Whatman #42 filter paper (98% retention of 2 μm particles).

From this filtered base solution, asphaltene samples were made by accurate dilution. Usually five sample vials were filled with 10, 7.5, 5, 3.5, and 2 ml of the base solution. Sufficient pure solvent was then pipetted, if necessary, into each sample to make a 10 ml solution.

The solid adsorbents had been heated under vacuum at 200°C for 24 hours before surface area characterization and were subsequently used in this state. It was found that approximately 2 to 4 g. of solids worked best with a volume of 10 ml of solution. The solid adsorbents were weighed in a capped vial and the amount of solids was the difference between the vial weight before and after mixing the solids and asphaltene solution.

The actual adsorption runs took place under the following procedure. The sample vial with the 10 ml asphaltene solution was placed in the extension clamp (attached to the stirrer) and lowered into the constant temperature bath until half the vial was submerged. The vial was left at this point for five minutes (10 minutes at 80°, 130°, and 180°C) to allow the solution to come to near temperature. The vial was uncapped, a powder funnel inserted, and the solid absorbent poured into the asphaltene solution. The vial was recapped tightly, the stirrer immediately started, and the stirrer adjusted so that the vial rotated approximately 30 revolutions per minute. From some previous work, it was determined that one hour of mixing time was sufficient to achieve equilibrium. However in all these experimental runs, the asphaltene solution and solid adsorbent were allowed to mix for two hours. At this point the stirrer was stopped with the vial upright and the vial brought to the surface of the bath fluid so the vial cap was out of the fluid. A waiting period of five minutes was allowed for a majority of the solids to settle to the bottom of the vial. Then the cap was removed and a 2 ml glass pipette was used to remove approximately 2 to 2.5 ml of solution from the top of the asphaltene solution.

The concentrations of the base solution and each of the asphaltene solutions after adsorption were determined in the same manner. A 2 ml glass syringe with Luer Lok tip was attached and locked to a Millipore Swinny Stainless (13 mm diameter) filter holder. A Millipore Fluoropore membrane filter of 0.5 μm pore size was used to filter out any solid absorbents in the asphaltene samples. For the base solution and each of the absorption samples, two cleaned vials were weighed. The samples were filtered through the Swinny filter and approximately 1 ml of solution was put in each vial, which were quickly capped. Two vials were used for each sample to maintain a check on the accuracy of the filtering and the method of concentration determination. For this reason the adsorption isotherms show two points for each adsorption sample.

Vacuum drying of the asphaltene samples was used to determine the concentration of all samples. This seems to be the best method for these asphaltenes as most other methods have disadvantages as discussed previously.[2] The vials were weighed to obtain the total sample weight and then dried. The drying procedure varied depending upon the solvent. For tetrahydrofuran (THF), the samples were allowed to dry in a ventilated hood until no liquid was present and then dried at full vacuum for 24 hours at room temperature. Toluene and pyridine samples were also allowed to dry in a ventilated hood and then vacuum dried at full vacuum at 50-60°C. Tetralin presents a particular problem because of its high boiling point (207°C). In earlier work, drying of samples containing tetralin still showed some tetralin present after vacuum drying for 48 hours at 50-60°C and even after an additional vacuum drying at 100-110°C. Finally is was shown by work with the VPO that no tetralin remained in samples if vacuum dried at 150-160°C. To dry the tetralin samples, the sample vials were placed in the vacuum oven, a vacuum pulled, and slowly the temperature was raised to 150-160°C, allowed to dry for 24 hours at this temperature, and then allowed to cool to room temperature before removing them. All samples for each adsorption run were dried together in a large vacuum oven so all samples in the run would be dried under identical conditions. This should help avoid errors in the concentration determination if any of the lower molecular weight asphaltenes are volatile to any extent. The volume of each sample was calculated from the total sample weight and a specific gravity equation which was a function of asphaltene concentration. The concentration was then the dried solids weight divided by the sample volume.

2. Equilibrium Adsorption Isotherm Results

The purpose of the equilibrium studies was to explain the effect of major variables on asphaltene adsorption. To better explain these effects, uniform, well characterized asphaltene samples were needed. Characterization of the asphaltenes from the batch extracts showed them to have a wide molecular weight distribution. Results from proton NMR also showed them to vary considerably in their chemical nature. However much more uniform asphaltenes of a narrower molecular weight distribution were obtained from the large scale GPC runs.

The major variables affecting asphaltene adsorption are temperature, solvent properties, surface area characteristics, plus the molecular

weight and chemical nature of the asphaltenes themselves. To determine each of these effects it was proposed to obtain several adsorption isotherms by varying the one factor of study and keeping all other conditions equivalent. This approach should give a clear view of the effect of the variable under study and also limit the total quantity of asphaltenes needed.

The first variable to be investigated was the effect of temperature. Tetralin was chosen as a solvent similar to coal liquids with a high boiling point (207°C) so a wide temperature range could be explored. Temperatures selected for the isotherms were 30°, 80°, 130°, and 180°C. Asphaltene fraction GPC-72-2 (MW 1250) was used in these experimental runs. Immediately, experimental problems developed in dissolving the high molecular weight material in tetralin. A solution of approximately 12.8 weight percent asphaltenes was made but after a day the asphaltenes had not completely dissolved. This solution was heated and stirred in the oil bath at 150°C to help solubilize the asphaltenes. It appeared that the asphaltenes were solubilized but very small particles could be seen near the liquid surface on the walls of the glass bottle. This solution was filtered twice through Whatman #42 filter paper and a filter cake was retained on the paper. From the resulting concentrations of the filtrate, approximately 60% of the asphaltene fraction was soluble in tetralin at room temperature.

The resulting filtrate was used in Adsorption Runs Number 16, 17, 18, and 19. The adsorption isotherms for these runs are shown in Figure 40. Experimental difficulties were experienced at 180°C when the vial caps loosened due to the high temperature and resulted in the loss of some asphaltene samples. Because of this, 15 ml asphaltene samples in the 50 ml round bottom flask were used along with the chain stirrer to obtain some data.

From Figure 40 it can be seen that an increase in temperature slowly lowers the amount of asphaltenes absorbed. This trend is observed from 30°, to 80°, to 130°C. However, when the temperature is raised to 180°C, the decrease in adsorption is more pronounced. This may be due to the fact that the temperature is approaching the solvent boiling point and the solvent is becoming much more thermally active.

The isotherms in the temperature study show a Langmuir type isotherm but with one discrepancy. The Langmuir isotherm reaches a level plateau at higher concentrations but most of the experimental asphaltene isotherms show a Langmuir like rise in adsorption followed by a slight decrease in adsorption as the concentration is increased. At first it was thought that this might be some experimental procedural error but the procedure was reevaluated and refined. It does not appear to be a procedural error but an observed phenomenon. This trend is seen with all asphaltene samples which have molecular weights greater than approximately 600, a preasphaltene fraction, and is seen in two solvents, tetralin and pyridine. Therefore, it would appear to be a property of the asphaltenes.

Higher concentration samples were run for the system of pyridine, asphaltenes (GPC-72-3 (MW 690)) and F-20 Alumina. Figure 41 shows the

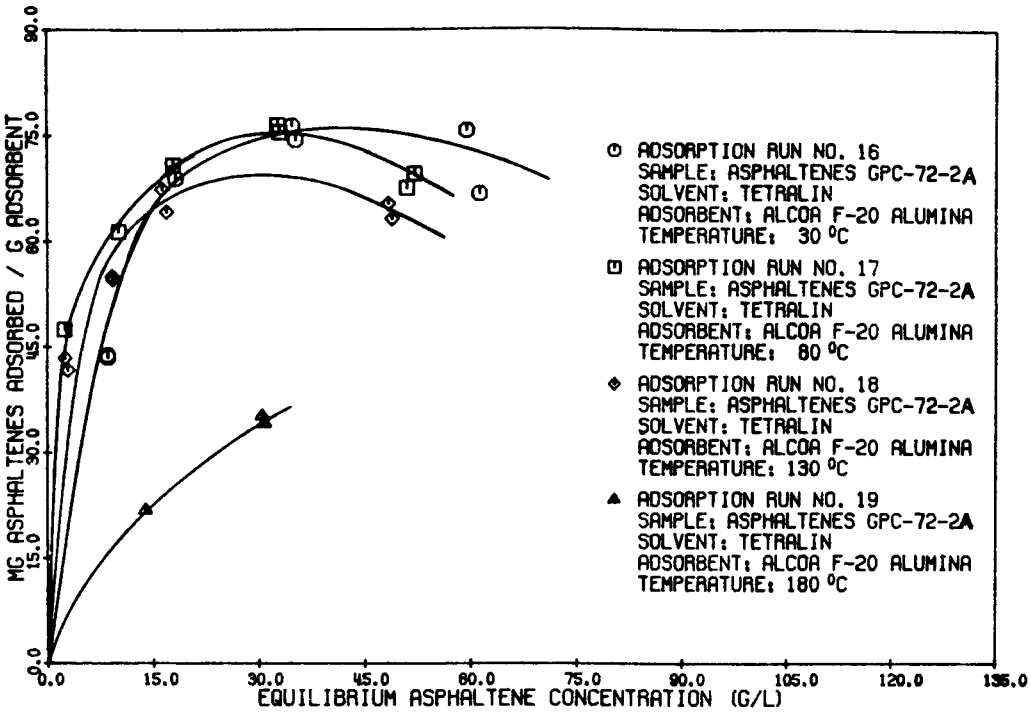

Figure 40. Effect of Temperature on the Adsorption of Asphaltenes from Fraction GPC-72-2 in Tetralin onto Alcoa F-20 Alumina.

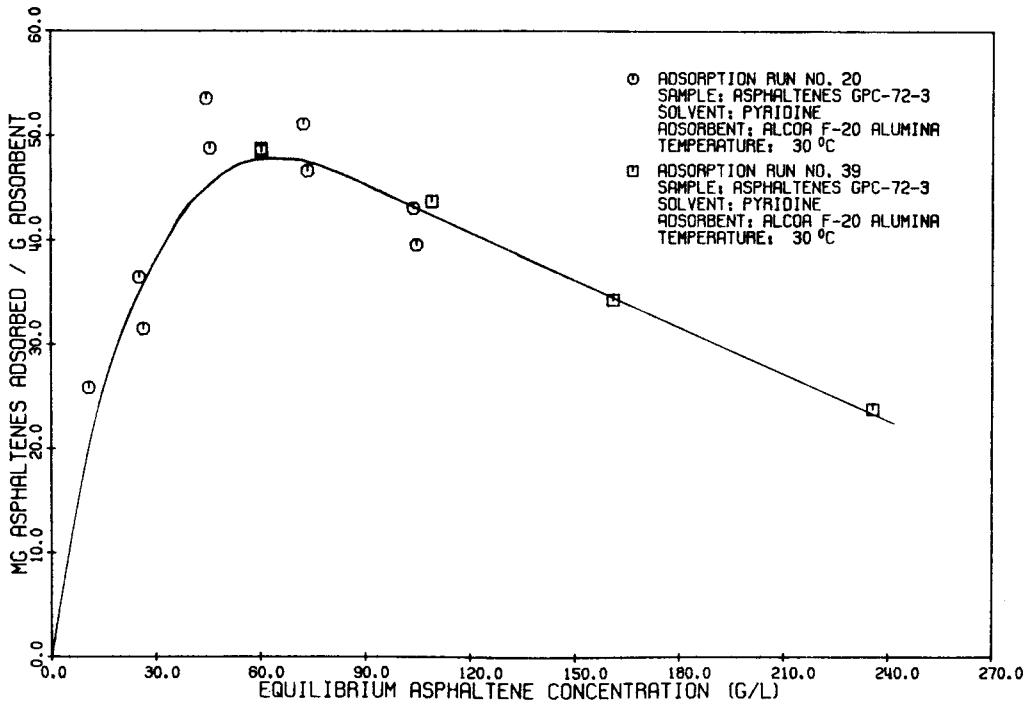

Figure 41. Effect of High Concentrations of Asphaltenes on the Adsorption of Asphaltenes from GPC-72-3 in Pyridine onto Alcoa F-20 Alumina.

results of two runs, one at lower concentrations and one at higher concentrations up to 25 wt. %. This graph shows the same continued trend of the amount of adsorption decreasing at higher concentrations. This decline seems surprisingly steep.

This phenomenon could be easily explained if the asphaltenes were associating with increases in concentration. If this were true, then as the asphaltene particles increase in size with increased asphaltene concentration, the larger particles would be excluded from more pores in the solid adsorbent. As pore exclusion increases, less surface area is available for adsorption of the asphaltenes. As a result the adsorption would decrease in the plateau region as is observed. As a consequence of the phenomenon, the curves drawn through the experimental data are drawn to best fit the data and are not Langmuir isotherms. For the cases where this phenomenon was not observed, the experimental data were fit to the Langmuir equation and the curve drawn from this equation.

For the second study, the effect of molecular weight on asphaltene adsorption, pyridine was chosen as the solvent. This was done because all the asphaltene fractions are quite soluble in this solvent. Also the preasphaltene extraction material is soluble in pyridine so that adsorption of this fraction can be compared to the adsorption of the asphaltenes. A temperature of 30°C was chosen as the temperature for these runs due to the convenience of working at this temperature plus the temperature study showed no great difference in adsorption between 30°C and 80°C.

The adsorption isotherms for five asphaltene fractions and one preasphaltene fraction are shown in Figures 42 and 43. All fractions seemed to show lower levels of adsorption in pyridine than in tetralin. The three highest molecular weight fractions shown in Figure 42 have isotherms which are fairly similar and all reach a declining plateau at about the same level of adsorption. As the molecular weight decreases below a certain value, there appears to be an accompanying decrease in adsorption. Fraction GPC-72-4 (MW 425), Figure 33, shows a slightly lower amount of adsorption. Fractions GPC-72-5 (MW 330) and GPC-72-6 (MW 305) show considerably less adsorption and so little adsorption that scatter in the adsorption data makes the shape of the isotherm uncertain.

This decreasing adsorption with decreasing molecular weight can be explained by examining the characteristics of each of the asphaltene fractions. As the molecular weight decreases, the weight percent of heteroatoms, oxygen, nitrogen, and sulfur also decrease. In some of the LEAC work, the adsorption between alumina and aromatic hydrocarbons was considerably stronger when the heteroatoms oxygen and nitrogen were present. This would appear to correlate the level of asphaltene adsorption with the molecular weight and heteroatom concentrations. The higher molecular weight fractions in Figure 42 all have significant amounts of heteroatoms so they are able to cover the entire surface of the alumina not restricted due to the size of the asphaltenes. The lighter molecular weight fractions with fewer heteroatoms only attain partial monolayer coverage. The data for the molecular weight study in pyridine is also plotted on a molar basis in Figures 44 and 45.

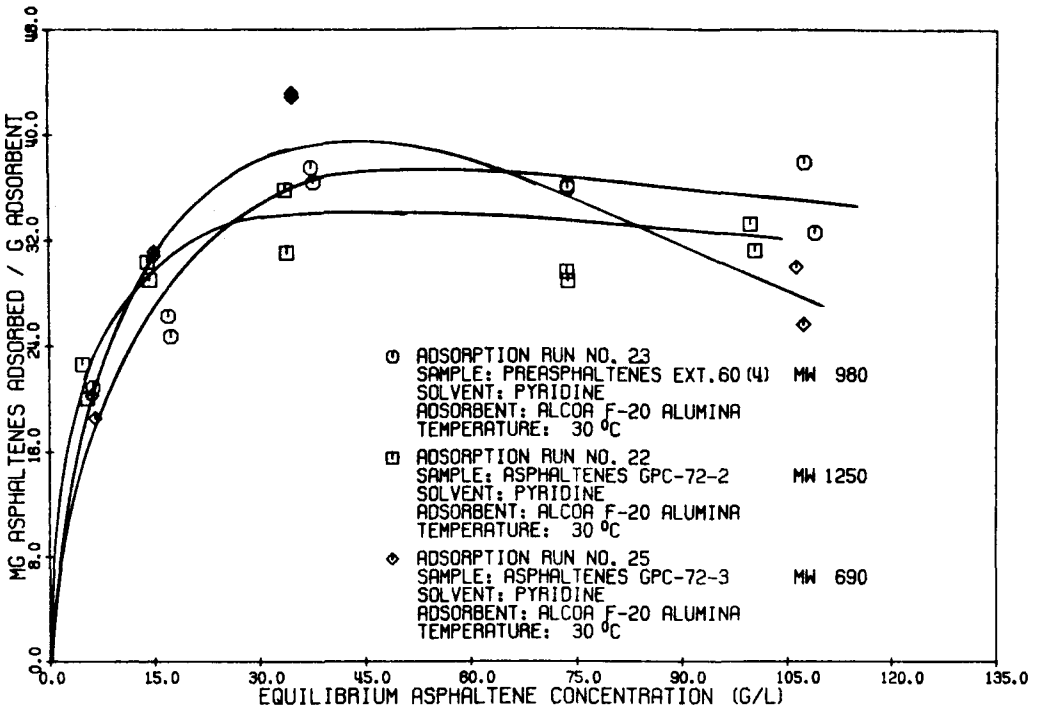

Figure 42. Effect of Molecular Weight on the Adsorption of Asphaltenes and Preasphaltenes in Pyridine onto Alcoa F-20 Alumina - Mass Concentration at 30°C.

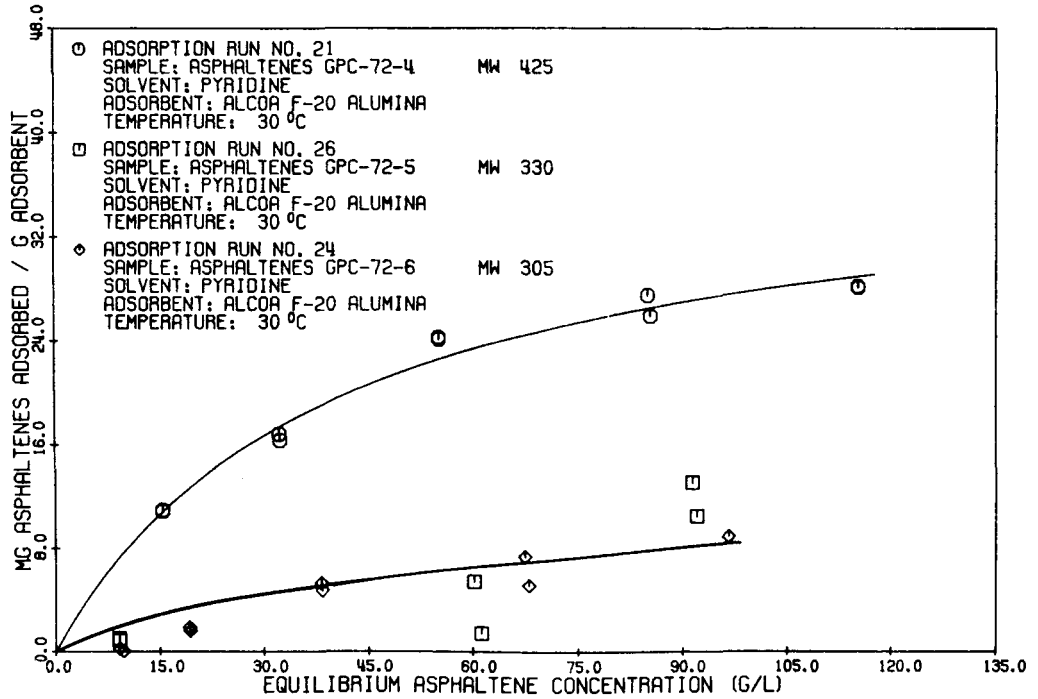

Figure 43. Effect of Molecular Weight on the Adsorption of Asphaltenes in Pyridine onto Alcoa F-20 Alumina - Mass Concentration at 30°C.

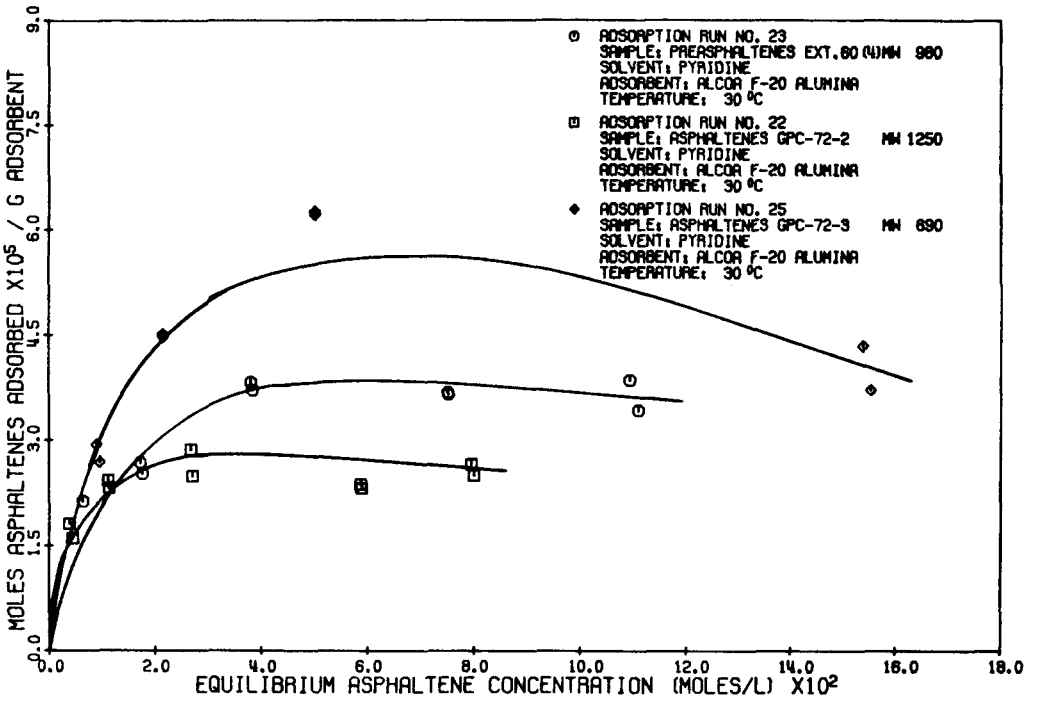

Figure 44. Effect of Molecular Weight on the Adsorption of Asphaltenes and Preasphaltenes in Pyridine onto Alcoa F-20 Alumina - Molecular Concentration at 30°C.

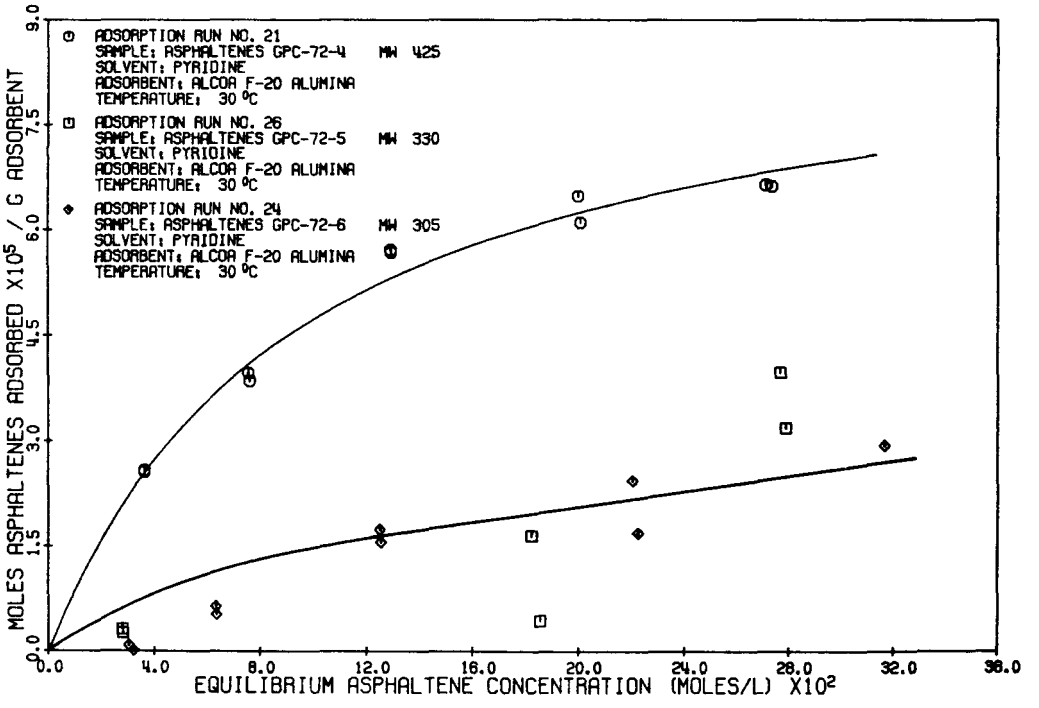

Figure 45. Effect of Molecular Weight on the Adsorption of Asphaltenes in Pyridine onto Alcoa F-20 Alumina - Molecular Concentration at 30°C.

Experimental adsorption runs were undertaken with alumina as adsorbent, tetralin as solvent, and four different molecular weight fractions. These isotherms are plotted in Figure 46 on a weight adsorbed basis and in Figure 47 on a molar adsorbed basis. Using tetralin as the solvent did create some problems with the higher molecular weight fractions. In preparation for Adsorption Run No. 16, only 60% of Fraction GPC-72-2 (MW 1250) dissolved in tetralin at room temperature. In preparation for Adsorption Run No. 30, there was again problems. Approximately 83.5% of Fraction GPC-72-3 (MW 690) dissolved in tetralin. At the present time, characterization of the soluble and insoluble portions of these two fractions is in progress. The soluble portions of Fractions GPC-72-2 and GPC-72-3 were used in Adsorption Runs Number 16A and 30A, respectively. Based on a weight adsorbed basis, the higher molecular weight fractions again appeared to achieve approximately the same level of adsorption. The lowest molecular weight fraction, GPC-72-5 (MW 330) shows a lower level of adsorption. The same trend was found in the adsorption results with pyridine.

Solvent properties considerably influence the amount of asphaltene adsorption observed. Tetralin, toluene, tetrahydrofuran, pyridine, and nitrobenzene were chosen as suitable solvents for this study because of their range of surface tension and dielectric constants. A low molecular weight fraction, GPC-72-5 (MW 330), was chosen as the asphaltene fraction for this study to avoid any problems with limited solubility.

The adsorption results for this solvent study are shown in Figure 48. A trend of decreasing adsorption with increasing solvent strength is observed. It would seem that the amount of asphaltene adsorption from a particular solvent is related to the degree of hydrogen bonding with the solvent. As shown previously by the chromatography work, the strength of adsorption to the alumina surface is strongest between the surface and the oxygen and nitrogen heteroatoms in the asphaltenes. The heteroatoms are attracted to the solid surface but can also be attracted to solvent molecules that hydrogen bond.

Asphaltene adsorption from pyridine seems to be the lowest because pyridine undergoes hydrogen bonding to the phenolic oxygen present in coal derived asphaltenes but also can adsorb directly onto the alumina. Tetrahydrofuran and nitrobenzene do hydrogen bond but not as strongly as pyridine. Therefore, asphaltenes in these solvents are more attracted to the solid surface than the solvent molecules. Toluene and tetralin do not hydrogen bond so the asphaltenes have little attraction to the solvent molecules and consequently show a larger adsorption on the alumina.

Asphaltene adsorption was investigated on seven solid adsorbents. Two of the solids are laboratory standards, Alcoa F-20 Activated Alumina and Grace 923 Silica Gel. The other five solids are materials which would be present in coal liquefaction processes or be available from supporting processes. These five are Celite 503 diatomaceous earth; a mineral matter from a Synthoil process run, Pittsburgh Seam, Ireland Mine Coal (Ext. 8); mineral matter from an H-Coal process run, Illinois No. 6 Coal, River King Mine (Ext. 60); Aero HDS-1442A desulfurization catalyst; and a Utah high volatile B gasifier char.

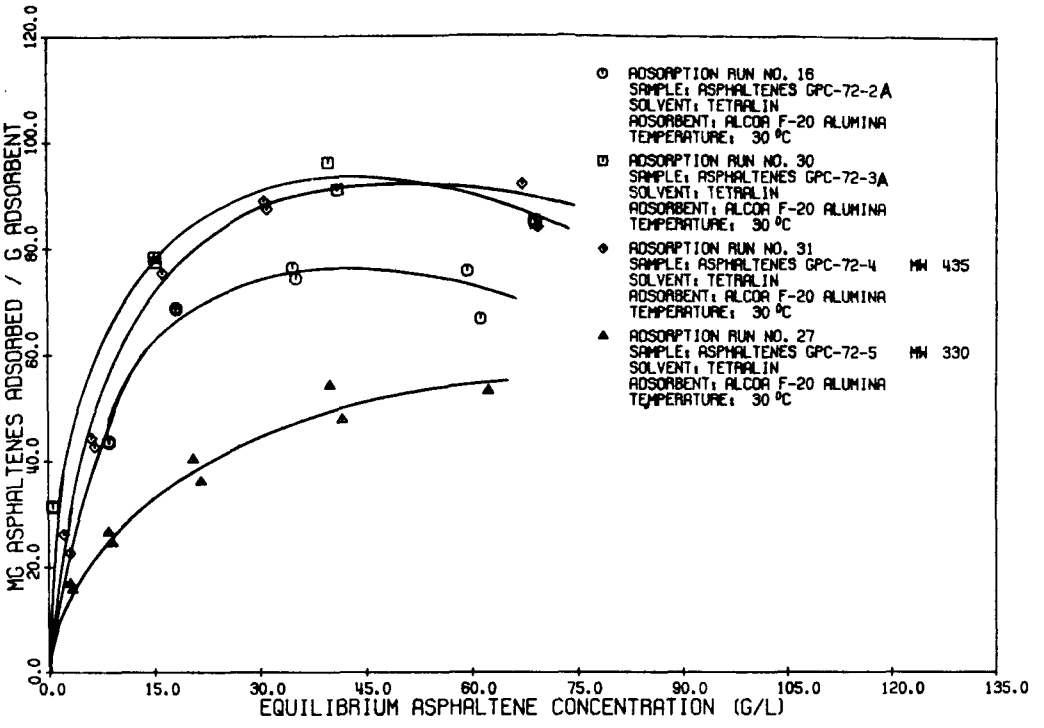

Figure 46. Effect of Molecular Weight on the Adsorption of Asphaltenes in Tetralin onto Alcoa F-20 Alumina - Mass Concentration at 30°C.

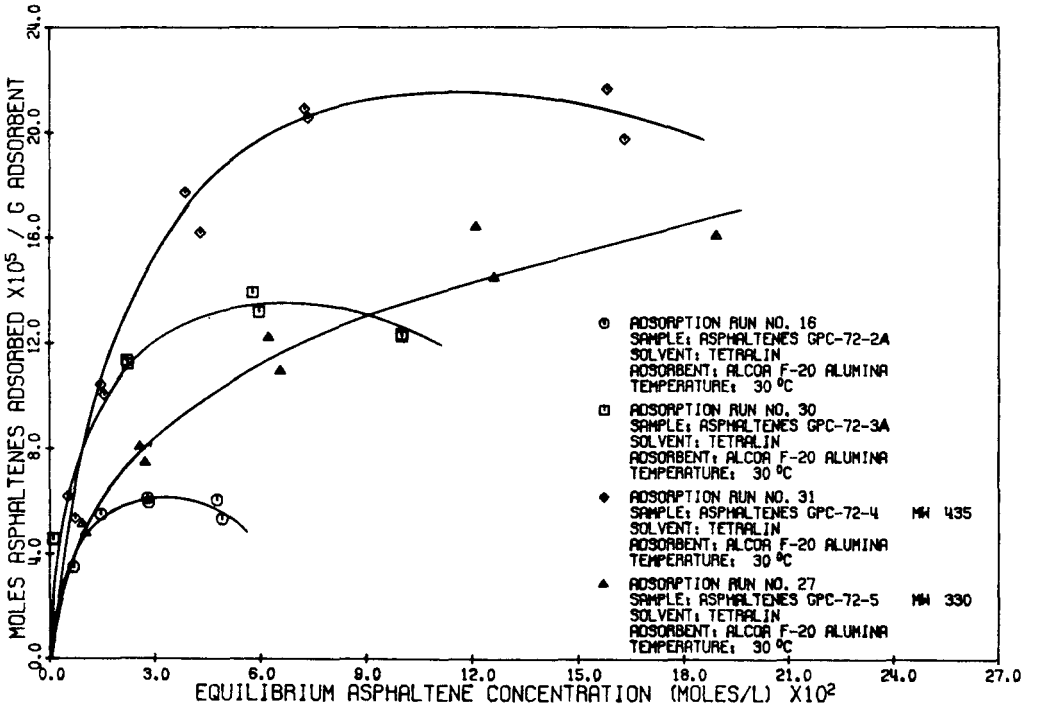

Figure 47. Effect of Molecular Weight on the Adsorption of Asphaltenes in Tetralin onto Alcoa F-20 Alumina - Molecular Concentration at 30°C.

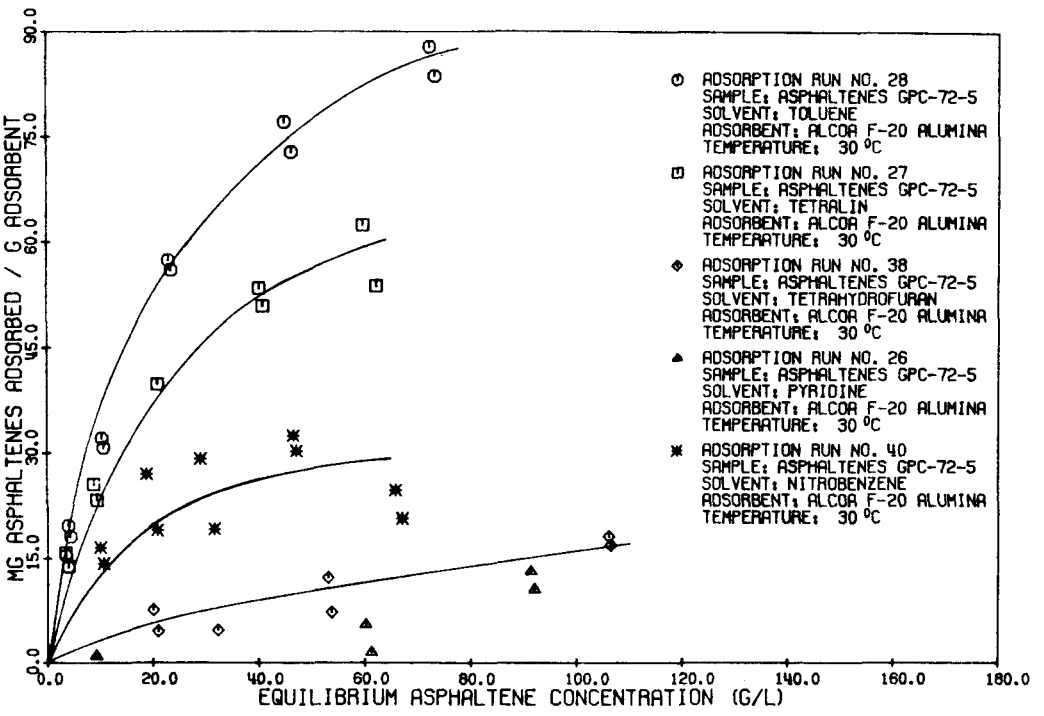

Figure 48. Effect of Solvent Properties on the Adsorption of Asphaltenes from Fraction GPC-72-5 in the Solvent onto Alcoa F-20 Alumina at 30°C.

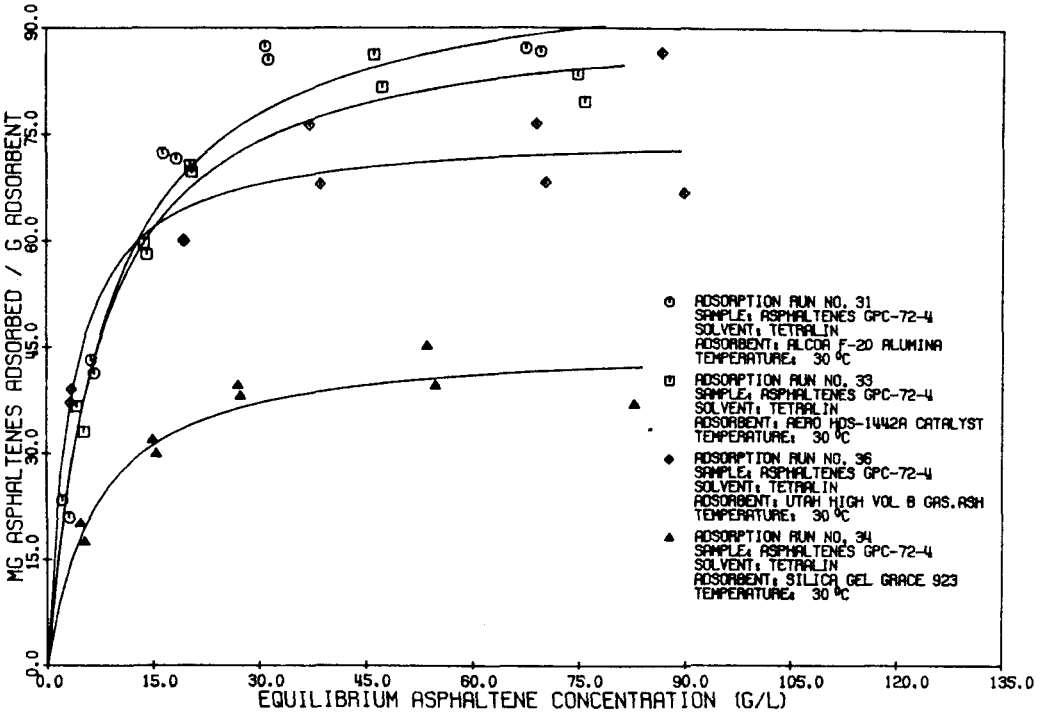

Figure 49. Effect of Solid Adsorbent on the Adsorption of Asphaltenes from Fraction GPC-72-4 in Tetralin onto the Adsorbent at 30°C.

The asphaltene adsorption isotherms on these seven solids are shown in Figures 49 and 50. There is a large difference in the level of adsorption of each solid which seems to result from the surface area characteristics of each solid. It would appear that the porous character and pore size distribution of each solid are the major importance.

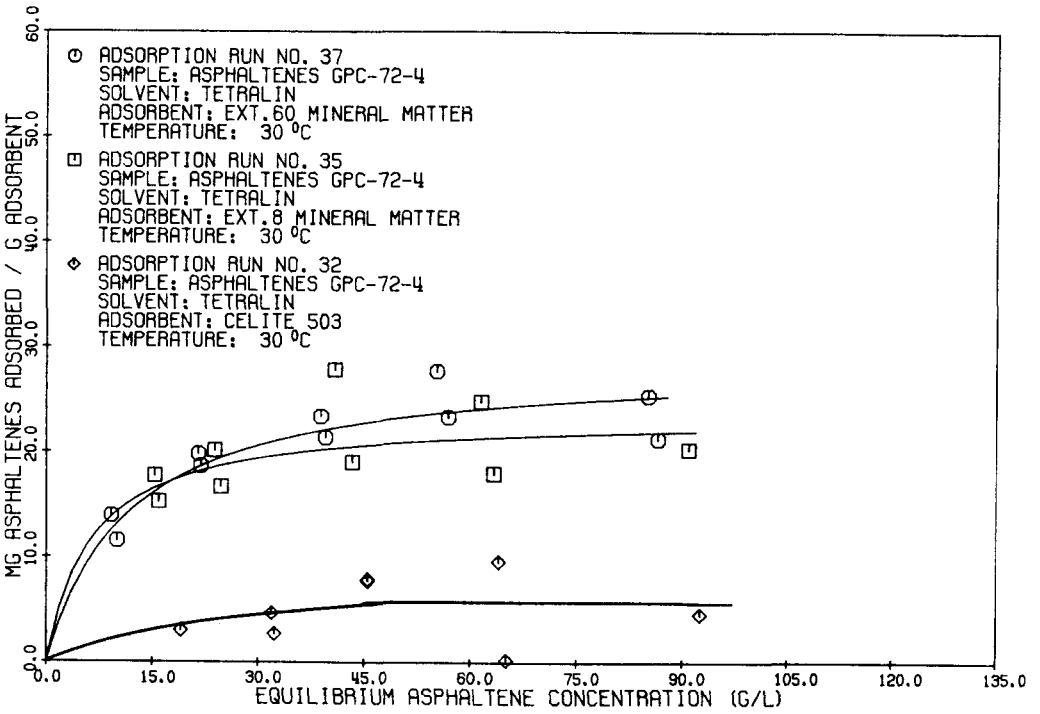

Figure 50. Effect of Solid Adsorbent on the Adsorption of Asphaltenes from Fraction GPC-72-4 in Tetralin onto the Adsorbent at 30°C.

The less porous solids, the diatomaceous earth and two coal mineral matter samples, show a large amount of asphaltene adsorption for their rather low surface areas. For the other more porous solids, the level of asphaltene adsorption seems to be dependent on the pore size. For instance the silica gel shows the highest surface area from BET nitrogen measurements, but this large area is associated with very fine pores. In respect to asphaltene adsorption, the silica gel shows a lower level than the three other porous solids of less surface area. By comparing the asphaltene adsorption with the surface area associated with a given pore diameter, the adsorption per surface area seems more consistent between all seven solids. Considering all seven solids, the asphaltene adsorption per surface area seems most consistent at a pore diameter of 40 Å and above. Asphaltene exclusion in smaller pores would explain the low asphaltene adsorption on silica gel.

Asphaltene Fraction GPC-72-4 has a molecular weight of 425 which would correspond to a particle size of 12-14 Å for a circular sheet. If

the asphaltenes are not circular in shape but more rod-like, as some evidence would indicate, then their size could be more like 20-25 Å. In a 40 Å pore, any asphaltene of molecular size 20 Å that adsorbs on the pore walls, would effectively block the pore to additional adsorption. Pore exclusion seems a very reasonable explanation of the observed asphaltene adsorption on these solids, but more work is needed in this area.

D. Flow System
(D. V. Addington)

The primary objective in the study of the flow system was to examine the flow of asphaltene solutions through a fixed bed, similar to the system of pressure precoat filtration through a filter cake and precoat material. Of particular interest in this study of fixed beds is the movement of the adsorption front down the bed and the shape of the "breakthrough" curve.

It has been reported that asphaltenes from crude oil when flowing through porous media tended to precipitate by an electrokinetic phenomenon known as the streaming potential. Part of this work is to measure the streaming potential in fixed bed flow to see if this phenomenon is occurring here. Also examination of the streaming potential may lead to a better understanding of coal derived asphaltenes in solution.

It was hoped that the equilibrium adsorption isotherms could be used to predict breakthrough curves in the flow system. Then comparing the breakthrough curves to the predicted curves, it would be possible to determine if any precipitation occurred due to the streaming potential.

1. Fixed Bed System

Several experimental runs were made in fixed beds by injecting asphaltene solutions in a step function manner. The breakthrough curves were followed by a continuous UV detector and continuous RI detector. The fronts tended to be broadening and there appeared to be a large amount of diffusion.

There was also observed to be some irreversible adsorption of part of the asphaltenes onto alumina and silica gel beds. This adsorbed asphaltene fraction generally could not be entirely eluted even by strong solvents such as pyridine or THF. This strong irreversible adsorption effectively prevented a comparison of the experimental breakthrough curves to the predictions obtained from the equilibrium isotherms.

2. Streaming Potential

The results of the streaming potential measurements have been more productive. Most of the experimental work on the streaming potential measurements have been completed. A few inconsistencies exist in the data and some further experimental work may be necessary.

a. Experimental Apparatus and Procedure

Streaming potentials were taken in the flow system under two procedures. Initially asphaltene solutions were pumped through a fixed bed at constant pressure drop to saturate the column and achieve steady streaming potential readings. Then the flow rate was varied and streaming potentials and streaming currents were measured at each flow rate.

The columns were Altex 252-00 6 mm-ID analytical column which had been shortened in length. One of two different length columns was used depending upon the solid particle size and the flow rate. 22 gauge platinum wire was run through the Teflon end plugs and set at 90° to the direction of flow. The smaller column was sized so that the electrodes were 0.75 in. apart and the larger column was sized for the electrodes to be 2.25 in. apart. The platinum wire was run through a short piece of tubing, a cross tee, and then through a plug which was sealed with silicon caulk.

Solvent was pumped from a solvent reservoir by a LDC Model 196 mini pump through an Altex 201-56 injection valve into the column to wet it and force out all air. The asphaltene samples were loaded into one of two injection column, the smaller one of 50 ml. volume and the larger one of 130 ml. volume. The asphaltene solutions were injected into the column through the injection valve and nitrogen pressure from a pressure regulator (0-90 psi) was used to control the flow rate. The elution volume was directed into a pipet for measurement. A timer was used to measure given volumes from which flow rates were calculated.

The platinum electrodes were connected to a Keithley 610C electrometer for measurement of the streaming potentials and streaming currents. The electrometer has an internal impedance of 10^{14} ohms on the volts scale and can measure down to 10^{-14} amps of current. The inlet electrode was connected to the electrometer ground.

Electrical conductivities of the asphaltene solutions were taken according to ASTM standard D3114-72. This d-c method used the Keithley 610C Electrometer and a Balsbough Model LRC-1 conductivity cell. A Radiometer Model MM2 RLC Meter was recently obtained and capacitances of the cell and solutions have been taken for some of the later experimental runs. These values will be used to obtain the dielectric constants of the asphaltene solutions.

b. Effect of Variables on Streaming Potential

Pressure precoat filtration involves the flow of asphaltenes in solution through a filter cake of mineral matter and through the precoat material. Flow through the built up filter cake is a short term phenomenon since in a rotary filter the filter cake is shaved off regularly. Therefore long term effects are of little importance. Flow through the precoat material, solids such as diatomaceous earth, is a long term phenomenon. Therefore, in these experiments it was proposed to study solids for both short term and long term effects on streaming potential.

Some early experimental runs indicated that different solids act quite differently in reaching column saturation and steady state conditions. For each of the experimental runs the asphaltenes were run through the column at constant pressure drop until a relatively constant streaming potential was measured.

Many of the solids which were examined attained a steady streaming potential value in about 5 ml. of asphaltene solution. One solid, alumina required the elution of a large volume of asphaltene solution before a steady streaming potential was achieved. Three solids actually changed the sign of the streaming potential during these constant pressure drop runs. In all the experimental runs at constant pressure drop, the flow rate slowly decreased but this may be the result of further packing of the bed rather than any precipitation of asphaltenes. This will have to be confirmed.

A great deal of the initial streaming potential work examined asphaltenes solutions and alumina since this solid had been used extensively in the equilibrium isotherm work. Unfortunately, the system of asphaltenes in THF flowing through alumina did not achieve steady state conditions rapidly. Figure 51 shows the time study for this system. The streaming potential continues to decrease faster than the flow rate. After 75 ml. of solution had passed through the bed, the flow rate was varied and streaming potential measurements taken. The results of these data are shown in Figure 52. At low flow rates the streaming potential and flow velocity were linear but at higher velocities the streaming potential levels off. These results were observed in several runs of this system and at even higher velocities the streaming potential actually decreased. Alumina was the only solid on which this phenomenon was observed, but it was also the only solid which was run at such high flow velocities. There is still an uncertainty about the mechanism for this type of phenomenon. It has been suggested that the higher velocities are shearing molecules off the alumina surface and disturbing the electric double layer but this has not been proven.

Three solids showed a change in the sign of the streaming potential during the time studies. They were the Ext. 18 Mineral Matter (THF-insolubles from H-Coal Vacuum Still Bottoms, Illinois No. 6 Coal), and two diatomaceous earths, Celite 503 and Celite 550. The time studies for these three solids, Ext. 18 Mineral Matter, Celite 503, and Celite 550, are shown in Figures 53, 54, and 55, respectfully. In each case pure THF shows a low negative streaming potential and then after injection of the asphaltene solution, the streaming potential becomes positive before drifting negative and eventually reaching a fairly constant value. Clearly some type of competitive adsorption between asphaltenes of opposite charge is taking place on these surfaces before a saturation point is reached.

After steady state streaming potentials were obtained, the flow rate was varied and measurements recorded. These plots of streaming potential versus velocity are shown in Figures 56, 57, and 58. Celite 550 is a larger particle size diatomaceous earth than Celite 503 with a pH of 8.0 compared to 10.0 for 503. A comparison of the streaming potentials on Celite 503 and Celite 550 showed approximately equal slopes so there appears to be little difference in surface properties.

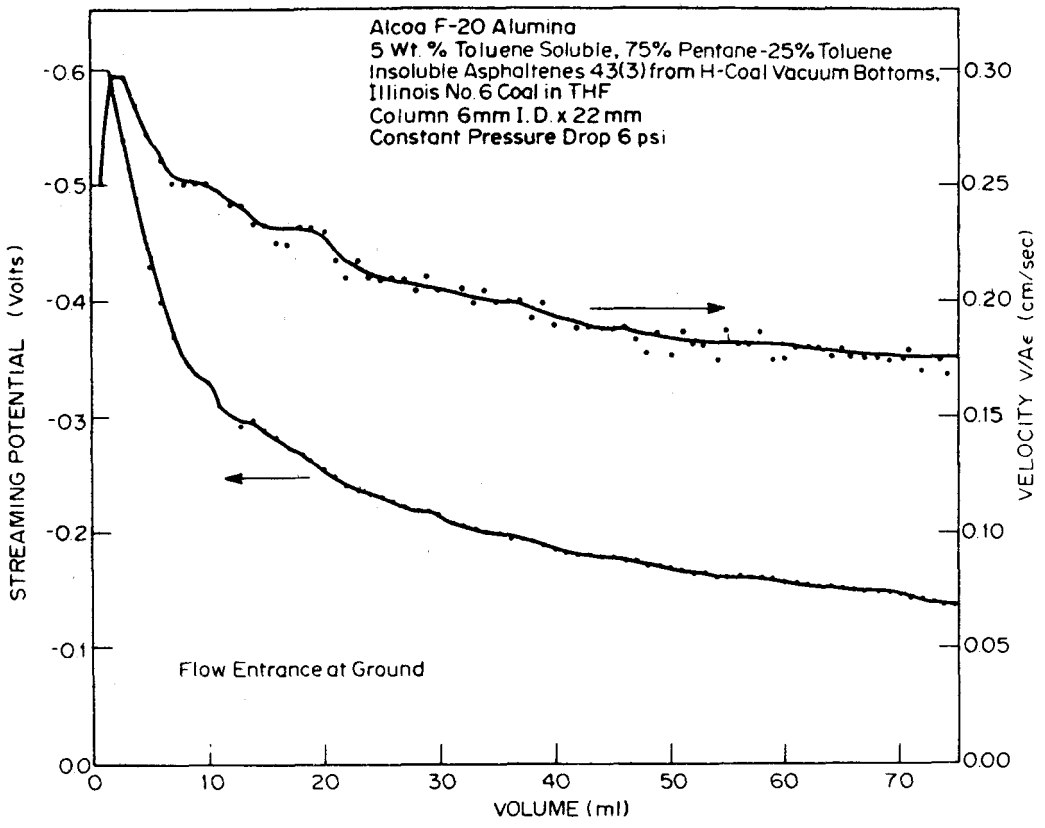

Figure 51. Time Study of Streaming Potential for Asphaltenes in Tetrahydrofuran Flowing Through Alcoa F-20 Alumina.

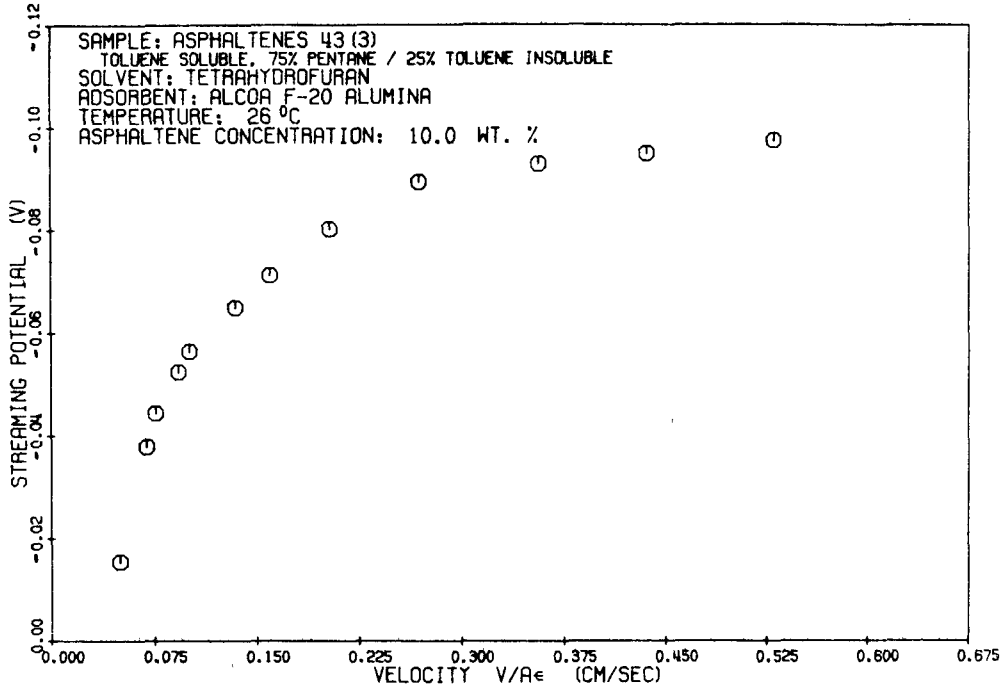

Figure 52. Streaming Potential vs. Flow Velocity of Asphaltenes in Tetrahydrofuran Flowing Through Alcoa F-20 Alumina (Saturated Column).

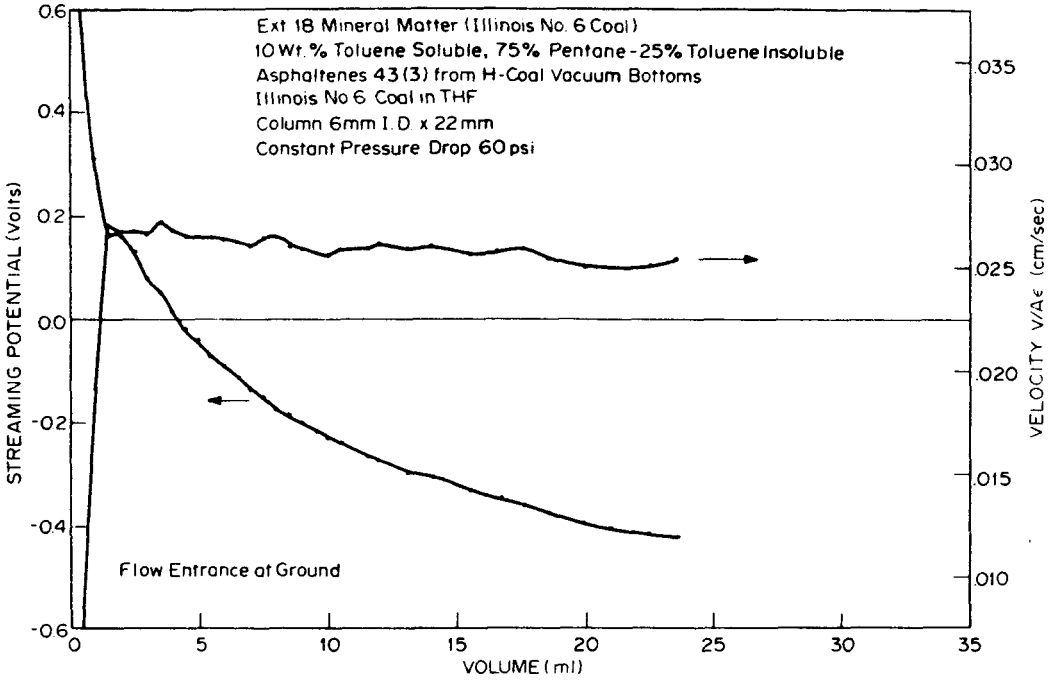

Figure 53. Time Study of Streaming Potential for Asphaltenes in Tetrahydrofuran Flowing Through Ext. 18 Mineral Matter.

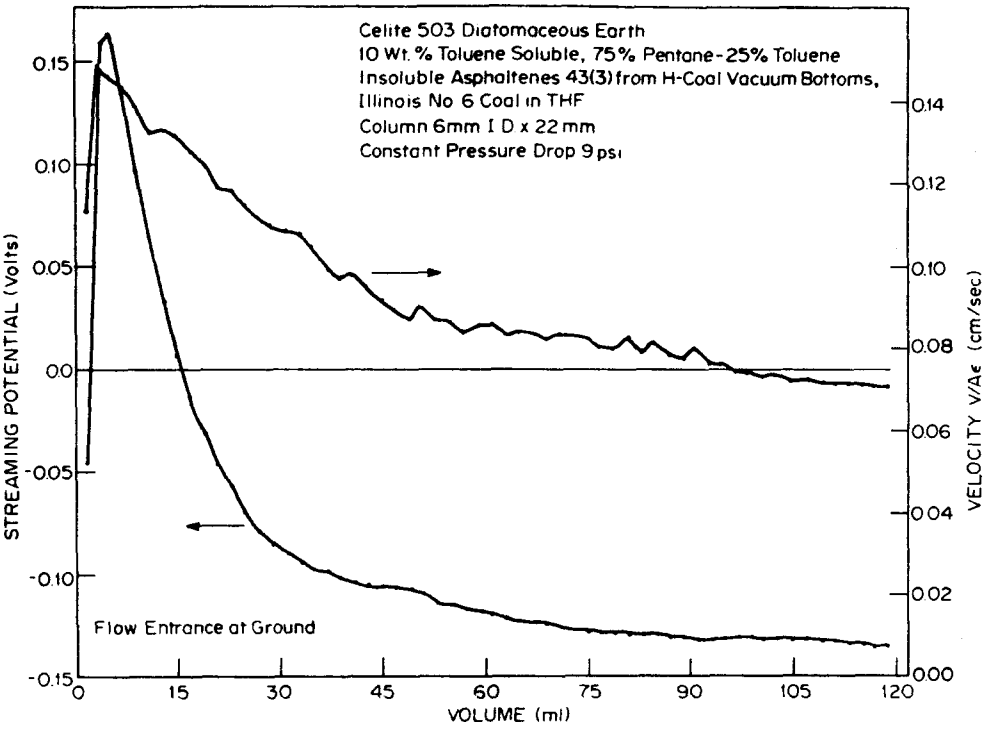

Figure 54. Time Study of Streaming Potential for Asphaltenes in Tetrahydrofuran Flowing Through Celite 503.

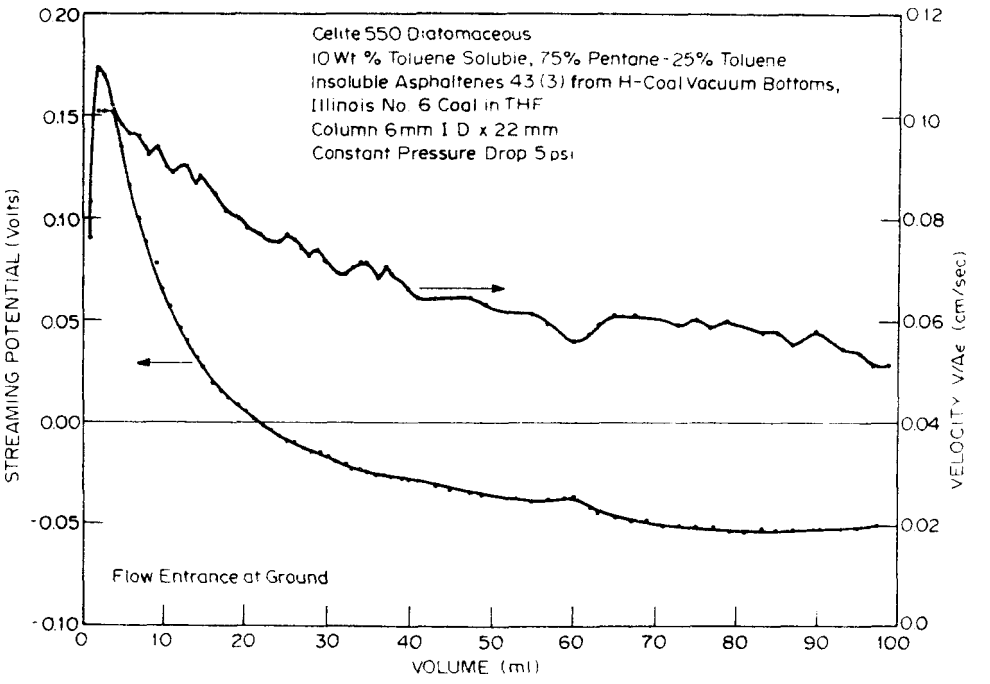

Figure 55. Time Study of Streaming Potential for Asphaltenes in Tetrahydrofuran Flowing Through Celite 550.

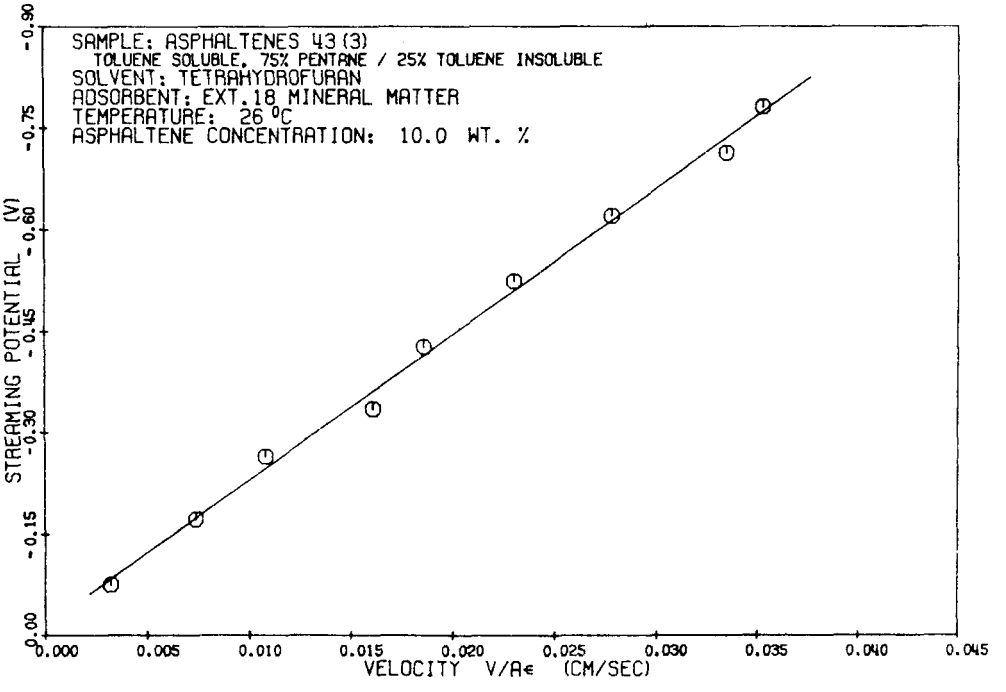

Figure 56. Streaming Potential vs. Flow Velocity of Asphaltenes in Tetrahydrofuran Flowing Through Ext. 18 Coal Mineral Matter (Saturated Column).

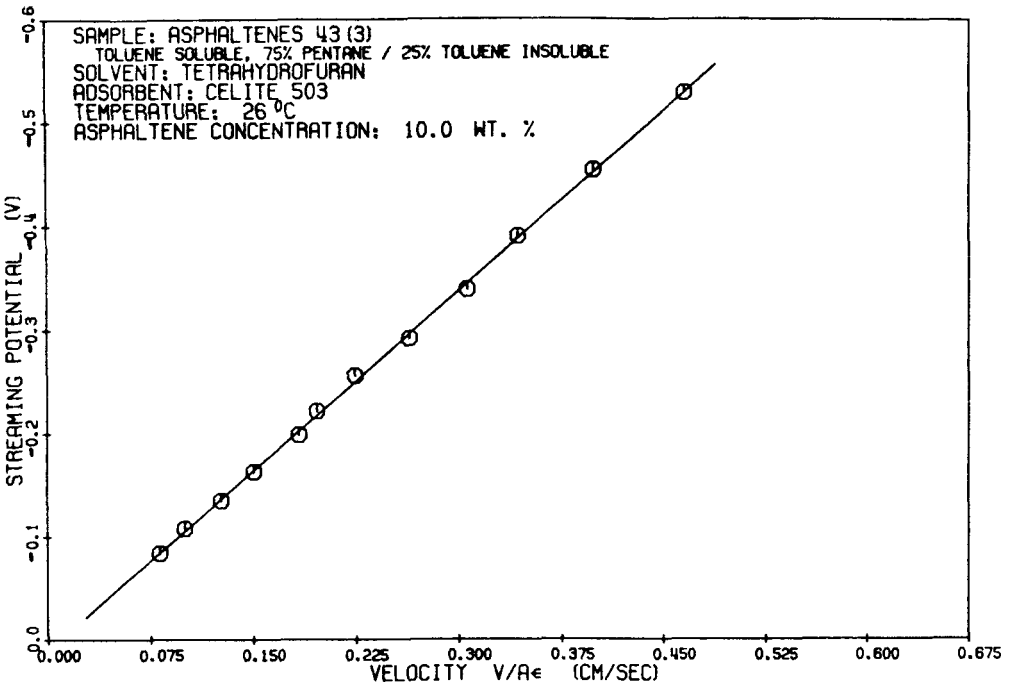

Figure 57. Streaming Potential vs. Flow Velocity of Asphaltenes in Tetrahydrofuran Flowing Through Celite 503 Diatomaceous Earth (Saturated Column).

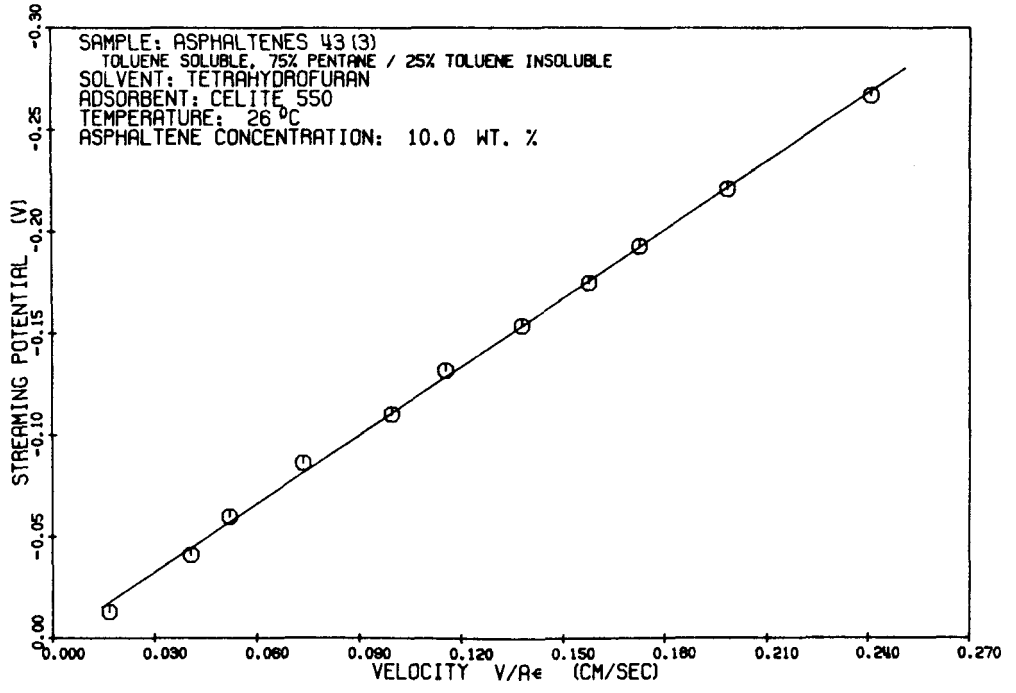

Figure 58. Streaming Potential vs. Flow Velocity of Asphaltenes in Tetrahydrofuran Flowing Through Celite 550 Diatomaceous Earth (Saturated Column).

All of the other solids which were investigated attained steady streaming potentials after the flow of approximately 5 ml. of asphaltenes in solution. The mineral matter from Ext. 8 of the Synthoil Centrifuge Cake was used as the solid adsorbent for studies on the effect of temperature, asphaltene concentration, asphaltene fraction, and solvent properties on the streaming potential.

The results of the temperature study are shown in Figure 59. The flow of a low molecular weight asphaltene 43(2) in tetralin was examined at temperatures of 26°, 80°, and 130°C. Increasing temperature results in increasing electrical conductivity of the asphaltenes solution which accounts for a portion of the decrease in streaming potential.

The concentration study investigated the streaming potential of five different concentrations of asphaltenes 43(3) in THF flowing through Ext. 8 Mineral Matter. The results for asphaltene concentrations of 5, 7.5, 10, 15, and 20 wt. % are shown in Figure 60. At low concentrations the streaming potential changes rapidly with increasing asphaltene concentration but shows less change at higher concentrations.

Figure 61 shows the results of the streaming potential for two different asphaltenes and one preasphaltene at 10 wt. % concentration in THF flowing through Ext. 8 Mineral Matter. The higher molecular weight materials in solution show a higher electrical conductivity which is one reason for the lower streaming potentials of those samples.

Streaming potentials were measured at equivalent conditions for a series of four solvents, tetralin, tetrahydrofuran, pyridine, and a mixture of 10% m-cresol and 90% tetralin. The results of this work are shown in Figure 62. From these data there appear to be interactions between the asphaltenes and solvents which clearly effect the streaming potential.

Four other solids were investigated to examine the effect of the solid surface on streaming potential. An Illinois No. 6 Coal was examined but THF solutions attacked the coal so tetralin was substituted as the solvent. These results are shown in Figure 63. A coal beneficiation refuse, a possible precoat substitute, was investigated and the results are shown in Figure 64. A Utah coal gasifier char was also investigated but this solid had a very high surface conductance and no streaming potential could be measured. A fixed bed of this material measured a resistance of only 40 ohms between electrodes 0.75 in. apart. This surface must be covered with graphite like material causing the high conductance. Finally the streaming potential of asphaltene solutions flowing through silica gel was examined. In contrast to the alumina, the streaming potential on the silica gel quickly reached steady state conditions. These results are shown in Figure 65.

A majority of the streaming potentials were negative in sign. Three systems did show consistently positive signs. The lower molecular weight asphaltene 43(2) in tetralin showed positive streaming potentials on both the Ext. 8 Mineral Matter and the Illinois No. 6 Coal. However, the sample asphaltenes in THF showed a negative potential on the Ext. 8 Mineral

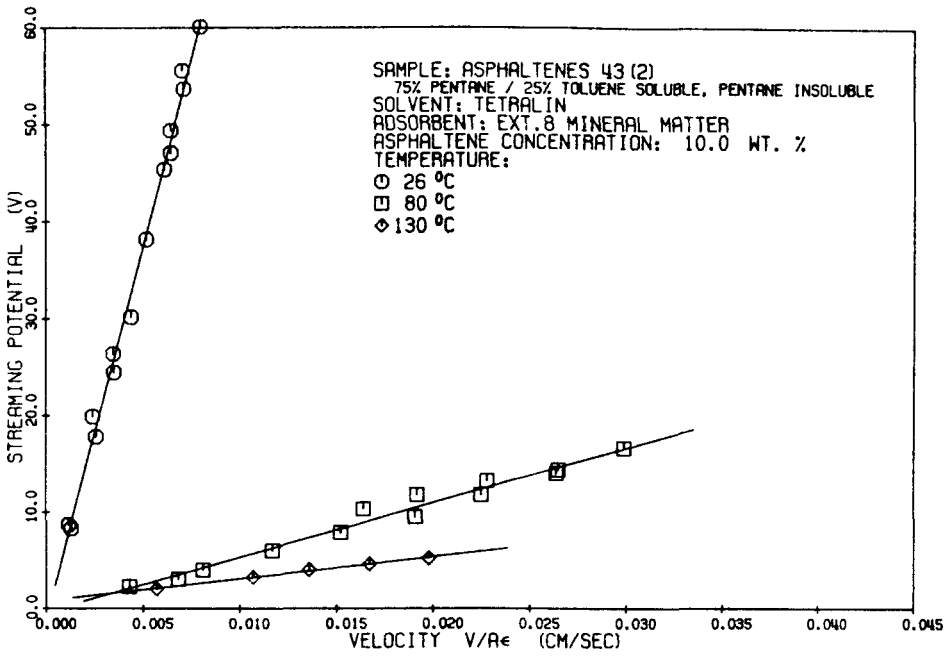

Figure 59. Effect of Temperature on Streaming Potential of Asphaltenes in Tetralin Flowing Through Coal Mineral Matter.

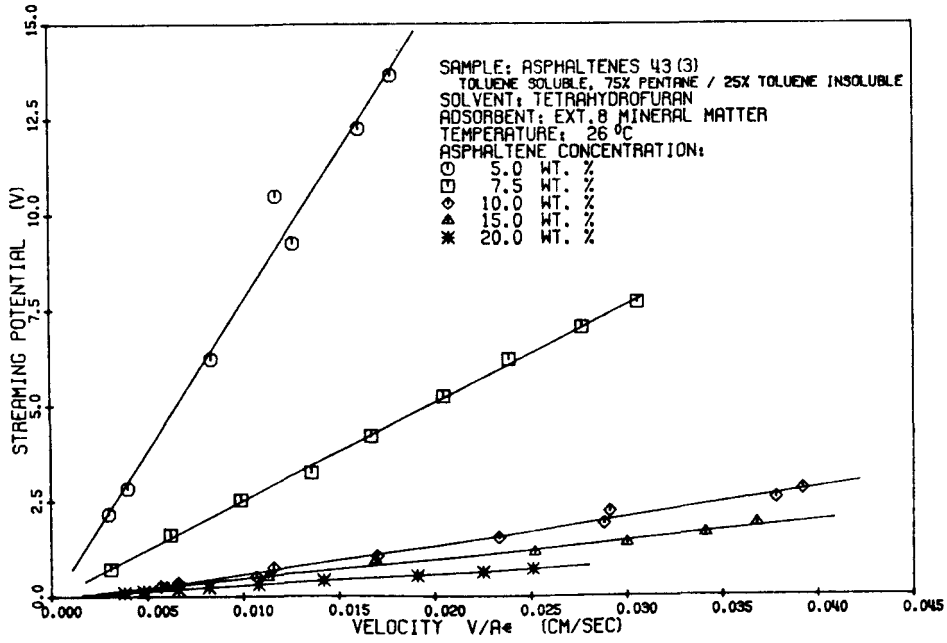

Figure 60. Effect of Asphaltene Concentrations on Streaming Potential of Asphaltenes in Tetrahydrofuran Flowing Through Coal Mineral Matter.

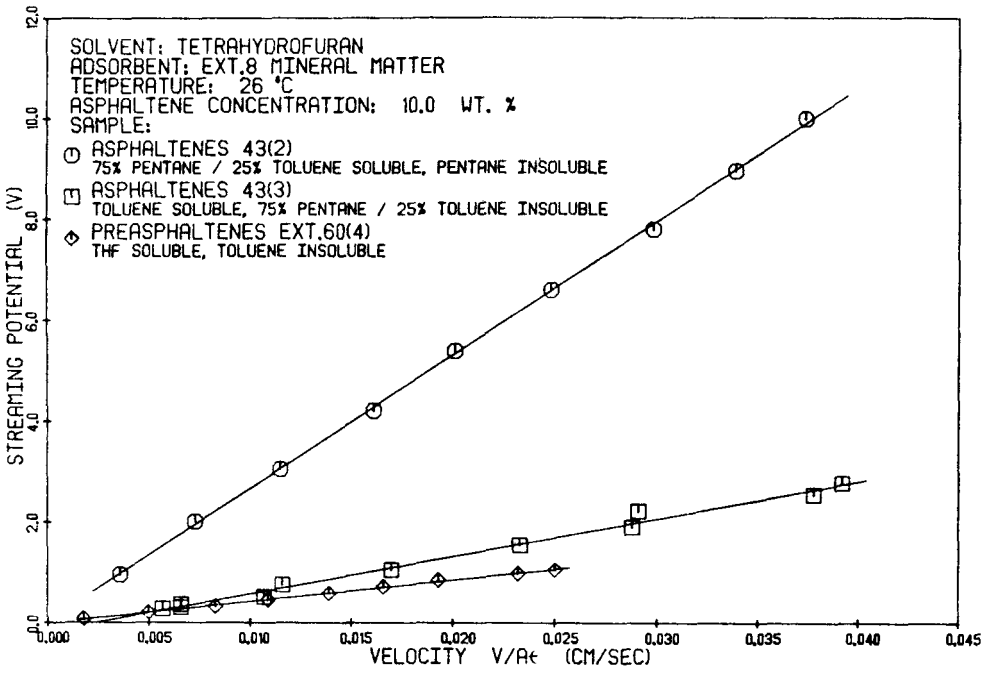

Figure 61. Effect of Asphaltene Fraction on Streaming Potential of Asphaltenes in Tetrahydrofuran Flowing Through Coal Mineral Matter.

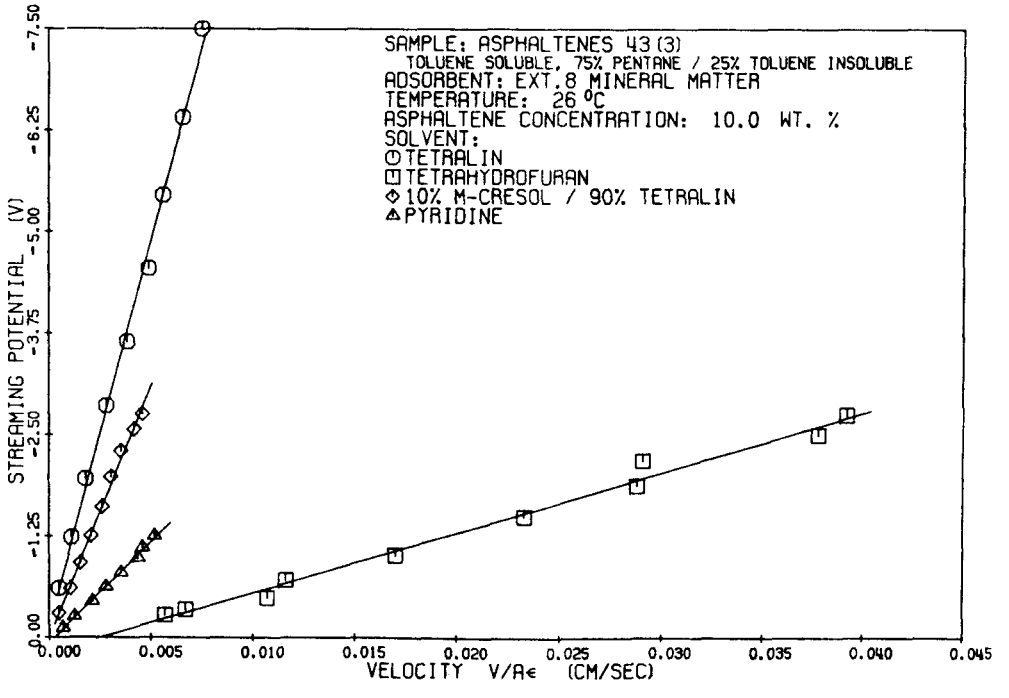

Figure 62. Effect of Solvent Properties on Streaming Potential of Asphaltene Solutions Flowing Through Coal Mineral Matter.

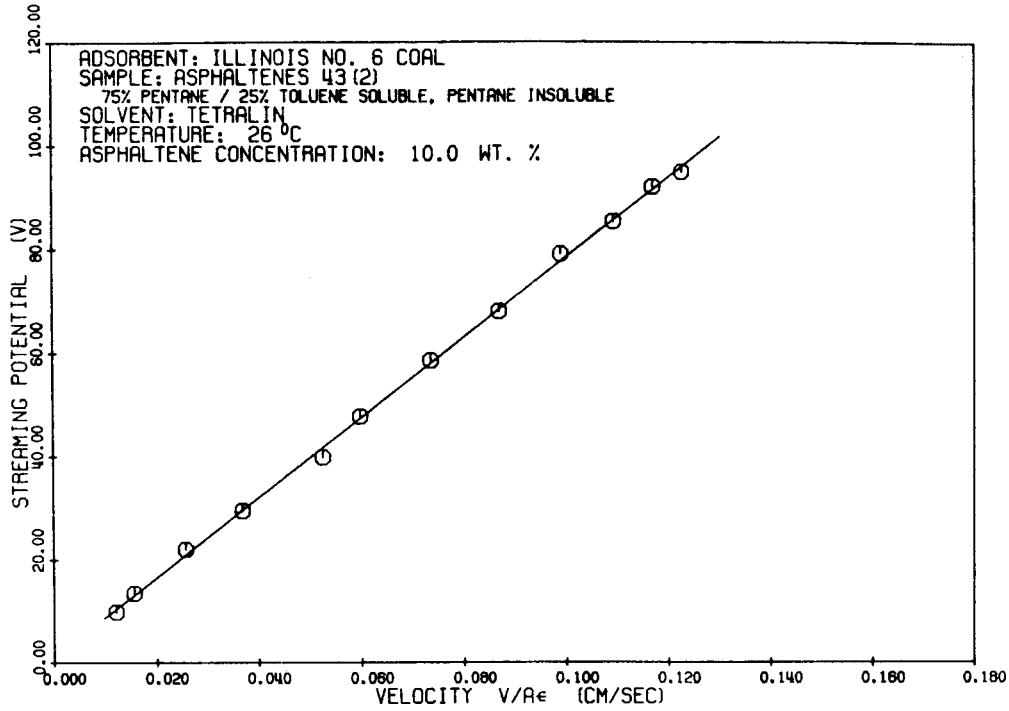

Figure 63. Streaming Potential vs. Flow Velocity of Asphaltenes in Tetralin Flowing Through Illinois No. 6 Coal.

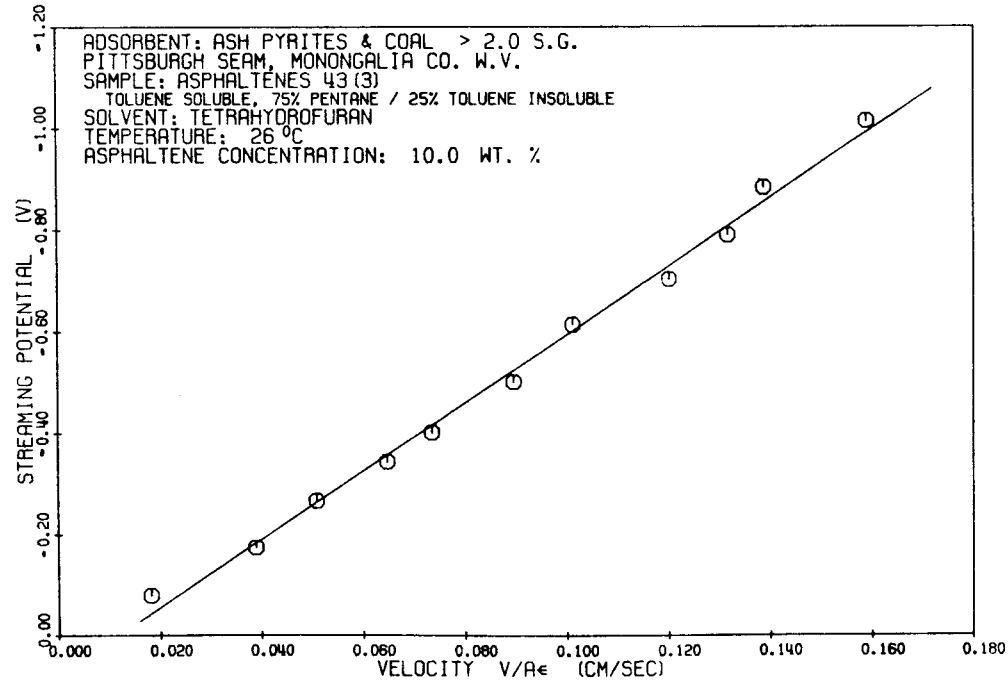

Figure 64. Streaming Potential vs. Flow Velocity of Asphaltenes in Tetrahydrofuran Flowing Through a Refuse from Coal Beneficiation.

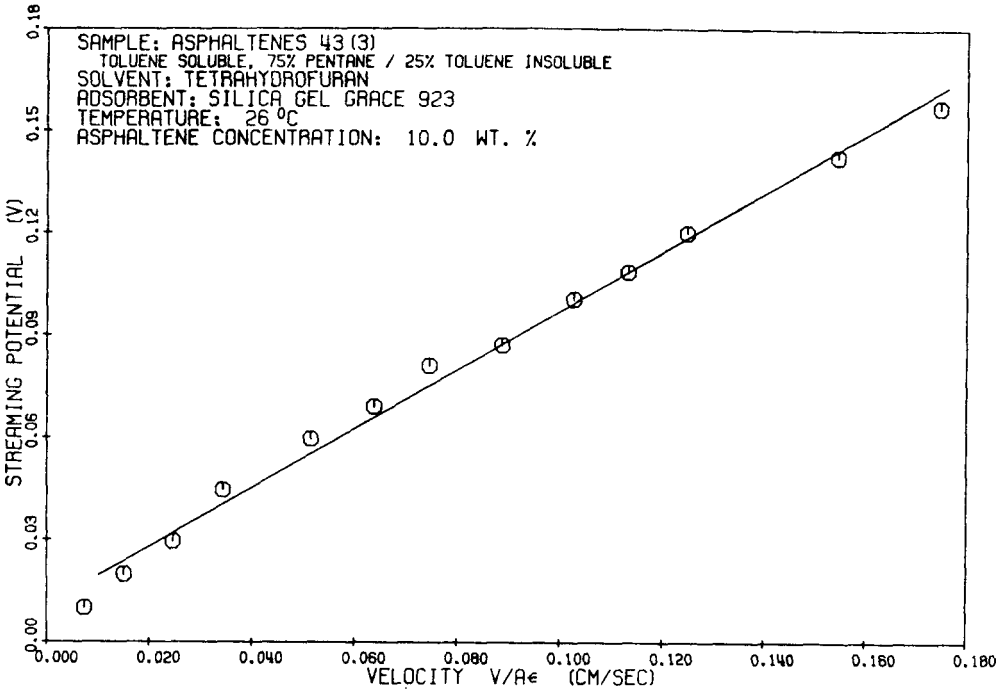

Figure 65. Streaming Potential vs. Flow Velocity of Asphaltenes in Tetrahydrofuran Flowing Through Silica Gel (Grace 923).

Matter. This sign change for this asphaltene fraction does correspond to a similar reversal of sign in some of the electrodeposition work. The higher molecular weight asphaltenes 43(3) in THF showed a negative potential on all the solids except the silica gel.

These data represent the experimental work to date. Analysis and interpretation of the results is currently being undertaken. Some general conclusions have been stated but more detailed analysis will be made and the results reported at a later date.

V. VISCOSITY AND SURFACE TENSION CHARACTERISTICS OF COAL LIQUIDS
(J. R. Cameron)

The work done this last year was devoted entirely to the rheological characterization of coal-derived liquids. This effort was directed in three areas. The first was initial experimental studies of viscosity involving the Ubbelohde and Brookfield viscometers. The second area involved literature studies pertinent to the microrheology of coal-derived liquids. The third area included studies in rheological theory and investigations into available experimental techniques of rheological characterization.

Over the past year, certain alterations to Task 5 as originally stated have proven necessary. This has come about due to increasing awareness of the nature of the problem and because the rheological part of Task 5 has been incorporated into a doctoral research program and as a consequence, requires a more in-depth investigation. Originally, the rheological characterization was to be done using Ubbelohde and Brookfield viscometers. Now, it appears that other devices might be more suited to this task. Originally, Task 5 specified viscosity to be correlated with temperature, coal constituent concentration and molecular weight, solvent type, and factors indicative of molecular association. However, microrheological studies have indicated that other parameters might be involved such as particle shape and size distribution, particle rigidity, and particle charge. Due to the complexity of a thorough rheological characterization, investigations of the originally specified narrow molecular weight range fractions and their mixtures might have to be dropped in favor of a more extensive investigation of the standard larger molecular weight range fractions. If this were done, molecular weight would cease to be a parameter being replaced in importance by particle size and/or molecular weight distribution.

A. Initial Experimental Studies

1. Brookfield Viscometer Studies

A Brookfield viscometer was modified to permit viscosity measurements at temperatures up to and possibly above 250°C. An extension to the UL adaptor was constructed and fitted with a nitrogen purge to keep the viscometer clean and cool at high temperature and to prevent oxidation of the liquid sample. The viscometer with modified adaptor was calibrated with tetralin. The windage viscosity correction at each rpm value was found to be a function of temperature. This was not expected. A second extension to the UL adaptor was constructed to allow for better nitrogen purging. Use of the Brookfield viscometer has been discontinued pending evaluation of other rheometric devices.

2. Ubbelohde Viscometer Studies

Seven narrow molecular weight range asphaltene fractions (GPC-77) were prepared by making three duplicate GPC runs in the 10.16-cm ID x 122-cm long GPC column. The feed material, procedure and fraction characterization are discussed in Section IB. Although analyses were not made on these fractions, they were prepared and processed as were the fractions for which analyses were made (GPC-72).

Viscosity runs were done on the Fraction GPC-77-4 (i.e., the fourth GPC fraction of the toluene soluble and 75%-pentane/25%-toluene-insoluble H-Coal asphaltene fraction) dissolved in tetralin at varying concentrations and temperatures. The concentrations ranged from 5 to 40% by weight of dissolved asphaltene fraction and the temperature ranged from 26° to 130°C. Calibrated Ubbelohde viscometers were used and the temperature was controlled in an oil bath. At a given temperature, the viscosity was seen to increase with increasing concentration. The effect of concentration on viscosity was more pronounced at lower temperatures.

Efforts to recover this fraction from tetralin for use in other solvents by precipitation with an excess of pentane proved unsuccessful. A certain portion remained in the pentane and as a result, the viscosity of the precipitated material when redissolved in tetralin was no longer the same. The portion remaining in the pentane was recovered and recombined with the precipitated material in tetralin. The resulting viscosity of this recombined solution was slightly less than that of the original solution indicating alteration due to material loss, molecular change due to the precipitation, or both. It should be noted that the first couple of fractions from GPC-77 would not dissolve completely in tetralin, making viscosity determinations with these fractions in tetralin impossible.

3. Studies on the Reversible Nature of Asphaltene Solutions

The apparent viscosity of a colloidal solution may depend on its temperature and concentration history. Previous exposures to elevated temperatures or concentration changes may alter the molecular structure of the colloidal particle with subsequent changes in the apparent solution viscosity. If however, the viscosity remains constant after a cyclical change in its physical state, the viscosity is considered reversible with respect to this change. For this work, the reversible nature of asphaltenes in tetralin was examined for two reasons. The first is that a knowledge of its reversible nature would give insight to other physical behavior such as surface tension, particle surface charge, and colloidal stability. Secondly, this knowledge would be valuable in planning viscosity measurements to assure reproducible results and to keep material use at a minimum.

The reversibility with respect to cyclical changes in temperature and concentration was examined using Fraction GPC-77-4 in tetralin. The cyclical concentration change was actually a drying process where the tetralin was driven off using distillation followed by vacuum drying.

Thus, this process combines any effects of the temperature and concentration change on the viscosity. The cyclical process used was as follows:

1) Preparation of a 8.85% by weight solution and the measurement of its apparent viscosity at 30°C
2) Distillation of this solution at 205°C for 1.1 hours giving a resulting concentration of 22.78% by weight and the subsequent measurement of its viscosity at 30°C
3) Distillation of this solution at 205°C to approximately 50% by weight after 2/3 hours and then vacuum drying at 75°C for 24 hours followed by vacuum drying at 150°C for 24 hours
4) Preparation of 22.78% by weight of these dried solids in tetralin and subsequent measurement of viscosity at 30°C
5) Dilution of this solution to 8.85% and subsequent measurement of its viscosity at 30°C

The resulting viscosities and densities were:

(Before Drying)	Density(g/ml)	Viscosity(cp)	Temperature(°C)	
8.85% by weight	0.978	3.02	30	
22.78% by weight	1.006	6.15	30	
(After Drying)	Density(g/ml)	Viscosity(cp)	Temperature(°C)	% Change
8.85% by weight	0.978	2.92	30	-(3.31)
22.78% by weight	1.006	7.03	30	+(14.3)

From the data it can be seen that at low concentrations the effects of temperature and drying on viscosity is not great. At higher concentrations the effect is more pronounced. However, the viscosity does not undergo a radical change and the densities remain constant indicating no effect on the volumes of mixing. Considering the severity of the drying process, this does not show a great departure from reversibility. This indicates that these asphaltenes are somewhat lyophilic in nature typical of colloid systems exhibiting behavior intermediate to lyophilic and lyophobic systems.

In the future, viscosity experiments will be planned to minimize temperature stresses even if additional material is required.

B. Background Studies in the Microrheology of Coal-Derived Liquids

Microrheology can be defined as those investigations directed toward the prediction of the macroscopic rheological behavior of a material from a detailed description of its chemical and physical character. A study of the microrheology of coal derived liquids was undertaken for two reasons. First, it would give insight about the parameters important to the

rheology of coal-derived liquids, thereby aiding in design of the experimental program. Secondly, it would aid in analysis and correlation of the results.

The microrheology of coal-derived liquids can be approached in different ways depending on the nature of the system. If the system consists of a solvent and particles of molecular size (i.e., of a size comparable to that of the solvent molecules) the system can be considered effectively homogeneous and a thermodynamic treatment applied. In this case viscosity would be correlated with the properties of the pure components and with thermodynamic parameters characteristic of the interactions between components. If the system consists of a solvent with particles of a considerably larger size, then the discrete molecular nature of the solvent can be ignored and an approach based on continuum hydrodynamics can be used.

Within the thermodynamic approach, there are two major semiempirical theories. The first is the absolute reaction rate theory of Eyring and co-workers which relates the viscosity exponentially to the free energy needed for a molecule to overcome the attractive force field of its neighbors, so that it can move to a new equilibrium position. The second semiempirical approach is the free volume theory which relates the viscosity exponentially to the probability of occurrence of an empty neighboring site into which a molecule can move. Bloomfield and co-workers have used both concepts of absolute rate and free volume theories in connection with the viscosity of binary liquid mixtures of short-chain normal alkanes.[38,39] They show that these theories, when used independently, correlate well for systems of n-alkanes of less than 12 carbons in benzene, predicting well the observed negative intrinsic viscosities. Hydrodynamic theory, which works well for long-chain molecules, fails to predict this behavior for short-chain molecules.

Continuum hydrodynamic theory, however, is useful for systems where the dispersed phase is so large that the solvent can be effectively considered as a continuum. The literature abounds with hydrodynamic treatments of dispersed systems. The first effort in this area was by Einstein who considered a dilute suspension of rigid noninteracting spheres in a Newtonian fluid ignoring wall effects and assuming low Reynolds number hydrodynamics.[40] He obtained a relation in which the intrinsic viscosity was a constant value of 2.5 and the viscosity was a linear function of the particle volume fractions. As a next step, Jeffery considered a similar system except with rigid ellipsoidal particles.[41] In this case, the resulting intrinsic viscosity varied between 2.0 and 2.5 depending on the shape of the ellipsoidal particle. Here, the disorienting force of Brownian motion is not considered and the equilibrium position of zero torque is assumed, thus giving lower intrinsic viscosities than might be expected for a real system. Sheraga treated the same system except he included Brownian forces.[42] As a measure of the Brownian force, he used the rotary diffusion constant. The ratio of the shear (the orienting force) to the rotary diffusion constant (the disorienting force) serves as an index for the importance of Brownian motion in energy dissipation. When this ratio is zero, there

is complete particle disorientation giving intrinsic viscosities greater than 2.5. For zero rotary diffusion in a shear field, this reduces to Jeffery's case with intrinsic viscosity less than 2.5.

The above mentioned treatments can be considered as only zeroth order approximations to suspension hydrodynamics since they ignore particle-particle interactions and only apply to very dilute solutions. There have been several attempts to treat first order interaction effects. Simha treated first order interaction effects by using a cell model approach.[43] Batchelor treated first order interaction effects using ensemble averages such as bulk stress and bulk velocity gradients to give an exact formula good to the second order of the volume fraction for pure straining flow.[44] For very concentrated suspensions, asymptotic solutions are in the process of being developed.[45]

In addition to concentration effects, there are other factors such as flocculation and solvation[46,47], particle size distribution[48], particle surface energy[44], wall effect[48], particle nonrigidity[49], and secondary electroviscous effects[50] for the case of charged colloidal systems.

The above theoretical treatment of these factors can serve as a guide for predicting the rheological behavior of colloidal coal-dervied liquids. This will be of considerable use when planning the experiments.

C. Rheological Theory and Experimentation

In the case of a system of spherical particles of uniform size suspended in a Newtonian medium, hydrodynamic theory and data indicate that the system will be Newtonian provided that particles are uniformly distributed and the suspension is not near the upper limit (volume fraction = 0.52) of loose packed-bed concentration.[48] This configuration certainly cannot be assumed for coal-derived liquids and thus, non-Newtonian behavior is to be expected. Through microrheology as described above, an estimation of the rheological behavior can be made. However, by making certain empirical observations, the complete rheological behavior can be specified for particular types of flow at a constant temperature, density, and strain. Rheology is the science of deformation and flow of matter and is concerned with determining the constitutive equation of a material primarily by observation. Usually an empirically determined flow curve (stress versus strain rate) is associated with the hypothetical model that fits the data best.

To become familiar with rheology, several books were reviewed.[51-53] For steady simple shearing flows of a homogeneous and incompressible fluid, rheological theory has shown that the stress tensor depends only on the shear rate and may be expressed in terms of three independent functions or viscometric functions.[51,53] These viscometric functions are functions of the shear stress or normal stresses. Experimental measurement of the shear stress and difference of normal stresses as a function of shear rate yields the desired constitutive equation for a homogeneous and incompressible fluid in simple shear flow.

A rheometer is a device which measures the viscometric functions. Work is currently being done to assess the relative merits of various rheometers. There are two general types of rheometers: the rotational type (cone-and-plate, parallel-plate, and coaxial cylinder) and the capillary type. The first type has capability of measuring both steady (viscometric functions) and oscillatory shearing flow properties. The second can measure steady flow properties. Of the first type, the Weissenberg rheogoniometer is the most commonly used device. A Weissenberg rheogoniometer is available for this project, however certain ancillaries would have to be purchased in order to allow for normal stress measurements. In addition, the problems of insensitivity to small normal stresses and "transducer hole" error would have to be overcome. Literature pertaining to the capillary viscometer is now being examined to determine its cost and advantages. One possible advantage would be the use of other than ambient pressures. Another is that fewer transducers are needed for operation than in the rotational type. The possibility of constructing such a viscometer is also under consideration.

CONCLUSIONS

This contract is a continuation of a previous study sponsored by NSF RANN. The conclusions presented here are in part based on a Ph.D. dissertation which was completed during the first quarter of this ERDA contract.[1]

Several factors have been found for the low filtrate flow rates encountered when filtering liquefied coal slurries. The principal factors are solids size, solids compressibility, softening of the carbonaceous solids at temperatures above 200°C, high liquid viscosities, interactions between the asphaltene micelles in the liquid phase and the filter cake solids, and interactions between the asphaltene micelles and the oils and resins in the liquid phase.

Suspended solids contained in the liquefied coal slurries consist of mineral solids, undissolved coal, and char. They range in size from less than 0.05 micron to greater than 1.0 micron in diameter. Even though a large percentage of the particle volume (mass) is contained in particles which are one micron or larger in diameter, the small (less than 0.2 micron in diameter) particles play a very important part in governing the flow properties of filter cakes formed when filtering liquefied coal slurries. The small particles largely determine the diameter of flow passages through these filter cakes. They do this by forming 'micro' filter cakes which fill the interstices between the large diameter particles forming the bulk of the 'macro' filter cakes.

Filter cake specific resistance varies as an inverse function of the number average particle size. THF-insoluble solids from SYNTHOIL product oil, H-Coal vacuum still bottoms and SYNTHOIL centrifuge cake had number average particle sizes of 0.067, 0.071, and 0.147 microns, respectively. When filtered from tetralin at 177°C, the specific resistances were 0.7×10^{12}, 0.6×10^{12}, and 0.31×10^{12} m/kg, respectively.

At temperatures below 200°C, the H-Coal filter cake solids compressibility was found to be 0.36. Thus, if filter pressure drop is doubled, filter cake specific resistance will increase by approximately 28% and the flow rate will increase only 56%.

The specific filtration resistance of the solids is temperature-dependent above 200°C. As the temperature is increased from 177 to 232°C, the specific cake resistance increases from 50 to 100%. The increase in resistance is believed to be associated with melting or softening of residual organic matter contained in the solids. The softened organic solids are subject to semi-plastic flow under the influence of the drag forces exerted by the flowing filtrate and block or partially block some of the flow passages in the filter cake.

Surface tension and reduced viscosity data for oils, resins, and asphaltenes in tetralin indicate intermolecular association and colloid

micellization in liquefied coal fractions. At asphaltene and preasphaltene concentrations above 15 weight percent, micelle formation is significant. The micelles interact with porous media through which they are flowing to give an apparent increase in specific cake resistance. This increase depends on the size of the micelles in relation to the size of the flow passages. Resins act to peptize the micelles, which limits their size.

As total liquid-phase asphaltene and preasphaltene concentrations are increased from 0 wt. % to values between 15 and 25 wt. %, an apparent increase in specific cake resistance occurs. The magnitude of this increase depends upon the composition of the liquid in which the asphaltenes and preasphaltenes are dissolved. When tetralin is used as the suspending medium, specific cake resistances approximately double. When oils and resins are used as the suspending media, specific cake resistances increase by only about 40%. Asphaltenes can also increase the flow resistance of precoat layers from 0 to 100%. However, this increase is insignificant when compared to the absolute resistance to flow of a typical filter cake.

It has been found possible to synthesize "model" asphaltene compounds which have either two or more heterocyclic rings joined by a saturated carbon chain or two or more phenolic groups joined in the same way. Both bis-(o-hydroxyphenyl)-alkanes and bis-heterocyclic compounds have been synthesized. The formation of para isomers of bis-(o-hydroxyphenyl)-alkanes has been a problem. It was found it could be avoided by blocking the para position with a methyl group. Purification methods are still needed. Bis-heterocyclic compounds have been synthesized by a modified Minisci procedure to give yields of about 7%.

The Clemmensen reduction method has been effective in the synthesis of bis-(hydroxyphenyl)alkanes. 1,5-bis-(hydroxy-5-methylphenyl)pentane, 1,6-bis-(2-hydroxy-5-methylphenyl)hexane and 1,4-bis-(2-hydroxy-5-methylphenyl)butane were effectively synthesized using the technique. The NMR spectra of synthesized 1,2-bis-(2-quinolyl)ethane account for the low field end of the "aliphatic" portion of asphaltene NMR spectra.

NMR spectra of mixtures of phenol and pyridine show that the shift of the phenolic proton depends significantly upon the ratio of phenol to pyridine. This is due to the deshielding effect of hydrogen bonding.

An effective solvent-acid system is needed to separate the asphaltenes and preasphaltenes into acidic, basic, and neutral fractions. The toluene-HCl system is satisfactory for asphaltenes but inadequate for preasphaltenes. The preasphaltenes are of particular interest since they contain more heteroatoms than do asphaltenes. Ideally the preasphaltenes should be soluble in the solvent and form a base-adduct which precipitates upon the additional of acid but which is recoverable in solution upon neutralization.

The 10.16-cm ID x 122-cm long GPC column containing 8% divinylbenzenestyrene copolymer was found to be effective for separating large

quantities of asphaltenes into fractions containing narrow ranges of molecular sizes. Toluene-soluble, 75%-pentane/25%-toluene-insoluble asphaltenes from vacuum still bottoms from the liquefaction of an Illinois No. 6 Coal in the Hydrocarbon Research, Inc. H-Coal process contained molecules with molecular weight in the range from 280 to 1350. The first two of seven GPC fractions contained 24% of the total mass and had molecules above a molecular weight of 1250. These fractions had the highest oxygen content, 7-8% by weight, with subsequent fractions containing less oxygen. The nitrogen content was fairly constant at 1.5% in all fractions while the sulfur content dropped from about 1% to 0.1%. Evidence of substantial intermolecular association was found in the first three GPC fractions. Hydrogen bonding is believed to be the major cause of association.

Neutron activation analysis for metals in asphaltene fractions from a GPC fractionation of toluene-soluble, 75%-pentane/25%-toluene-insoluble asphaltenes from Hydrocarbon Research, Inc., H-Coal vacuum bottoms from an Illinois No. 6, River King Mine Coal showed higher metals levels in the higher molecular weight fractions. There is a close relationship between the concentration of metals and the levels of heteroatoms present.

Electrophoresis experiments with asphaltene and preasphaltene fractions in pyridine, THF, m-cresol, benzene, and tetralin show evidence of positive and negative charges in solution. Pyridine, THF and m-cresol, which can participate in hydrogen bonding, are more effective at peptizing asphaltene and preasphaltene micelles. This is evident by the increased electrical conductivity of solutions and by the increase in deposits on the electrodes. Much more material deposits on the positive electrode when asphaltenes and preasphaltenes are dissolved in pyridine and m-cresol. Asphaltenes and preasphaltenes behave differently in THF with comparable deposits occurring on both electrode from preasphaltene solutions. More deposits occur on the negative electrode in the poorer solvents, benzene and toluene.

Adsorption experiments on the second to fifth GPC fractions mentioned above showed that adsorption increases with molecular weight when the same solvents, solids and temperatures are used. Solvents, such as pyridine and THF, which effectively alter hydrogen bonding, reduce adsorption by a factor of 5 to 8. Alumina has the highest affinity for adsorption in comparison of seven solids with the same asphaltene fraction in tetralin at 30°C. At asphaltene concentrations above 40 g/l for the first four GPC fractions, intermolecular association is apparent with subsequent cluster exclusion from the smaller pores of alumina. The solvents in order of highest to least adsorption onto alumina of a 330 molecular weight asphaltene fraction were: toluene, tetralin, nitrobenzene, THF, and pyridine.

Streaming potential measurements with asphaltenes in different solutions give results consistent with the electrophoresis work.

The LEAC method is useful in the measurement of the contribution of heteroatoms to adsorption or to intermolecular association. Adsorption experiments with water deactivated alumina reveal that the compounds with

basic nitrogen and hydroxyl groups have a higher affinity for adsorption. The acidic and basic fractions of the asphaltenes from an Illinois No. 6 Coal contain compounds with such groups as indicated by the large elution volume required. A synthesized model compound with two basic nitrogents had a 50% retention elution volume seven times larger than 5,6-benzoquinolene which contains one basic nitrogen atom.

Viscosity measurements on an asphaltene fraction in tetralin before and after vacuum drying the asphaltenes at 150°C for 24 hours showed a 14.3% increase at an asphaltene concentration of 23% by weight, but little difference was observed at 9% by weight.

REFERENCES

1. Briggs, D. E., et al., "Studies on the Separation of Coal Extract from Solid Residue in Liquefied Coal," NSF-AER Report NSF-AER 7515213, December 1976.

2. Minisci, F., Tetrahedron, 27, 3575,

3. Walker, Jr., P. L., et al., "Characterization of Mineral Matter in Coal and Coal Liquefaction Residues," Electric Power Research Institute Report, EPRI AF-417, June 1977.

4. Unlirzaucher, J., Ber. 73b, 391, 1940.

5. Coleman, R. F. and J. Perkin, Analyst, 84, 233, 1959.

6. Coleman, R. F. and J. Perkin, Analyst, 85, 154, 1960.

7. Veal, D. J. and C. F. Cook, Anal. Chem., 34, 178, 1962.

8. Steele, E. L. and N. W. Meinke, Anal. Chem., 34, 185, 1962.

9. Anders, O. V. and D. W. Briden, Anal. Chem., 36, 287, 1964.

10. Burk, Jr., E. H., and H. W. Kutta, "Investigations on the Nature of Preasphaltenes Derived from Solvent Refined Coal Conversion Products," Stanford Research Incorporated, Coal Chemistry Workshop, August 1976.

11. Sternberg, H. W., R. Raymond, and F. K. Schweighardt, Science, 188, 49, 1975.

12. Snyder, L. R., Accounts of Chemical Research, 3, 290, 1970.

13. Grosskreutz, T. C., "Small-Angle Scattering of X-rays," Handbook of X-rays, ed. Emmet F. Kaebble, McGraw-Hill Book Company, N. Y., 1967.

14. Beeman, Kaesbey, Anderegg, and Webb, Handbuch der Physik, 32, Springer-Verlag, OHG, Berling, 1957.

15. Guinier, A., G. Fournet, C. B. Walker, and K. L. Yudowitch, Small Angle Scattering of X-rays, John Wiley & Sons, Inc., N. Y., N. Y., 1955.

16. Pilz, I., "Small-Angle X-ray Scattering," in Physical Principles and Techniques of Protein Chemistry, Part C, ed. by Sydney J. Leach, Interscience, 1973.

17. Hendricks, R. W. and P. W. Schmidt, Acta Physica Austricaca, 26(3), 97, 1976.

18. Jellinch, M. H., E. Solomon, and I. Fankuchen, Ind. Eng. Chem. Anal. Ed., 18, 172, 1966.

19. Hight, Jr., R., W. T. Higdon, and P. W. Schmidt, "Small Angle X-ray Scattering Study of Sodium Montmorillonite Clay Suspensions," J. Chem. Phys., 33(6), 1656, 1960.

20. Bale, H. D. and P. W. Schmidt, "Small Angle X-ray Scattering from Aluminum Hydroxide Gel," J. Phys. Chem., 62, 1179, 1958.

21. Hight, Jr., R., W. T. Hijdon, and P. W. Schmidt, "Small Angle X-ray Scattering from Montmorillonite Clay Suspensions II," J. Chem. Phys., 37(3), 502, 1962.

22. Reiss-Husson, R and Luzzati, Vittorio, "Small Angle X-ray Scattering Study of the Structure of Soap and Detergent Micelles," J. Colloid and Interface Sci., 21, 534, 1966.

23. Luzzati, V., J. Witz, and Nicolaieff, "Determination de la Masse et des Dimensions des Proteines en Solution par la Diffusion Centrale des Rayons X Mesuree a l'Echelle Absolue = Exemple du Lysozyme," J. Mol. Biol., 3, 367, 1961.

24. Ritland, H. N., P. Kaesbey, and W. W. Beeman, "An X-ray Investigation of the Shapes and Hydrations of Several Protein Molecules in Solution," J. Chem. Phys., 18(9), 1237, 1950.

25. Siegel, L. A., "Small Angle X-ray Scattering from Solutions of Aerosol OT in Nonaqueous Media," J. Chem. Phys., 29(5), 1091, 1958.

26. Dwiggins, Jr., C. W., "A Small Angle X-ray Scattering Study of the Colloidal Nature of Petroleum," J. Phys. Chem., 69(10), 3500, 1965.

27. Yen, T. F. and J. P. Dickie, "Macrostructures of the Asphaltic Fractions by Various Instrumental Methods," Analytical Chemistry, 39(14), 1847, 1967.

28. Yen, T. F. and S. S. Pollack, "Structural Studies of Asphaltics by X-ray Small Angle Scattering," Analytical Chemistry, 42(6), 523, 1970.

29. Preckshot, G. W., N. G. DeLisle, C. E. Cottrell, and D. L. Katz, "Asphaltic Substances in Crude Oils," Trans. AIME, 151, 183, 1943.

30. Csanyi, L. H. and B. S. Bassi, "Analysis of Asphalts by Electrical Means," Proc. Assoc. Asphalt Paving Tech., 27, 52, 1958.

31. Wright, J. R. and R. R. Minesinger, "The Electrophoretic Mobility of Asphaltenes in Nitromethane," J. Colloid Sci., 18, 223, 1963.

32. Briggs, D. E. and P. A. S. Smith, "Physical and Chemical Behavior of Liquefied Coal in Coal Liquefaction and Solids Separations," University of Michigan Proposal DRDA-76-1416-T1 to ERDA, March 29, 1976.

33. Rodgers, B. R., Oak Ridge National Laboratory, Oak Ridge, Tennessee, Personal Communication, October 13, 1976.

34. Snyder, L. R., J. Chromatog., 5, 430, 1961.

35. Snyder, L. R., J. Chromatog., 6, 22, 1961.

36. Heftman, E., Chromtography, 2nd Ed., Reinhold Publ. Corp., N. Y., N. Y., 1967.

37. Snyder, L. R., J. Phys. Chem., 72(2), 489, 1968.

38. Bloomfield, V. A. and R. K. Dewan, "Viscosity of Liquid Mixtures," J. Phys. Chem., 75, 20, pp. 3113-3119, 1971.

39. Dewan, R. K., V. A. Bloomfield, and P. B. Berget, "Intrinsic Viscosity of Short-Chain Normal Alkanes," J. Phys. Chem., 75, 20, pp. 3120-3124, 1971.

40. Einstein, A., Ann. Physik, 19, 4, 289, 1906.

41. Jeffery, G. B., "The Motion of Ellipsoidal Particles Immersed in a Viscous Fluid," Roy. Soc. Proc. Series A, 102, pp. 161-179, 1922.

42. Scheraga, H. A., "Non-Newtonian Viscosity of Solutions of Ellipsoidal Particles," J. Chem. Phys., 23, 8, pp. 1526-1532, 1954.

43. Simha, R., "The Influence of Brownian Movement on the Viscosity of Solutions," J. Phys. Chem. 44, pp. 25-34, 1940.

44. Batchelor, G. K. and J. T. Green, "The Determination of the Bulk Stress in a Suspension of Spherical Particles to Order C^2," J. Fluid Mech., 56, Part 3, pp. 401-427, 1972.

45. Frankel, N. A. and Andreas Acrivos, "On the Viscosity of a Concentrated Suspensions of Solid Spheres," Chem. Eng. Sci., 22, pp. 847-853, 1967.

46. Vand, V., "Viscosity of Solutions and Suspensions, I," J. Physical and Colloidal Chemistry, 52, pp. 277-299, 1948.

47. Vand, V., "Viscosity of Solutions and Suspensions, II," Ibid, pp. 300-314.,

48. Happel, J. and H. Brenner, Low Reynolds Number Hydrodynamics with Special Attention to Particulate Media, Prentice-Hall, Inc., Englewood Cliffs, New Jersey, 1965.

49. Oldroyd, J. G., "The Elastic and Viscous Properties of Emulsions and Suspensions," Roy. Soc., Proc., London, Series A, 218, pp. 122-132, 1953.

50. Russel, W. B., "Low-Shear Limit of the Secondary Electroviscous Effects," J. Colloid Enterface Science, 55, 3, pp. 590-604, June, 1976.

51. Frederickson, A. G., Principles and Applications of Rheology, Prentice-Hall, Inc., Englewood Cliffs, New Jersey, 1964.

52. Brodkey, R. S., The Phenomena of Fluid Motions, Addison-Wesley Pub. Co., Reading, Massachusetts, 1967.

53. Han, C. D., Rheology in Polymer Processing, Academic Press, New York, N. Y., 1976.

☆U.S. GOVERNMENT PRINTING OFFICE: 1978-740-206/39